RHODES UNIVERSITY

Grahamstown • 6140 • South Africa

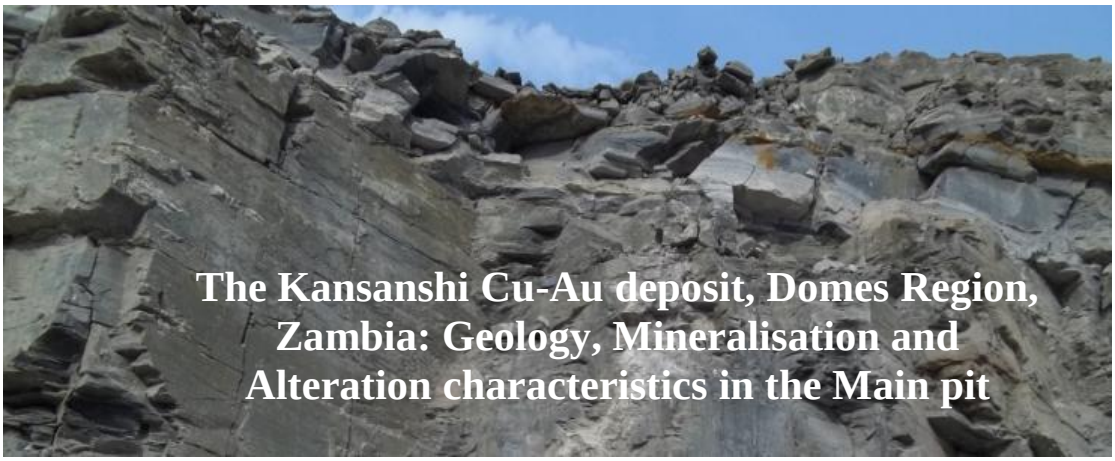

The Kansanshi Cu-Au deposit, Domes Region, Zambia: Geology, Mineralisation and Alteration characteristics in the Main pit

By

Donald T Chinyuku

A thesis submitted in fulfillment of the requirements for the degree of

MASTER OF SCIENCE
(Exploration Geology Cwk/Thesis)

MSc Exploration Geology Programme
Geology Department
Rhodes University
P.O. Box 94
Grahamstown 6140
South Africa

25 November 2013

ACKNOWLEDGEMENTS

My sincere thanks go to First Quantum Minerals (Kansanshi Mine) for funding my studies and permission to use geological information for my thesis. Of special mention is Mr. Meiring Burger (Mine Manager) and Mr. Alain Mouton (then Chief Geologist) for making this all possible and believing in me. Many thanks to Rob Grafen-Greaney and Stergios for 'sowing the seed'. To Louis van Heerden (Chief Geologist) for allowing me time to do my studies and taking time out of your busy schedule to review my thesis. To Professor Yong Yao, thanks for the guidance throughout the studies and for supervising my thesis. Mrs. Ashley Goddard the Exploration Geology secretary and Michelle Booysen are immensely thanked for all the arrangements (accommodation and transport) during attendance of module courses. To my classmates, thanks for making the attendance of module courses and field trips across South Africa worthwhile. To Nico Bleeker, Clay Kaila and Jimmy for all the encouraging words when the chips were down. Seona, Chris, Pieter Fourie, James Mwale and my fellow workmates for keeping me focused on the goal. To my entire family, thank you for being my pillar of strength and motivator during the academic programme.

DECLARATION

I, Donald T Chinyuku, declare this thesis to be my own work. It is submitted in fulfillment of the Degree of Master of Science at Rhodes University. It has not been submitted before for any degree or examination in any other University or tertiary institution.

Signature of the candidate: …….

Date: ……

Dedicated to my wife Rosebud and my boys Tanatswa and Anotidaishe, thank you for all the support and sacrifice during this journey.

ABSTRACT

The Kansanshi Cu-Au deposit located in the Domes region of the North West province of Zambia is characterised by structurally controlled high angle veins and associated alteration halos. The northwest trending Kansanshi antiform flanks the Solwezi syncline to the north and hosts the Kansanshi deposit and consists of tillites and metasedimentary rocks. Mineralisation is associated with Neoproterozoic Pan African deformation events experienced during the formation of the Lufilian fold belt; however recent findings confirm that structures in the form of reverse and normal faults and drag folds are critical controls on mineralisation within the deposit, Main pit in particular. Low angle faults occurring below the current pit are believed to have served as major fluid pathways during mineralisation. Age dating data from the Kansanshi deposit suggest that mineralisation took place between 512 and 503 Ma indicating that the event was associated with metamorphism. Two types of alteration are dominant within the Main pit (Kansanshi deposit) with the type and intensity of alteration being largely controlled by lithological units. Albite alteration occurs dominantly in phyllites and schists whereas dolomitisation is prevalent in calcareous units. Alteration is associated with mineralisation, and therefore is used as a condition for predicting vein or disseminated mineralisation.

The high Au tenor at Kansanshi can be attributed to gold grains occurring in association with melonite ($NiTe_2$) and microfractured pyrite intergrown with chalcopyrite in sulphide and quartz dominated veins and veinlets. Analysis of gold grade distribution within the Main pit shows a clear concentration of the element along the major north-south trending structures like the 4800 and 5400 zones, possibly through supergene enrichment in the oxide-transition-sulphide zones. It is imperative that exploration for Kansanshi-type deposits will require geochemical and geophysical studies, understanding of the geology of an area to identify the three lithostratigraphic units (red beds, evaporites and reducing strata).

Keywords*: Kansanshi antiform, Pan African deformation, Cu-Au mineralisation*

TABLE OF CONTENTS

Acknowledgements ii
ABSTRACT v
1. INTRODUCTION 8
1.1. Introduction and Background 8
1.2 Location of study area 8
1.3 Mine History 10
1.4 Historical work 11
1.5 Aims of study 11
1.6 Methodology 12
2. GEOLOGICAL SETTING 14
2.1 Introduction 14
2.2 Regional and Local setting 14
2.3 Structure, Deformation and Metamorphism 16
3. REGIONAL GEOLOGY 19
3.1 Introduction 19
3.2 Stratigraphy 19
3.2.1 Basement 21
3.2.2 Katanga Supergroup of Zambian and Congo Copper belts 22
3.2.3 Regional Lithostratigraphic correlation of Katanga Supergroup 24
3.3 Tectonics and Structures 25
3.3.1 Orogenic events in the Lufilian Fold Belt 27
3.4 Metamorphism 28
3.5 Magmatism (Intrusive activity) 29
4. MINE GEOLOGY 30
4.1 Introduction 30
4.2 Stratigraphy 31
4.2.1 Quartz-Feldspar-Mica Schist (QFMS) 33
4.2.2 Upper Dolomite (UD) 34
4.2.3 Upper Pebble Schist (UPS) 35
4.2.4 Top most Marble (TMM) 36
4.2.5 Kansanshi Mine Formation 37

4.2.5.1 Upper Mixed Clastics (UMC) 37
4.2.5.2 Upper Marble (UM) 39
4.2.5.3 Middle Mixed Clastics (MMC) 39
4.2.5.4 Lower Calcareous Schist (LCS) 40
4.2.5.5 Lower Marble (LM) 41
4.2.6 Lower Pebble Schist 42
4.2.7 Lower Dolomite (LD) 43
4.2.8 Micaeous Calcareous Schist (MCS) 44
4.3 Structures 45
4.3.1 Large scale structures 46
4.4 Metamorphism 48
4.4.1 Age of metamorphism 50
4.5 Magmatism (Intrusive activity) 51
5. MINERALISATION AND ALTERATION TYPES 53
5.1 Introduction 53
5.2 Ore body and mineralisation characteristics 53
5.2.1 Mineralisation controls 57
5.3 Types of mineralisation 58
5.3.1 Vein mineralisation 58
5.3.1.1 Stage 1: Quartz-carbonate sulphide veins 59
5.3.1.2 Stage 2: Carbonate sulphide-U-Th rich veins 61
5.3.1.3 Stage 3: Sulphide veins 62
5.3.2 Breccia/Stock mineralisation 62
5.3.3 Disseminated sulphide mineralisation 63
5.3.4 Distribution and geometry of vein mineralisation 64
5.3.5 Age of mineralisation 65
5.4 Mineral association and zonation of copper mineralisation 66
5.5 Alteration types and characteristics 67
5.5.1 Albite-carbonate alteration 67
5.5.2 Carbonate alteration 71
5.5.3 Other significant alteration types 72
5.6 Gold mineralisation 73
6. GENETIC IMPLICATION FOR THE DEPOSIT 77
6.1 Introduction 77
6.2 Formation of Sediment hosted copper deposits 77
6.3 Regional genetic models 80

6.4 Localised genetic models 82
6.4.1 Fold-thrust belt model 83
6.4.2 Extensional fault-fold model 84
6.5 Source of metals 86
7. EXPLORATION IMPLICATION FOR THE DEPOSIT 87
7.1 Introduction 87
7.2 Historical and current exploration considerations 87
7.3 Geophysical techniques 89
7.3.1 Electromagnetic surveys 90
7.3.2 Aeromagnetic surveys 92
7.3.3 Radiometric surveys 93
7.3.4 Other geophysical techniques applied to the Kansanshi deposit 95
7.4 Geochemistry 97
7.5 Drilling, estimation and orebody modelling 98
7.6 Exploration ideas for CACB deposits 104
8. DISCUSSION 106
8.1 Introduction 106
8.2 Controls on mineralisation 106
8.3 Relationship of mineralisation and stratigraphy 108
8.4 Copper and Gold mineralisation 109
8.5 Ore Genesis at Kansanshi 110
8.6 Exploration techniques 111
9. CONCLUSIONS/SUMMARY 113
9.1 Further study/Recommendations 115
REFERENCES 116
APPENDIX ONE – GLOSSARY 123
APPENDIX TWO – QUICKLOGS 124
APPENDIX THREE – QUICKLOG PLAN 129
APPENDIX THREE – GEOLOGY MAP OF MAIN PIT 130

LIST OF FIGURES

Figure 1. Location map of the Kansanshi Cu-Au deposit.

Figure 2. Image of Kansanshi Mine lease area.

Figure 3. Tectonic setting and Structural domains of the Lufilian Fold Belt.

Figure 4. Geological map of the North West Province of Zambia.

Figure 5. Schematic section of Lufilian fold belt showing tectonic zones.

Figure 5a. Geological map of the Solwezi area, illustrating structures (faults and folds) affecting the Kansanshi deposit.

Figure 6. Traditional Stratigraphy of the Katangan Supergroup.

Figure 7. Regional stratigraphy of Katangan Supergroup

Figure 7a. Regional Lithostratigraphic sequence of the Congolese and Zambian Copperbelts.

Figure 8. Regional structures of the Lufilian fold belt

Figure 9. Distribution of gabbros in the Domes Region of the NW of Zambia.

Figure 10. Regional Geology map of the Kansanshi Mine area also showing the Main Pit.

Figure 11. Generalised Tectono-stratigraphy of Kansanshi Mine.

Figure 12: Detailed stratigraphy of the Kansanshi Mine.

Figure 13. Core of Quartz-Feldspar-Mica Schist.

Figure 14. Dolomite with intercalations of biotite.

Figure 15. Pebble Schist (LPS) showing porphyroblasts of garnet.

Figure 16. Photograph of Top Most Marble (altered/bleached).

Figure 17. Photography of garnetiferous mica schist (Knotted Schist) of the UMC unit.

Figure 18. Photograph of carbonaceous phyllite (CBPH) of the UMC.

Figure 19. Photograph of the marble unit of the UM horizon.

Figure 20. Photograph of biotite schist (BS) and knotted schist (KS) of the MMC unit.

Figure 21. Photograph of calcareous biotite schist (CLBS) of the LCS unit showing compositional banding.

Figure 22. Photograph of marble and altered (albitised) phyllite of the LM unit.

Figure 23. Photograph of PS unit of the LPS showing porphyroblasts of scapolite and 'elongated quartz pebbles'

Figure 24. Siltstone unit in the LPS showing the presence of 'iron formation' and black magnetite.

Figure 25. Photograph of the carbonate unit of the LD with intercalations of biotite.

Figure 26. Dolomite-magnesite-biotite schists of the MCS.

Figure 27. High grade Cu intersections showing the 4800 and 5400 zones.

Figure 28. P-T diagram indicating metamorphic facies for Kansanshi metasediments.

Figure 29. Progression of metamorphism associated with deformation.

Figure 30. (A) Distribution of Gabbros within the confines of the Main pit area.

Figure 30. (B) Gabbro intrusion as on the pit wall in Main 6.

Figure 31. Kansanshi Orebody (Main and NW Pits) located along the crest of the antiform.

Figure 32. Graphical representation of the vein distribution in the Main Pit.

Figure 33. Residual and fresh marble contact as seen in core.

Figure 34: Vein mineralisation confined by calcareous units.

Figure 35. Schematic cross section through the Kansanshi vein system.

Figure 36: Quartz-carbonate-chalcopyrite vein in core from Main pit.

Figure 37. Carbonate-sulphide-rich veins in the Main pit.

Figure 38. High grade chalcopyrite vein hosted in Knotted schist.

Figure 39. Oxide mineralisation consisting of malachite, chrysocolla, tenorite within a 'Oxide vein'

Figure 40. Disseminated sulphide and blebs of Molybdenite mineralisation.

Figure 41: Sketch showing the prevalence of veins in the clastic units.

Figure 42. Range of mineralisation and metamorphic ages obtained for the Kansanshi deposit.

Figure 43. Albite carbonate alteration with chalcopyrite and molybdenite mineralisation.

Figure 44. Zonation of alteration in different lithologies.

Figure 45. Bleached Albite alteration zones in LCS.

Figure 46. Dolomitisation alteration in LCS.

Figure 47. Sericite alteration in core.

Figure 48. Scapolite alteration associated with sulphide dissemination (Py) in marble.

Figure 49. Gold grade trends in Main pit.

Figure 50. Section of the Main pit dome apex/pimple showing domain with high Au:TCu.

Figure 51. Metal content of sediment-hosted deposits plotted against age of host rocks.

Figure 52. Schematic section of an intracratonic basin, host to sediment-hosted stratiform Cu deposits.

Figure 53. Regional genetic model for CACB deposits.

Figure 54. Simplified Genetic model for the Main Pit

Figure 55. Sketch of fold-thrust model for mineralisation at Kansanshi.

Figure 56: Sketch of fault-fold model for mineralisation at Kansanshi

Figure 57. Section through the Main pit showing thickening of the PS and clastic units.

Figure 58. Location map of Geophysical surveys done in the Kansanshi Mining lease area.

Figure 59. Generalised EM survey setup.

Figure 60. Image of electromagnetic survey done on the Kansanshi Mining Lease area.

Figure 61. Total Magnetic Intensity image of Solwezi area showing Kansanshi Antiform and Solwezi Dome.

Figure 62. RTP images from (A) 1997 survey and (B) 2010 survey.

Figure 63. Schematic of airborne radiometric surveys.

Figure 64. Ternary image of K,U,Th of the Solwezi area.

Figure 65. Chargeability image of the SE Dome.

Figure 66. Results of soil sampling geochemical survey showing the Kansanshi anomaly.

Figure 67: Kansanshi and SE Dome drilling.

Figure 68. Section showing the impact of intrusive on lithological units.

Figure 69. Section 11400N showing the Main pit domal structure, thickening of the LPS and deep ‘seated’ mineralisation in the LPS and LD.

LIST OF TABLES

Table 1: List of boreholes and characteristics reviewed.

Table 2: Katangan Stratigraphic Column for Copperbelt – Solwezi Area.

Table 3: Historical and Current holes drilled within the Kansanshi deposit for the MRE.

Table 4: Block model extents for Kansanshi Mine.

Table 5: Block model attributes for Kansanshi Mine.

Table 6: Kansanshi and SE Dome Mineral Resource Estimate as at 30th November 2012.

CHAPTER 1: INTRODUCTION

1.1 Introduction and Background

The Kansanshi Cu-Au deposit located north of the Solwezi dome (Domes region) in the North West province of Zambia is characterised by structurally controlled high angle quartz-carbonate veins and associated alteration halos. The mineralisation, in the form of veins, cuts metasedimentary sequences which were deformed by the Lufilian Orogeny. The Kansanshi deposit which is located higher up in the stratigraphy is unique in that, the style and probable timing of mineralisation is different from that of the traditional Zambian Copperbelt deposits (Broughton et al., 2002). It is difficult to correlate it to the copper belt deposits, however additional drilling campaigns in the last couple of years has provided information to better understand this deposit.

Copper ore constitutes the primary beneficiation target, in the form of sulphide, transition and oxide which is the product of supergene weathering of mineralisation close to surface. Mining is currently focussed on two pits, Main and North West pits which are located on dome structures along the northwest trending Kansanshi Antiform.

The Kansanshi plant produces copper as concentrate and cathode at a ratio of 1.5:1. 2012 total copper production was 261,351 tonnes. Gold occurs as a substantial secondary product, amounting to 136,056oz of production in 2012 (FQM website, 2012).

1.2 Location of study area

The Kansanshi deposit is located 10-12 km from Solwezi in the North western province of Zambia and approximately 160 km west of the traditional Copperbelt deposits, refer to figure 1. The Main pit, which is one the deposits located along the Kansanshi Antiform, is the focus of this study, figure 2.

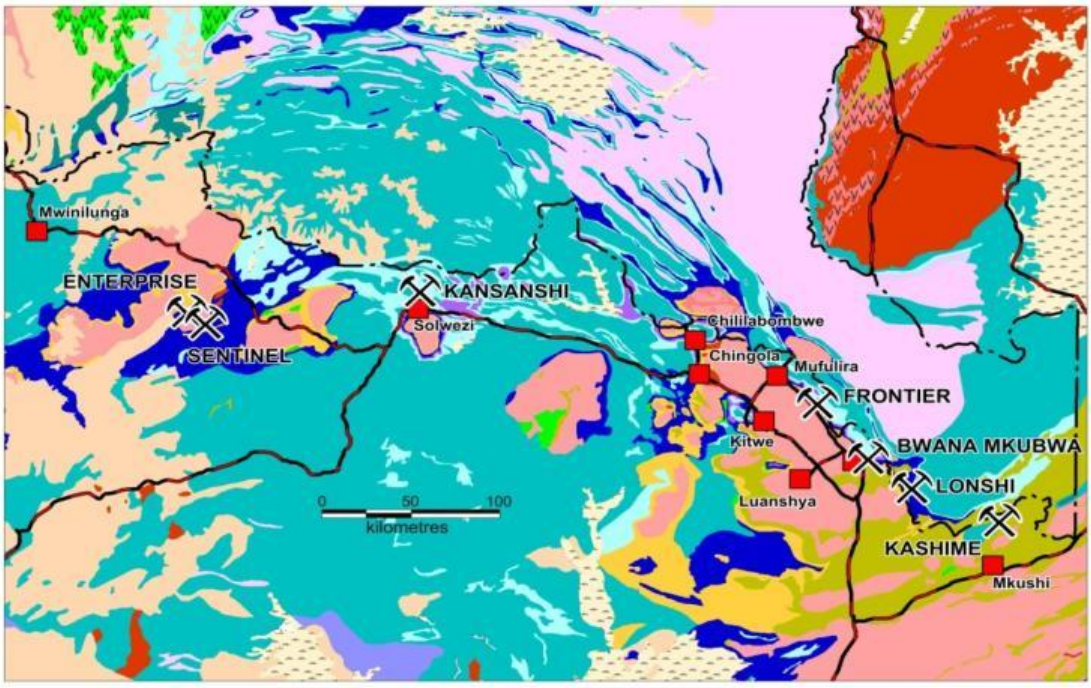

Figure 1. Location map of the Kansanshi Cu-Au deposit. (Kansanshi Resource and Exploration team, 2013)

Figure 2. Image of Kansanshi Mine lease area indicating the study area, Main pit outlined in red. (Google Earth, 2012)

1.3 Mine History

Kansanshi which means ‘important hill’ in the local language (Kaonde) was stacked out by George Grey on 6 September 1899. The deposit represents one of the earliest deposits and has seen intermittent production since 1906. Approximately 16,000t of hand sorted ore averaging 20 to 24% Cu was smelted between 1908 and 1914 producing 2,800t of blister copper (98% Cu) and 1,350oz of Au. This represents the first commercial production of copper in Zambia (Broughton et al., 2002).

The outbreak of World War One saw the closure of the mine, only to resume operation in 1927 after a change in ownership. A resource development campaign was embarked on in the following years only to be abandoned in 1932 owing to the global economic depression. In 1954, Anglo American Corporation bought the deposit and embarked on major underground development and installed a sulphide concentrator on site. Between 1956 and 1957 103,000t of sulphide ore at 3.81% was mined from the underground operations until 1958 when operations were stopped owing to flooding.

1969 saw the birth of the Zambia Consolidated Copper Mines (ZCCM) through nationalisation, which resulted in the acquisition of Kansanshi in the same year. The company embarked on drilling programmes within the Kansanshi deposit, which lead to the start of an open pit operation in 1977. Production was erratic until closure of the pit in January 1998 owing to privatisation of the ZCCM operations.

Cyprus Amax Minerals Company noticed the potential that the deposit had and acquired it in 1997. They established a prefeasibility study which involved drilling, remodelling of the geology and extensive metallurgical test work. This culminated in a resource estimate of 267 Mt at 1.28% Cu and 0.16g/t Au in 2000 (Broughton et al., 2002).

In August 2001, First Quantum Mineral (FQM) acquired an 80% stake in the deposit and formed a company called Kansanshi Mining PLC with ZCCM. The company embarked on a feasibility study thereafter. This resulted in the mine reaching commercial production in April 2005 and is currently the largest copper producer by volume in Africa.

1.4 Historical work

A lot of projects and papers have been written on sediment hosted copper deposits; however the focus has been on the traditional Zambian Copperbelt (ZCB) and Congolese Copperbelt (CCB) deposits. Not a lot of research was done on the deposits in the Domes region. It's only now that work is being undertaken to get a better understanding of the geology and mineralisation style in the latter. Various works has been done on the Kansanshi deposit in the early 2000s in the form of masters and doctorate thesis. Torrealday (2000) described the mineralisation and alteration of the deposit; this was followed by Barron (2003) who gave a description of the stratigraphy, metamorphism and tectonic history of the Solwezi area.

Various papers have been written on the history, geology and vein mineralisation of the Kansanshi deposit and prospects of copper deposits in the Domes region. These include Meheghel (1981), Broughton et al. (2002), Torrealday et al. (2000) and Hitzman et al. (2012).

There are a lot of unpublished reports and internal communication done by consultants and peers, which cover mapping, structural investigations, petrology studies and geophysics surveys.

Not much work has been done to understand the occurrences of gold in the Kansanshi deposit except for a project done by Goodship (2010) and a gold deportment study that was done by SGS on falcon concentrates from the three streams of ore.

1.5 Aims of the study

The main objective of this study is to review and document recent findings on the geology, mineralisation and alteration characteristics of the Kansanshi deposit with reference to the Main pit. The aims of the study are highlighted below;

1. Better understanding on controls of mineralisation (vein and stratiform) – folding/thrusting.
2. Significance of Lower Pebble Schist and Lower Dolomite mineralisation in relation to vein hosted mineralisation higher up the stratigraphic sequence.
3. Review of genetic models for sediment-hosted Cu deposits with relation to the Kansanshi deposit.
4. Relationship of alteration and mineralisation.

The objectives of the study will be achieved through review of additional information that is available through recent regional and resource definition drill core, assay data and recent geophysical surveys.

1.6 Methodology

In order to reach the study purpose, a number of methods are used:

A review and update of the geology, mineralisation and alteration was the focus for this thesis in the light of new findings or information concerning the Kansanshi deposit.

This was achieved through review of historical data and new findings (literature review). Field work was undertaken in the Main pit to identify mineralisation style and alteration trends. This was consolidated by review of logging of 12 boreholes, refer to Table 1 and Appendix 2 and 3 for quick logs and plan indicating location of these boreholes.

Table 1. List of boreholes and characteristics reviewed

Hole ID	From	To	Category	Item
KRDD662	98.6	100.25	Lithology	Gabbro
KRDD660	31	33.6	Lithology	Pebble Schist (UPS)
KRDD625	137.7	142.55	Lithology	Marble (TMM)
KRDD704	76	78.75	Lithology	knotted Schist and Phyllite (UMC)
KRDD704	153.6	156.2	Lithology	Marble (UM)
KRDD704	203.75	207.4	Lithology	Biotite Schist and Phyllite (MMC)
KRDD535	130.45	135.9	Lithology	Calcareous Biotite Schist (LCS)
KRDD609	29.9	34.5	Lithology	Marble and Phyllite (LM)
KRDD609	80.6	85.4	Lithology	Pebble Schist (LPS)
KRDD609	335.35	339.8	Lithology	Dolomite (LD)
KRX029	82	85.5	Lithology	Quartz-Feldspar-Mica Schist
KRDD475	255.85	259.6	Alteration	Carbonate
KRDD475	350.95	353.6	Alteration	Dolomitisation
KRDD533	218.8	219.75	Alteration	K-feldspar and Green Muscovite
KRDD420	186.85	188.5	Alteration	Scapolite
KRDD455	211.7	214.2	Alteration	Scapolite (marble)
KRDD559	113.3	114.5	Alteration	Plagioclase (Albite)
KRDD559	175	176.2	Alteration	De-dolomitisation

Review of historical and recent geophysical and geochemical surveys of areas around the deposit was also done.

Pit visits involved identification of stratigraphic unit within the Main pit. This was followed up with identification of mineralisation and alteration characteristics. This was consolidated by looking at core from the same area.

CHAPTER 2: GEOLOGICAL SETTING

2.1 Introduction

The Kansanshi deposit is geologically located in the Lufilian Arc which is a fold and thrust belt that developed owing to the Pan African Orogeny. Tectonism within the fold belt is related to the collision of the Congo and Kalahari cratons. The Katangan Supergroup metasediments lie unconformably on the granite and schist basement (Broughton et al., 2002). The Lufilian arc is divided into deformational zones which represent different tectono-stratigraphic zones. Metamorphic grade within the fold belt ranges from lower greenschist in the External Fold and Thrust belt to amphibolite in the Domes region (Selley et al., 2005).

2.2 Regional and Local setting

The Kansanshi deposit found in the Solwezi area, Zambia is geologically situated in the centre of the Lufilian Arc (Domes Region), a fold thrust belt that developed during the Neoproterozoic Pan African deformation. The Arc spans approximately 700km from Angola, Democratic Republic of Congo (DRC) into Zambia (Broughton et al., 2002). Cratons of influence on the Lufilian arc are the Congolese Craton, the Bengweulu block associated with the Tanzanian Craton in the northeast of Zambia and the Kalahari Craton in the southeast and southwest of Zambia (Hanson et al., 1990, Porada and Berhorst, 2000). The Lufilian fold belt is separated from the Zambezi belt in the south by the sinistral Mwembeshi Shear Zone (MSZ).

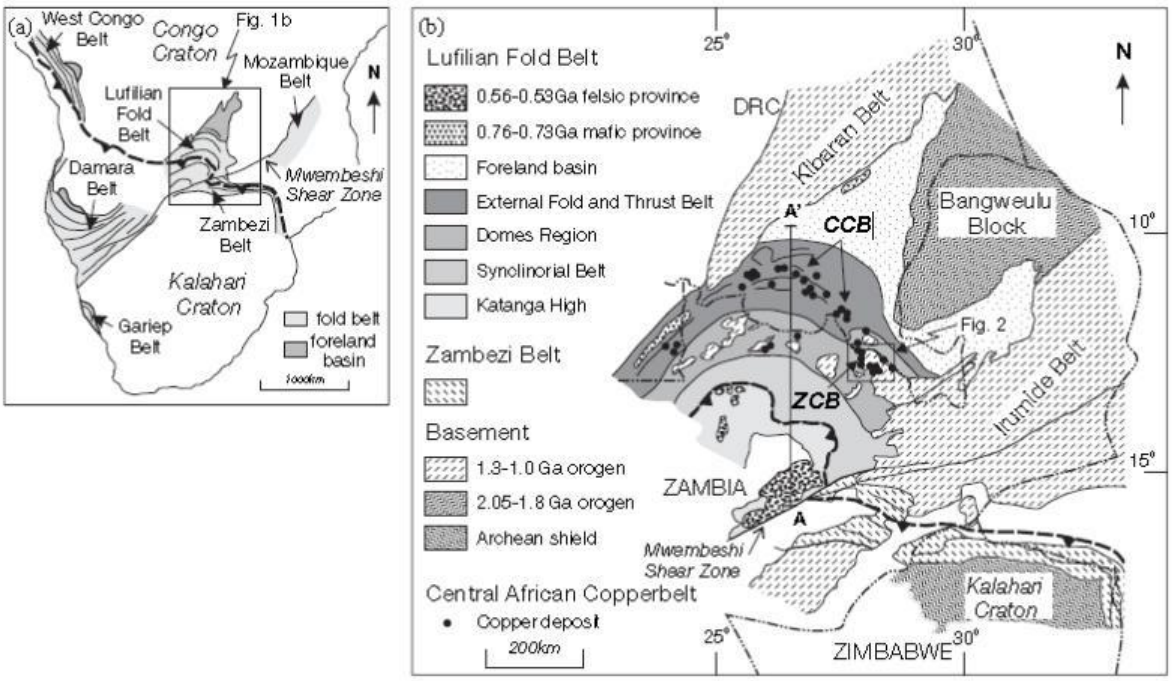

Figure 3. Tectonic setting and Structural domains of the Lufilian Fold Belt (Selley et al., 2005)

The Lufilian Fold Belt consists of metasedimentary rocks of the late Proterozoic Katangan Supergroup which lie unconformably on the basement which consists of Palaeoproterozoic magmatic arc sequences comprising of Lufubu schists and intrusive granitoids whose ages range from 1873-1994 Ma (Master et al., 2005). Rocks of the Katangan Supergroup are believed to be of Kibaran age (maximum age of sedimentation of 880 Ma) which is related to the age of the Nchanga Granite which appears to define a magmatic province accompanying deposition in the Lufilian fold belt (Porada and Berhorst, 2000).

Tecto-genesis in the Lufilian fold belt is related to ca. 560-550 Ma collision of the Kalahari and Congo cratons (Porada and Berhorst, 2000), along a southeast-northwest trending feature linking the Mozambique and the West Congo belt, figure 3. This collision resulted in northeast directed thrusting involving deep crustal detachments and forward propagating thrust faults (Porada and Berhorst, 2000). According to Unrug (1988), the Lufilian fold belt exists as the evolution of two arms of the tripe rift junction.

The Domes Region of the Zambian Copper Belt (ZCB) consists characteristically of poly deformed crystalline basement inliers or domes, figure 4. The Kansanshi deposit is located 12-15 km north of the Solwezi Dome, one of the basement quartzose schists,

gneisses and granites distributed east-west along the central part of the Lufilian arc (Broughton et al., 2002).

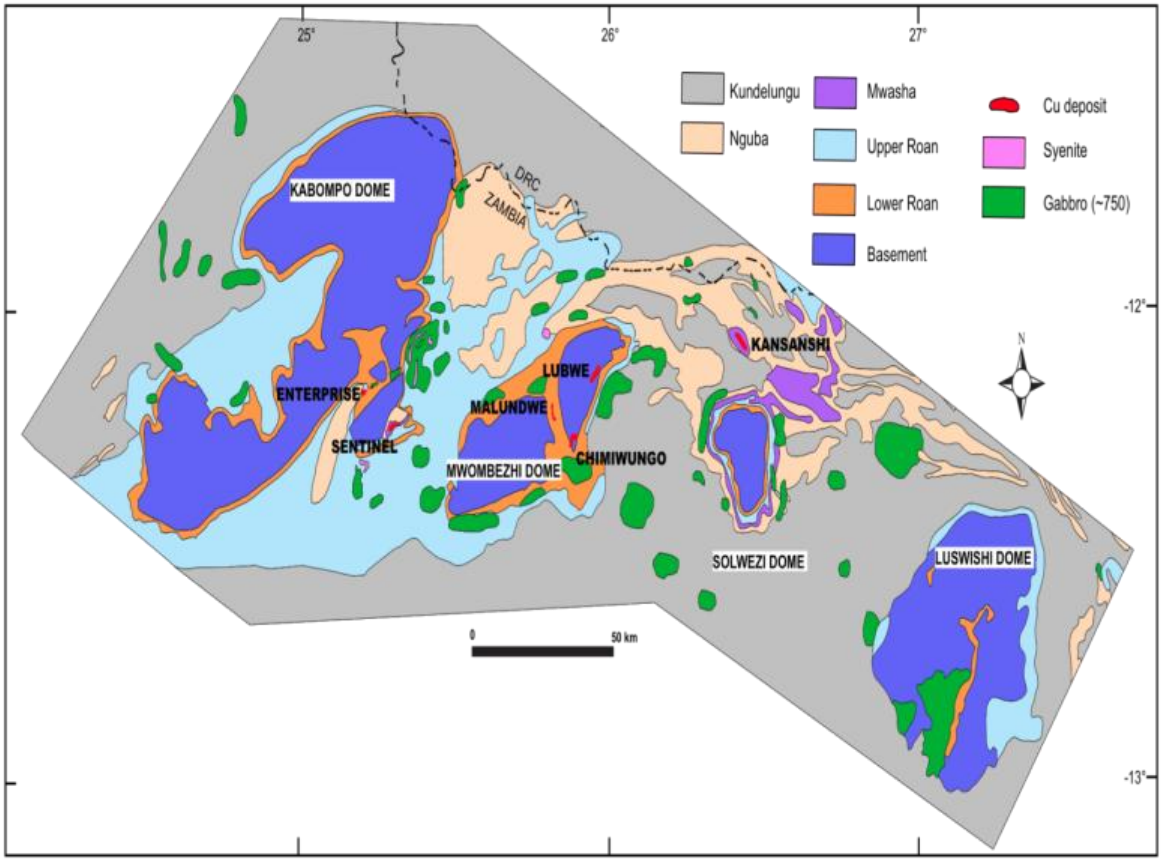

Figure 4. Geological map of the North West Province of Zambia (Domes Region) showing distribution of the domes and associated deposits. (Hitzman et al., 2012)

2.3 Structure, Deformation and Metamorphism

The Lufilian arc forms an arcuate belt with apparent deformational zones or regions (Barron, 2003). These are the Forelands (west and north), the External Fold and Thrust Belt, the Domes Region, the Synclinorial Belt and the Katanga High (Selly et al., 2005). These zones represent new tectono-stratigraphic domains based on more detailed regional mapping and use of airborne geophysics, figure 5. Figure 5a below summarises the local geology and structures of the Solwezi area (Kansanshi deposit).

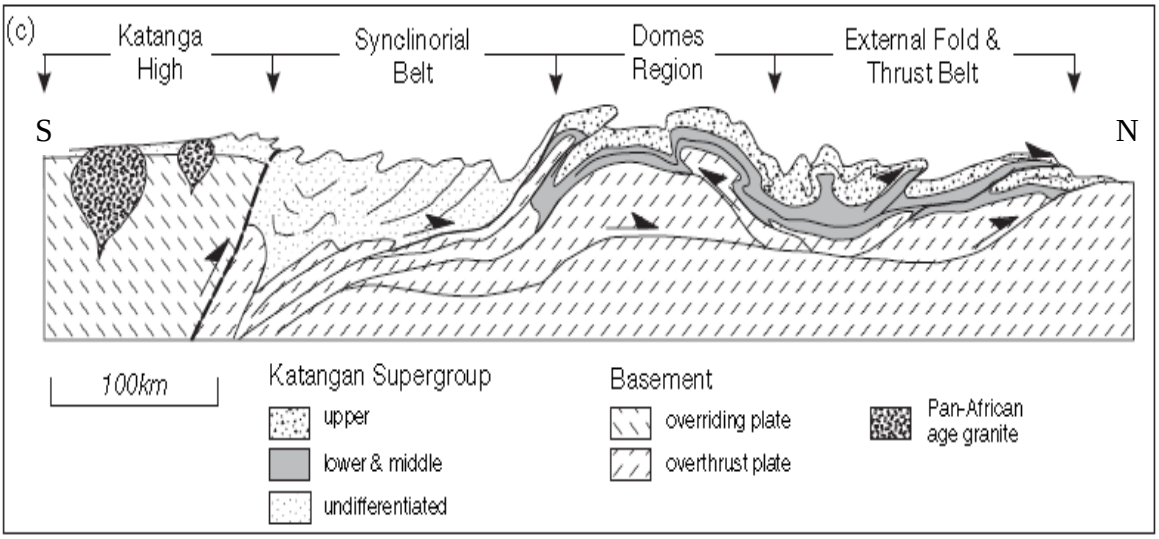

Figure 5. Schematic section of Lufilian fold belt showing tectonic zones, looking west. (Selly et al., 2005)

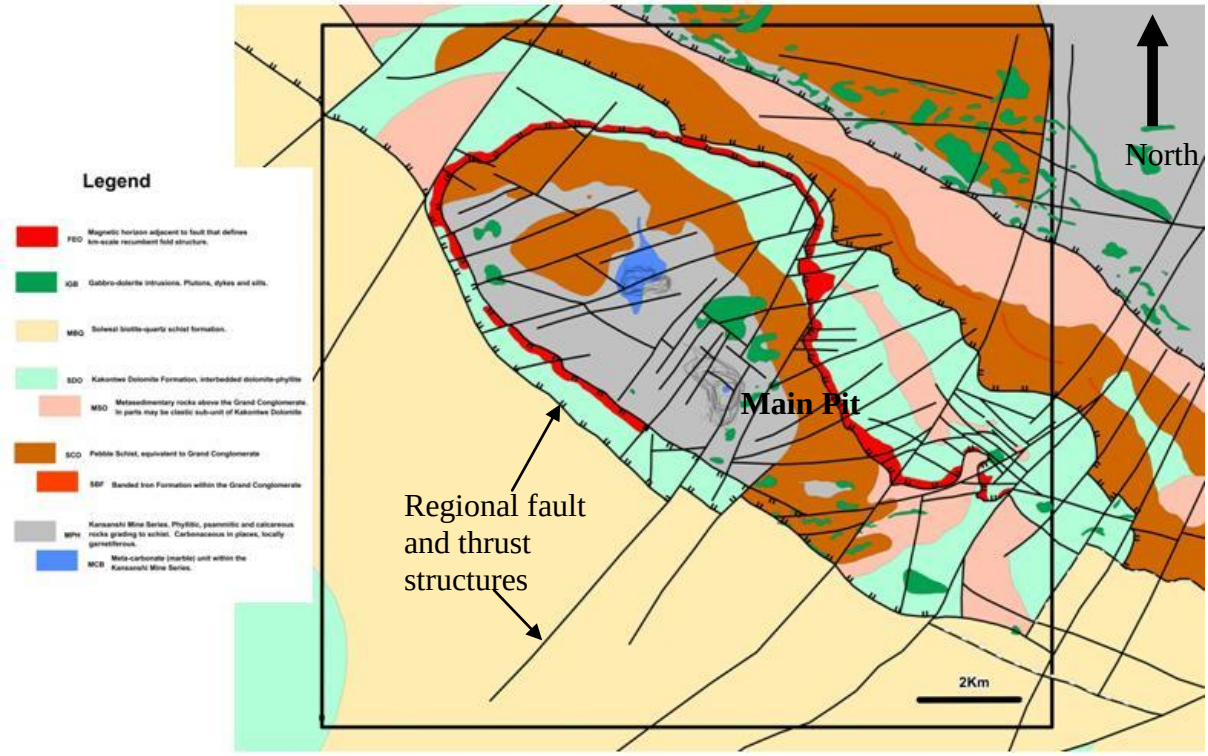

Figure 5a. Geological map of the Solwezi area, illustrating structures (faults and folds) affecting the Kansanshi deposit. (Fourie et al., 2012)

Lufilian deformation is characterised by northward verging rigid 'thin skinned' nappes and thrusts evolving into thick skinned more ductile structures owing to increased thickness and metamorphic grade (Barron, 2003).

Metamorphism varies within the different tectonic zones. Metamorphic grade encountered in the Katangan metasediments is generally lower greenschist and reduces to sub-greenschist facies towards the External Fold and Thrust Belt (Barron, 2003). Metamorphic grade is generally higher at the boundary between the External Fold and Thrust Belt and the Domes Region, upper greenschist to amphibolite facies (Barron, 2003). This area is characterised by growth of garnet and hornblende porphyroblasts. This is a notable feature in the schist found within the Kansanshi deposit.

CHAPTER 3: REGIONAL GEOLOGY

3.1 Introduction

The Central African Copperbelt occurs as an arcuate belt of Late Proterozoic sediment-hosted copper deposits. The deposits are coincident with the Lufilian arc, a major tectonic province characterized by broadly north-directed fold and thrust structures. The stratigraphic classification of the Katangan Supergroup has changed over the years as noted by the recent changes in the names of the Groups and the Subgroups. Based on Wendorff, (2003a) and Master et al. (2005), the Katangan Supergroup is divided into the Roan, Nguba, Kundelungu, Fungurume and Biano Groups. The various zones or regions of the Lufilian fold belt represent different levels of deformation, metamorphism and structures. Intrusive activity is a characteristic feature of the Katangan basin and is represented by gabbroic sills or dykes and stocks intruding the lower section of the Katangan sequence.

3.2 Stratigraphy

The preserved stratigraphic record of the Lufilian fold belt is characterised by a thick succession of metasedimentary and metavolcanic rocks of the Katanga Supergroup of variable thickness of ca. 5-7km (Selly et al., 2005). The rocks were deposited on a major unconformity and overlie a crystalline basement comprising of granites, gneisses and schists of Eburnean age and schists and quartzites of Kibaran age (Porada and Berhost, 2000).

The Katanga sequence was traditionally divided into the Roan, Lower and Upper Kundelungu Supergroup based on classification by Cailteux et al. (1994), refer to figure 6

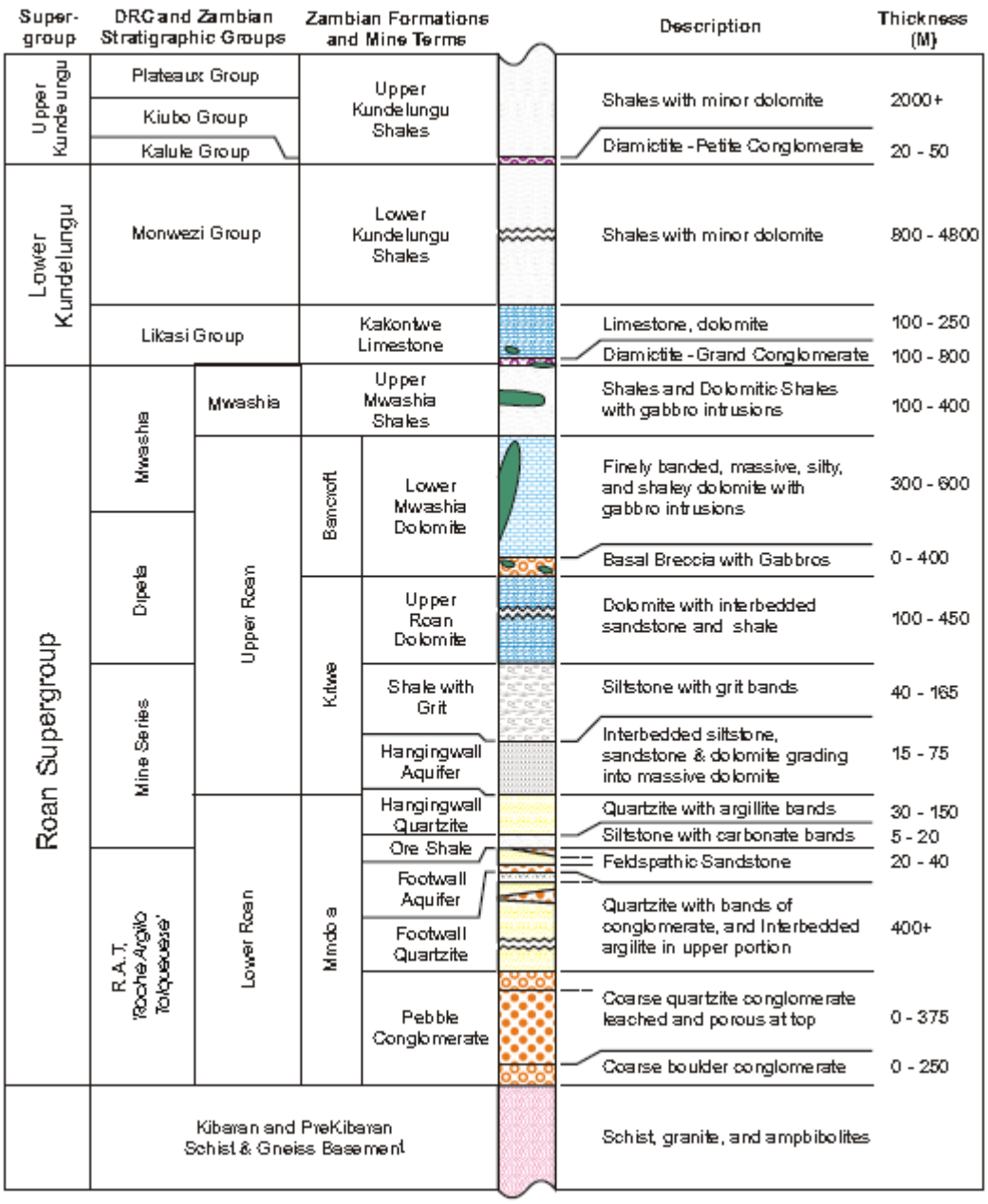

Figure 6. Traditional Stratigraphy of the Katangan Supergroup (Barron, 2003)

The recent classification scheme put forward by Wendorff (2003a) and Master et al. (2005) (similar to Cailteux et al., 2005a and Selly et al., 2005) subdivides the Katangan Supergroup into the Roan, Nguba, Kundelungu, Fungurume and Biano Groups, figure 7. This lithostratigraphic classification will be adopted in this thesis.

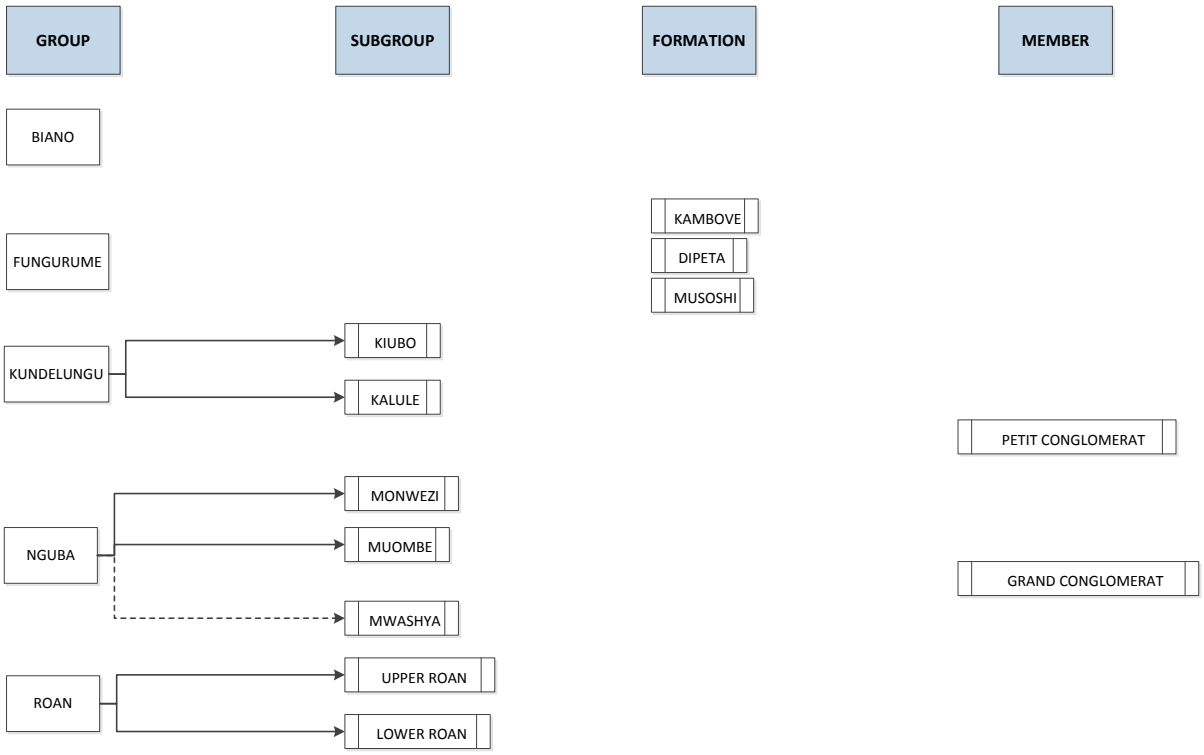

Figure 7. Regional stratigraphy of Katangan Supergroup (modified from Master et al., 2005)

3.2.1 Basement

Rocks constituting the basement in the Copperbelt are the oldest in the region, occurring as part of the Kasai Shield (part of the Archaean Congo Craton). The pre-Katangan basement rocks consist of quartzite, schist, gneiss and granitic intrusions ranging in age from Archaean to Neoproterozoic. The Muva Group consisting of quartzitic and metapelitic metasedimentary rocks, Mesoproterozoic in age was deposited on the basement after 1941 Ma. This age is based on detrital zircons (Rainaud et al., 2005). Rocks of the Muva Group were deformed and intruded by felsic intrusions associated with the Irumide Belt between 1384 and 1102 Ma (Barron, 2003).

Intrusion of the basement by the Neoproterozoic Nchanga Granite at 883± 10Ma (Master et al., 2005) and the Lusaka Granite at 865 +65/-44 Ma marks the final event to affect the pre-Katangan basement. This culminated in the unconformable deposition of the Katangan Supergroup on the Nchanga Granite within the Zambian Copperbelt (Barron, 2003).

3.2.2 Katanga Supergroup of the Zambian (ZCB) and Congo Copper belts (CCB)

The Neoproterozoic Katanga Supergroup overlies the basement with a marked angular unconformity and spans a depositional time interval of 1000 to 500 Ma. Deposition of the Katanga sediments is believed to have commenced between 880-870 Ma, based on the age of the basal Kafue Rhyolite (Porada and Berhorst, 2000). Different sedimentation ages for the Katangan Supergroup have been placed at between 877±11 Ma, the age of basement granite and 750 Ma the age of overlying diamictite and volcanic rocks (Barra et al., 2004).

Katangan sediments were deposited in an intracontinental rift basin which experienced three phase of basin evolution. The first two phases involved uplift followed by rapid fault controlled subsidence (rifting) and clastic sedimentation (Unrug, 1998). Both phases were associated with bimodal magmatism which resulted from two thermal events. Phase three consisted of localised uplift and creation of an unconformity surface in the basin followed by moderate subsidence (Unrug, 1998).

The Roan Group (formerly Roan Supergroup), the lower most unit in the Katangan succession represents the first phase of basin evolution (uplift and rifting resulting in deposition of coarse conglomerates at the base). This group is divided into the siliciclastic Lower Roan and the dolomitic Upper Roan Subgroups which consists of conglomerates, quartzites, arkoses, shales, siltstones (redbeds) and dolomitic shales and anhydrite bearing dolostones respectively (Master et al., 2005). Above the basal arkoses/redbeds lies a cyclic sequence of predominantly reduced, fine grained siliciclastic rocks (argillite, siltstone, arkosic sandstone, dolomitic argillite and sandstone). The occurrence of scattered anhydrite beds and the abundance of metamorphic scapolite indicate the former presence of evaporates (Torrealday, 2000). This portion of the Roan Group hosts the stratiform copper deposits of the Zambian Copper belt and is termed the Ore Shale. Breccias of angular to rounded fragments of dolostones and argillites are a common occurrence within the dolomitic unit of the Upper Roan Subgroup and are spatially associated with gabbro sills. These breccias have been interpreted as zones of tectonic transport (Binda and Porada, 1995), however Hitzman, (1999) and Torrealday, (2000) suggest that these could be collapse zones due to evaporate dissolution.

Dating of microcline bearing metamorphic veins within the Ore Shale unit from Luanshya Mine, Zambia and Musoshi Mine in DRC using Rb-Sr technique suggest a minimum age

for the Roan Group of 870±42 Ma (Master et al., 2005). Rainaud et al. (2005), suggests that the Lufubu Metamorphic Complex and the Bengweulu Block magmatic arc terrane are the sources of the Roan Group sediments. This is based on dating of detrital zircons.

The Nguba Group incorporates the Mwashya and Lower Kundelungu Groups, based on the classification of Wendorff, (2003) and Cailteux, (2003) (Master et al., 2005), but occurs as a subgroup of the Roan Group according to the classification in Hitzman et al.(2012). The Mwashya Subgroup is now considered as the lowermost unit of the Nguba Group as opposed to previous classifications where it was classified as the topmost unit of the Roan Group. This is because it rests on an erosional unconformity on the Upper Roan Subgroup and is conformable with the overlying Grand Conglomerat Member (Master et al., 2005). The Mwashya consists of carbonates and black shale which range in thickness from 50 to 700 metres and are associated with stratiform iron formation which makes it a regional marker unit/horizon (Master et al., 2005). Dating of gabbroic bodies within the Solwezi area gives dates of 745±7.8 Ma and 753±8.6 Ma which is believed to be associated with mafic magmatism of the Mwashya subgroup (Master et al., 2005). This unit is overlain by the Grand Conglomerat, a glacial tillite which shows a sequence of debris flow and diamictites containing interbeds of laminated siltstone and coarse lithic sandstone (Selly et al., 2005). This unit is related to the Sturtian diamictites deposited ca. 740 Ma. This unit is overlain by a thick metamorphosed sequence consisting of dolomitic shale, dolostone and limestone (Kansanshi Mine Series). The Nguba Group is believed to represent a phase of rapid subsidence in the basin which resulted in the deposition of ca. 5000m of pelitic sediments. This can be correlated to the rocks within the Kansanshi deposit (Torrealday, 2000).

The Petit Conglomerat Member, a second diamictite horizon marks the base of the Kundelungu Group, formerly known as the Upper Kundelungu. This horizon is glacial in origin based on the widespread presence of faceted and striated clasts whose origin is intra- and extrabasinal (Master et al., 2005). Overlying the Petit Conglomerat is a molasse sequence comprised of dolomitic shales, pink limestones, sandy shales and sandstones.

The Fungurume Group, a newly defined horizon in the Katangan Supergroup is a syntectonic basin fills that rest unconformably on the Nguba Group. This horizon consists of continental red beds of the Mutoshi Formation, marine mixed clastic and carbonates of the Dipeta Formation and olistostromes of the Kambove Formation (Master et al., 2005).

The Fungurume Group is overlain by the Biano Group also known as the Plateaux Subgroup (Cailteux, 2003). This horizon consists of post orogenic pink to red siltstones and sandstones deposited in an oxidising environment. These red siltstones in the CCB can be correlated to the uppermost redbeds within the Luapula Beds of north western Zambia (Master et al., 2005).

Existing literature for the northern Zambia suggest that the Katangan Supergroup forms a coherent sedimentary sequence, however aeromagnetic data indicate the area consists of complicated thrust sheets. These have recently been reinterpreted as structurally repeated units.

3.2.3 Regional Lithostratigraphic correlation of the Katangan Supergroup

It has always been recognised since the early regional mineral exploration days, that the major stratigraphical units of the Katangan sequence in Zambia and the DRC could be correlated. With this in mind the Stratigraphic terms Kundelungu, Mwashya(Mwashia – DRC) and Grand Conglomerat have been assumed to have correlative unit in both Zambia and the DRC (Grey, 1930, Cailteux *et al*., 1994). Recent attempts to make regional correlation have made use of facies analysis, sequence stratigraphy and metamorphic equivalents to the sedimentary protoliths (Cailteux *et al*., 1995; Porada and Berhorst, 2000). The only regionally extensive time-stratigraphic horizon is the Grand Conglomerat which has been correlated with the Sturtian Rapitan glacial epoch. However even with the use of this Stratigraphic timeline, regional stratigraphic correlation remain difficult, especially between rock packages within the different deformation regions of the Lufilian fold belt, figure 7a.

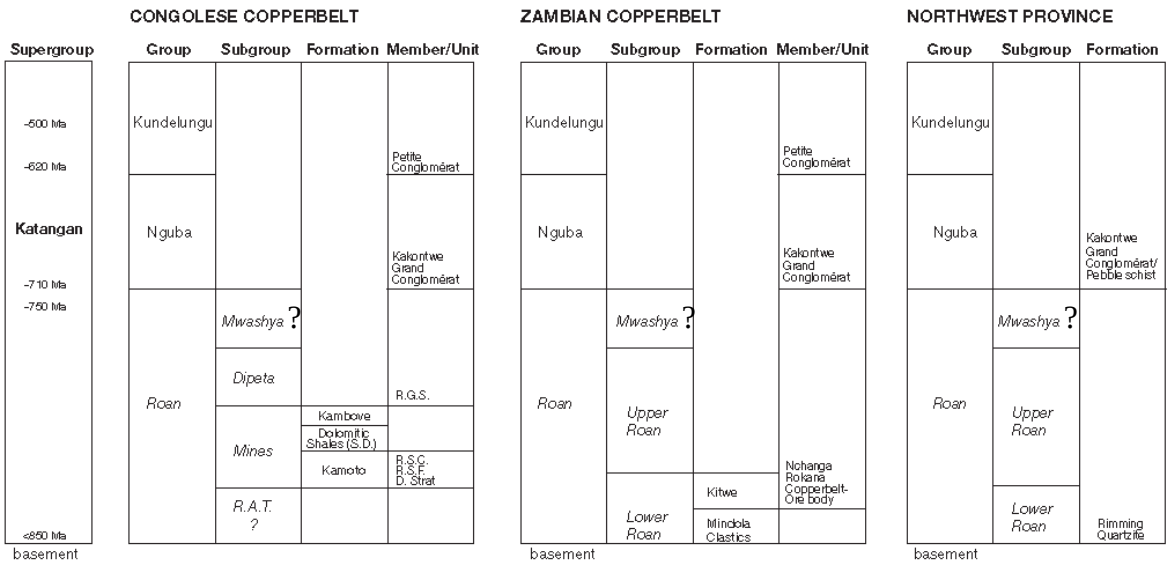

Figure 7a. Regional Lithostratigraphic sequence of the Congolese and Zambian Copperbelts (modified from Hitzman et al., 2012)

3.3 Tectonics and Structures

The Lufilian fold belt consists of five deformational/tectonic regions as highlighted in Chapter 2 i.e. the Forelands (west and north), the External Fold and Thrust Belt, the Domes Region, the Synclinorial Belt and the Katanga High, figure 8. The initial two regions are mainly exposed in the DRC whereas the Domes Region, the Synclinorial Belt and the Katanga High are explicitly exposed in Zambia.

From north to south, the Forelands (west and north) consist of Katangan sediments deposited on the Kasai shield and the undeformed section of the Kundelungu basin (the Kundelungu Aulacogen). This zone is relatively undeformed and weakly metamorphosed. The contact with the next zone is marked by thrust faults.

The External fold and thrust belt consists of a thin skinned geometry with complex macro scale fragmentation and thrusts responsible for repetition of the Katangan sequence. This tectonic zone lacks basement which is considered to indicate widespread decoupling along evaporitic strata at depth i.e. lower strata was thrust emplaced at the top of the tectonic pile (Kampunzu and Cailteux, 1999; Porada and Berhorst, 2000; Jackson et al., 2003).

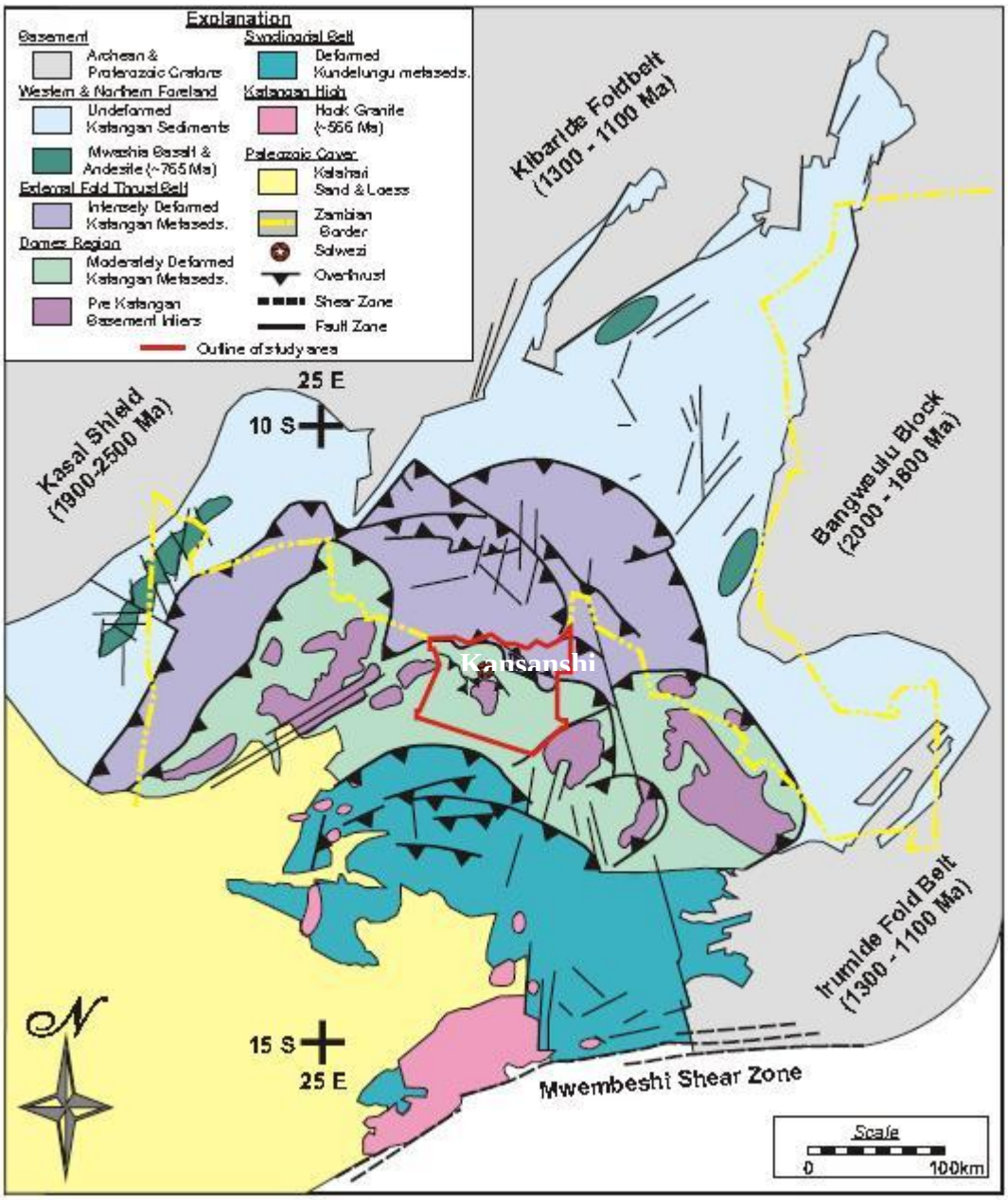

Figure 8. Regional structures of the Lufilian fold belt with the study area highlighted in red. (Barron, 2003)

The Domes Region of the Lufilian fold belt (study area) predominantly consists of polydeformed crystalline basement inliers (domes). The Katangan sequence in this zone is folded and variably metamorphosed. Axial traces of the metasedimentary rock folds are deflected around the domes (Barron, 2003).

Moving south, the contact between the Domes and Synclinorial Belt is not clear but is believed to exist as concealed thrust faults. According to Unrug (1988), this belt is described as moderately deformed, greenschist facies Katangan rocks. The Synclinorial

Belt could represent another thin skinned fold and thrust belt near the core of the Lufilian arc (Porada and Berhorst, 2000).

The Katangan High, which occurs to the extreme southern end of the fold belt is characterised by the Hook Granite complex (Barron, 2003). This is a syntectonic multiphase intrusive batholith that emplaced into the Nguba and Kundelungu (formerly Lower and Upper Kundelungu Groups) sediments during the early stages of the Lufilian deformation.

3.3.1 Orogenic events in the Lufilian Fold Belt

Three compressive orogenic events have been identified in the Lufilian fold belt for a period of over 300 Ma based on geochronology and regional correlations (Cahen et al., 1984). These events include the Lomanian Orogeny at ca. 950 Ma, the Lusakan folding at ca. 840 Ma and the Lufilian Orogeny between >656 and 503 Ma (Porada and Berhorst, 2000).

The Lomanian Orogeny was originally described from the north-western portion of the Kibaran arc where it affects rocks of the post-Kibaran Mbuji-Mayi Supergroup. This orogenic event produced southwest-northeast striking faults during a first deformational phase at 976±10 Ma (Porada and Berhorst, 2000). A subsequent phase resulted in thrusting and south-southwest-north-northeast trending folds. The Lomanian Orogeny was extended to the Lufilian fold belt by correlating the Mbuji-Mayi Supergroup with the Roan Group of the Katangan sequence. The event was also related to the main deformation and metamorphism in central Zambia and early recumbent folding and thrusting in the Domes region of the Lufilian fold belt (Porada and Berhorst, 2000). However recent age determinations on zircons of the Nchanga Granite yielded an age of 877±11 Ma (SHRIMP U-Pb) which shows that the onset of the Katangan deposition post-dates the Lomanian Orogeny and therefore not related to the evolution of the Lufilian fold belt.

The Lusakan folding event, dated at 865+65/-48 Ma from discordant zircons from the Lusaka Granite has been correlated to the Nchanga Granite. Based on recent age determination, these two granites, together with a few other intrusive bodies and rhyolites, emplaced in the age range of 880-845 Ma define a magmatic province preceding or accompanying the onset of deposition in the Lufilian fold belt (Porada and Berhorst, 2000). This new data therefore shows that the Lusaka granite predates Katangan

deposition and thus not syntectonic to the Lusakan folding event of ca. 840 Ma and therefore had minor or no effect on the evolution of the Lufilian fold belt.

The Lufilian Orogeny which manifested in a major NE directed thrusting and subsequent folding involving basement and the Katangan sequence accounted for the most of the deformation in the Lufilian fold belt. Cahen et al. (1984) divided the Lufilian Orogeny in the External Fold-Thrust Belt of the Katanga Province in the DRC into three phases;

- the Kolwezian phase (D_1), which involved north-directed thrusting and folding with associated south vergent back thrusting and back folding,
- the Kundelungu phase (D_2), with southward folding in the autochthonous Katangan sequence. D_2 structures deformed D_1 fabrics creating complex interference folds,
- the Monwezian phase (D_3), with strike slip faulting on east-west trends. During this event new metamorphic minerals grew and deformation fabrics were produced. (Key et al., 2001).

Cahen et al. (1984) attempted to correlate the above phases (in the Lufilian Arc in Zambia) to F_2 fold structures post-dating recumbent F_1 folding, shearing and thrusting that is a result of the Lusakan folding and/or Lomanian Orogeny. However both structures would have to be included in the Lufilian Orogeny as the latter two orogenic events did not affect the Lufilian fold belt (Porada and Berhorst, 2000). Barron, (2003) correlated the three phases of deformation to the western Lufilian arc in the NW of Zambia.

3.4 Metamorphism

The early phase D_1 event of folding and thrusting was associated with metamorphism that reached amphibolite facies grade in some parts of the Lufilian fold belt. The degree of metamorphism increases from greenschist in the Forelands region up to amphibolite facies in the External Fold and Thrust Belt and the Domes Region (Tembo et al., 2000). This facies of metamorphism was characterised by the porphyroblastic growth of garnet and hornblende (Barron, 2003). The geothermal gradient established for this regional metamorphism is 30-45°C/km.

3.5 Magmatism (Intrusive activity)

There is evidence of gabbroic sills or dykes and stocks intruding the lower section of the Katangan sequence below the Nguba Group including the basement gneiss and schist complex throughout the Zambian and Congolese Copperbelts (Barron, 2003), refer to figure 9. Gabbros are commonly hosted in the Mwashya Subgroup at or immediately above the contact with the Upper Roan Subgroup (Porada and Berhorst, 2000), however within the Main pit, these bodies can be located higher up the sequence within the clastics (UMC). Gabbros are found as individual bodies within bedding concordant and discordant breccia zones. They generally form stocks, sills and lenticular or podiform bodies, generally less than 100m thick and difficult to correlate between widely spaced drill holes.

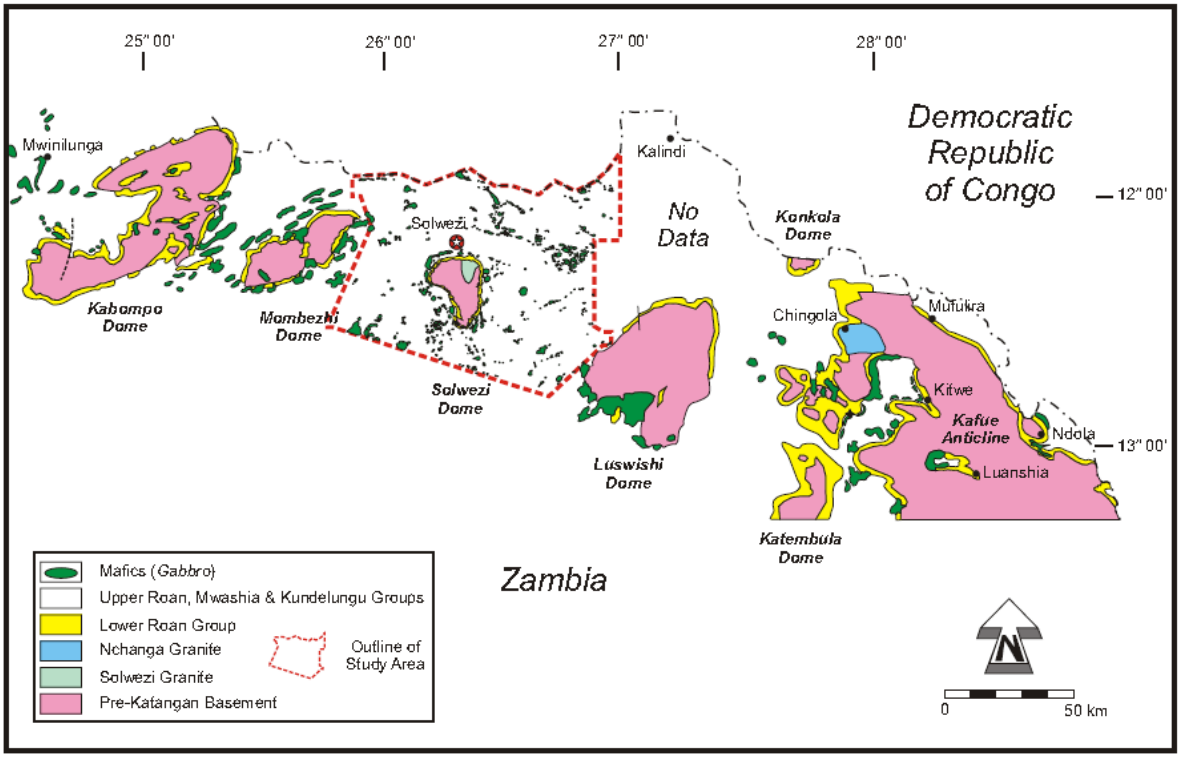

Figure 9. Distribution of gabbros in the Domes Region of the NW of Zambia. (Barron, 2003).

CHAPTER 4: MINE GEOLOGY

4.1 Introduction

The Kansanshi Cu-Au deposit, located ca. 15km north of the Solwezi Dome (North western Zambia), one of the many inliers of basement quartzose schists, gneisses and granites which trend east-west along the inner Lufilian fold belt (Broughton et al., 2002). Rocks exposed in the southern limb of an east-west trending and west plunging syncline, referred to as the Solwezi Syncline can be correlated to the Mines Series of the Zambian Copper Belt (ZCB). A basal series of metamorphosed siliciclastic rocks are host to disseminated Cu and U mineralisation (Lumwana deposit); can be correlated to the Lower Roan Subgroup (Arthurs, 1974; Broughton et al., 2002). Overlying calcareous schists and marbles are correlated to the Upper Roan and Mwashya Subgroups (Arthurs, 1974). The Chafugoma Marble Formation and the schists of the Solwezi Biotite Quartzite Formation (SBQF) overlie the Mines Series in the core of the Solwezi syncline, Table 2 and figure 10.

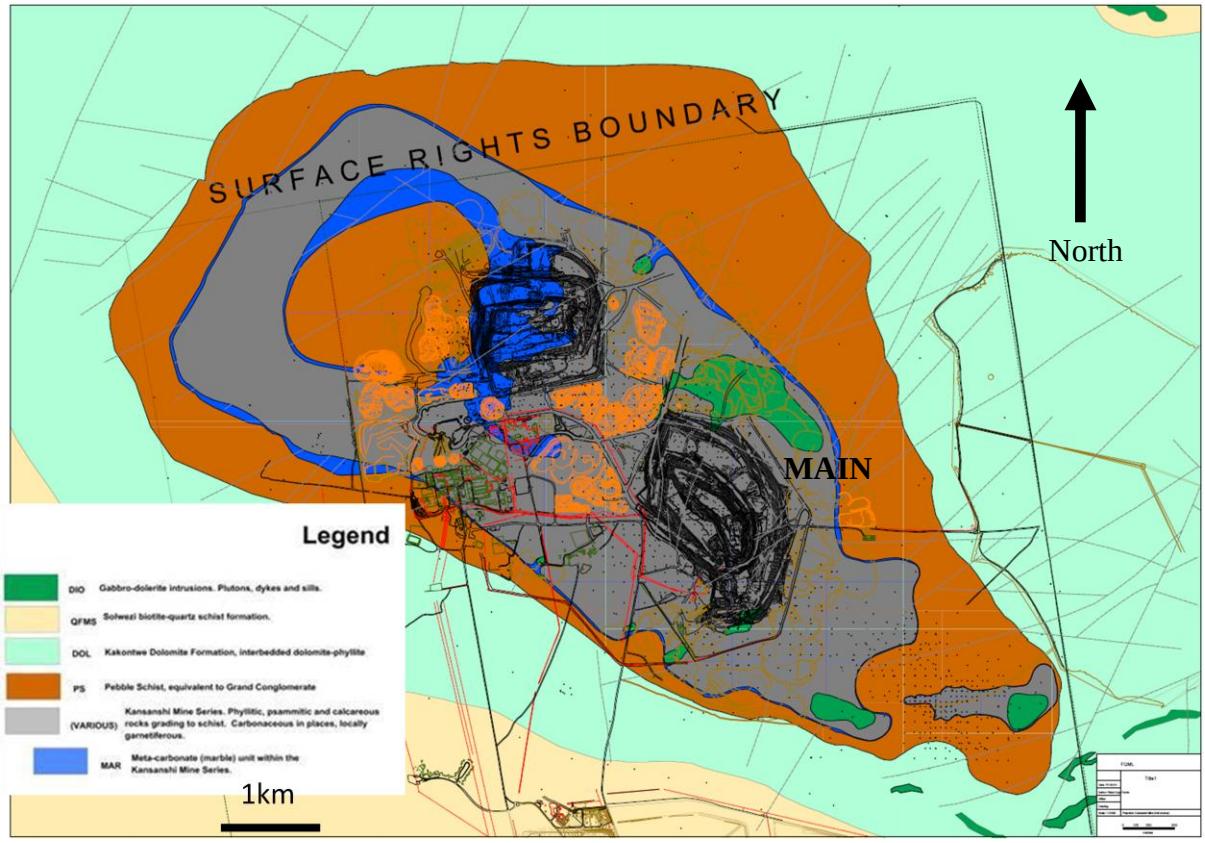

Figure 10. Regional Geology map of the Kansanshi Mine area also showing the Main Pit. (Fourie et al., 2012)

Table 2. KATANGAN STRATIGRAPHIC COLUMN FOR COPPERBELT – SOLWEZI AREA (adapted from Cyprus Amax Prefeasibility report, 2000)

SYSTEM	SERIES	COPPERBELT GROUP/ FORMATION		SOLWEZI FORMATION (Cyprus Amax report)	SOLWEZI FORMATION (after Arthurs, 1974)	SOLWEZI LITHOLOGY
KATANGA SUPERGROUP	LOWER KUNDELUNGU	Lower Kundelungu Shale Fm	UNCERTAIN CORRELATION	Solwezi Biotite-Quartz Fm	Solwezi Biotite-Quartz Fm	(calc) biotite-hornblende-quartz-musc-schists, phyllite
		Kakontwe Limestone		Upper Dolomite Fm	Chafugoma Marble Fm	Dolomite, minor phyllite
				Upper Pebble Schist Fm	Pelitic Fm	Calcareous pebble schist, knotted schist, bio-musc schist; scapolite
				Kansanshi Mine Fm	Pelitic Fm	Marble, calc biotite schist, locally carbonaceous phyllite, knotted schist; scapolite
		Grand Conglomerate/ Tillite Fm		Lower Pebble Schist Fm	Paraconglomerate Fm	Calcareous pebble schist, knotted schist, bio-musc schist; scapolite
	(COPPER BELT) MINE SERIES	Mwashia Group (argillaceous)		Mwashia?	Chafugoma Marble Fm Lower Unit ("Tectonic melange")	Marbles, calc-biotite schists, scapolite Calc-bio schists, marble, (local ironstone), scapolite
		Upper Roan Group (dolomitic)		Upper Roan?	Upper Roan?	Dolomite-muscovite schists
		Lower Roan Group (arenaceous)		Lower Roan?	Lower Roan?	Quartzite, quartz-mica schists

The northwest trending Kansanshi Antiform which flanks the Solwezi syncline to the north and hosts the Kansanshi deposit, consists of tillites and metasedimentary rocks which according to Broughton et al. (2002), correspond to the Nguba Group.

The Kansanshi Antiform is defined to a limited extent by the outcrop and radiometric signature of the Upper Dolomite, and a thin magnetic unit at its base. The average trend of the antiform is about 310^{o}. On the flanks of the antiform the rocks dip away to the NE and SW, generally at 10^{o} to 30^{o}. Southeast of the Kansanshi area the surface expression of the Upper Dolomite is disrupted by faulting and overlap by the Solwezi Biotite Quartz Formation, and hence the nature of the fold is unclear (Cyprus Amax, 2000).

4.2 Stratigraphy

The stratigraphy of the Kansanshi Mine area/lease has to a greater extent being derived from regional drilling due to the poor outcrop exposures in the area. The rock sequence of the Kansanshi deposit and the surrounding area was previously divided into four major units, which from top to bottom are termed the Upper Dolomite Formation, the Upper Pebble Schist Formation, the Kansanshi Mine Formation, and the Lower Pebble Schist Formation. Owing to more drilling and geophysical surveys in the area, the Kansanshi Mine sequence is better understood and consists of the following units; Quartz-Feldspar-

Mica-Schist Formation (QFMS), Upper Dolomite Formation, the Upper Pebble Schist Formation, **the Kansanshi Mine Formation**, Lower Pebble Schist Formation, Lower Dolomite Formation and Micaceous Calcareous Schist (MCS), figure 11.

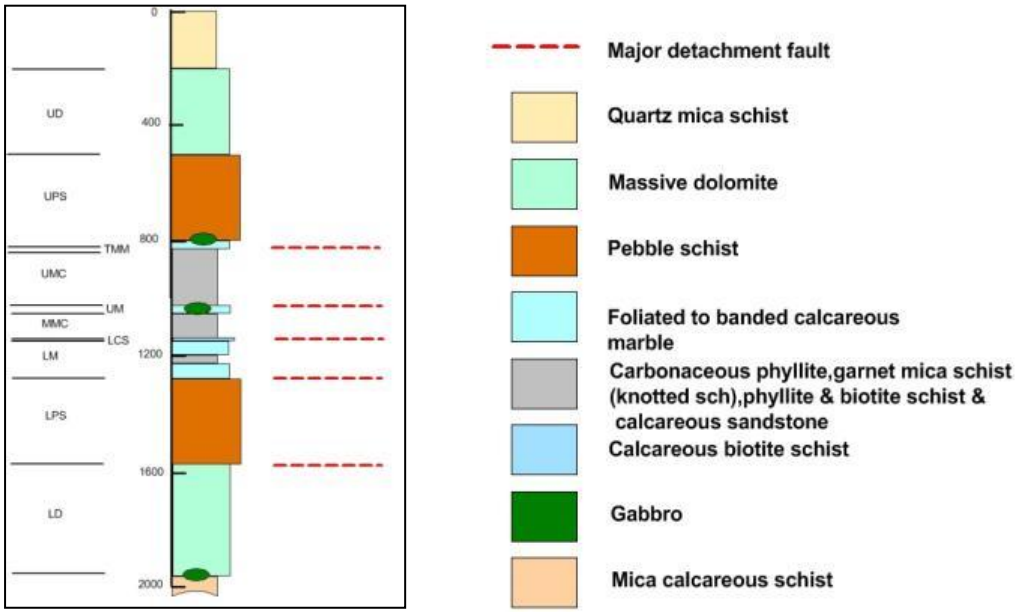

Figure 11. Generalised Tectono-stratigraphy of Kansanshi Mine (Kansanshi Resource and Exploration team, 2013)

Individual lithological units with the Kansanshi deposit (Mine pit) are readily correlated into a local metamorphic stratigraphy; however regional stratigraphic correlations are not clear owing to overprinting by metamorphism and structural complexities (Broughton et al., 2002). Gradational contacts are a common feature of the deposit and are characteristically overprinted by hydrothermal alteration. The Kansanshi Mine Formation collectively consists of a sequence of phyllites, knotted schists, calcareous schists and marbles represented by the following lithological units; Upper Mixed Clastics (UMC), Upper Marble (UM), Middle Mixed Clastics (MMC), Lower Calcareous Sequence and Lower marble, figure 12.

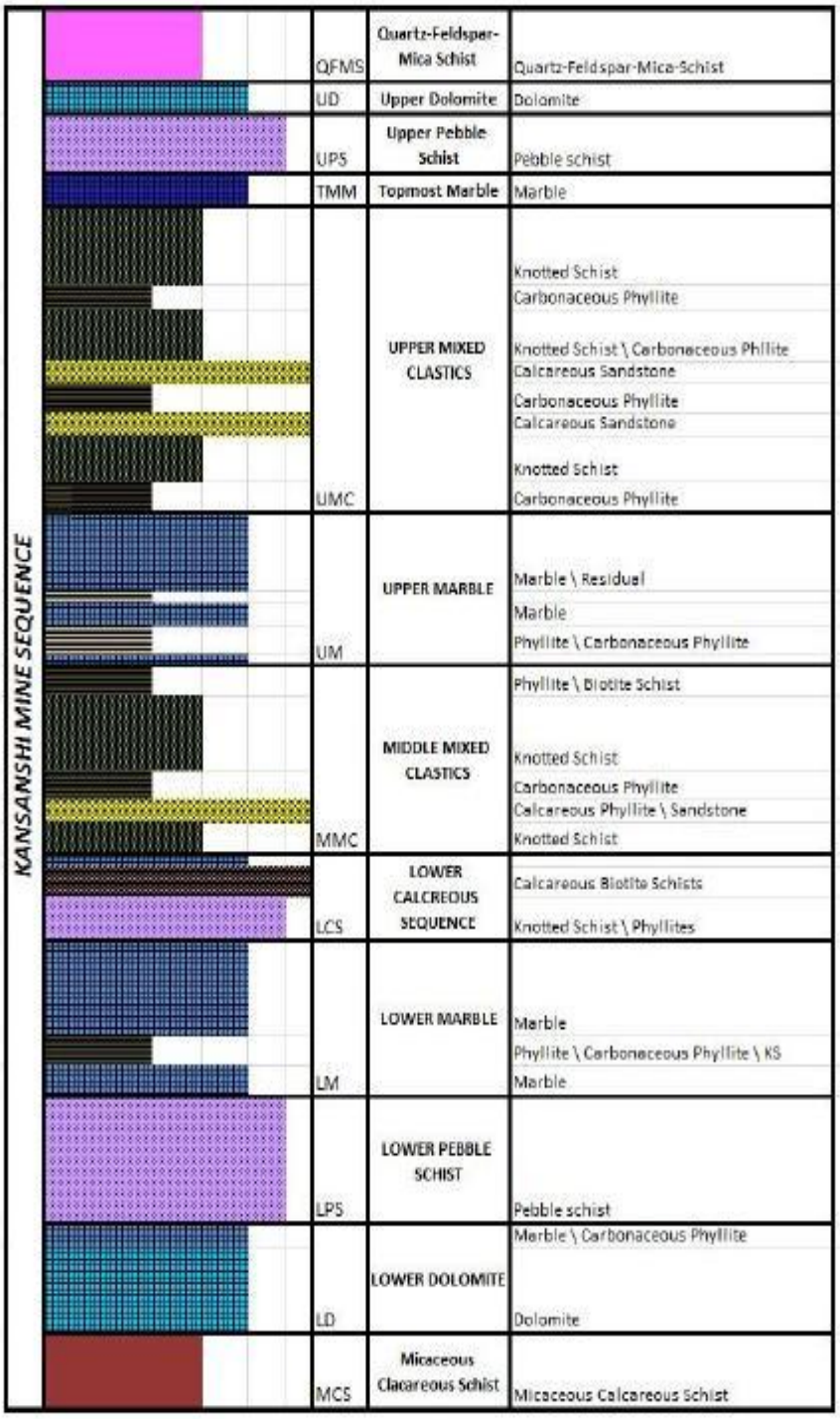

Figure 12. Detailed stratigraphy of the Kansanshi Mine (modified from Cyprus Amax, 2000)

4.2.1 Quartz-Feldspar-Mica Schist (QFMS)

The Quartz-Feldspar-Mica Schist unit caps the Kansanshi stratigraphy and occurs more on a regional scale as opposed to a mine scale. Not much of it is found in the confines of the main pit. The unit consists of fine-grained rocks which contain an abundance of quartz, biotite and muscovite aligned in a weak metamorphic foliation and porphyroblasts

of scapolite which tend to occur in the plane of foliation. Carbonates in the form of dolomite also occur in significant amounts as small anhedral grains, figure 13.

Figure 13. Core of Quartz-Feldspar-Mica Schist. (KRX029, 83.5m)

QFMS is believed to have formed as fine-grained silty sediments composed of clastic grains, detrital clays, carbonates and saline chemical sedimentary components (Mason, 2013). The foliated porphyroblastic metamorphic assemblage of quartz+carbonate+muscovite+biotite+scapolite+kyanite+zoisite can be attributed to recrystallisation as a result of regional metamorphism. The presence of kyanite in QFMS is a clear indication that load pressure during metamorphism was high in relation to temperature (Mason, 2013).

4.2.2 Upper Dolomite (UD)

The QFMS unit is underlain by a sequence of dolomite and dolomitic marble referred to as the Upper Dolomite. The unit consists of a sequence of pale brown-grey to medium grey, fined grained saccharoidal iron-poor dolomite. The unit tends to form low ground and swampy ground (Cyprus Amax, 2000). The footwall contact of the UD is characterised by a 10-15m thick unit which consists of a massive and pyrrhotite bearing coarse grained sediment, figure 14.

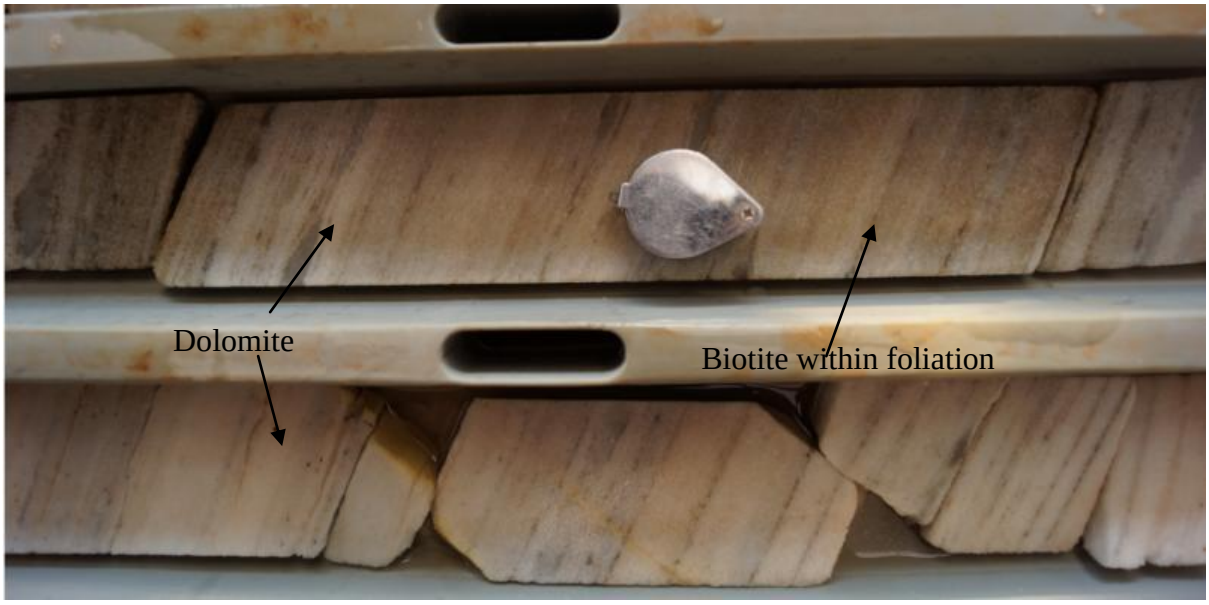

Figure 14. Dolomite with intercalations of biotite. (KRDD609, 335.35m)

4.2.3 Upper Pebble Schist (UPS)

The UPS unit is a sequence of non-layered, biotite bearing, commonly calcareous and locally garnet bearing (knotted) schists which contain ca. five percent exotic clasts, figure 15. The clast types include dolomite, metasiltstone, massive quartz, quartzite and rarely granite (Broughton et al., 2002). The unit is characterised by a low sulphide content (<1% Po) and low vein abundance. The unit is 'folded or thrust' on the north western portion of the deposit giving rise to a unit loosely termed 'Middle Pebble Schist (MPS)'. The footwall contact of the UPS is characterised by extensive development of mm to cm sized dark grey to black, poikiloblastic, frequently subhedral to euhedral porphyroblasts of scapolite.

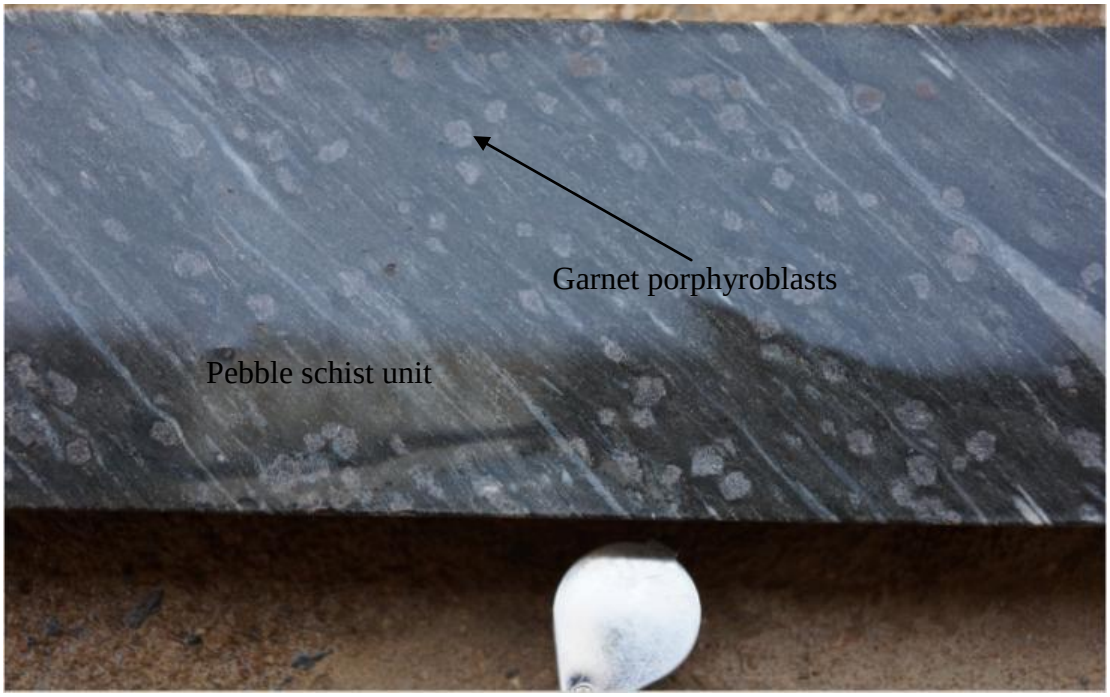

Figure 15. Pebble Schist (UPS) showing porphyroblasts of garnet. (KRDD 660, 31-33.60m)

Carbonate alteration and thin marble units is a common feature at the contact. Similarity between the UPS and knotted schist matrix could be interpreted as a transitional contact that has subsequently undergone deformation and dislocation, suggesting either an unconformity or a faulted contact (Cyprus Amax, 2000).

4.2.4 Top Most Marble (TMM)

The TMM is a relatively thin unit of ca. 5m and underlies the UPS. The unit typically consists of marble with calcite and dolomite alteration. The TMM tends to be sparsely mineralised with sulphide disseminations (Cpy, Py and Po) as a result of the alteration, figure 16.

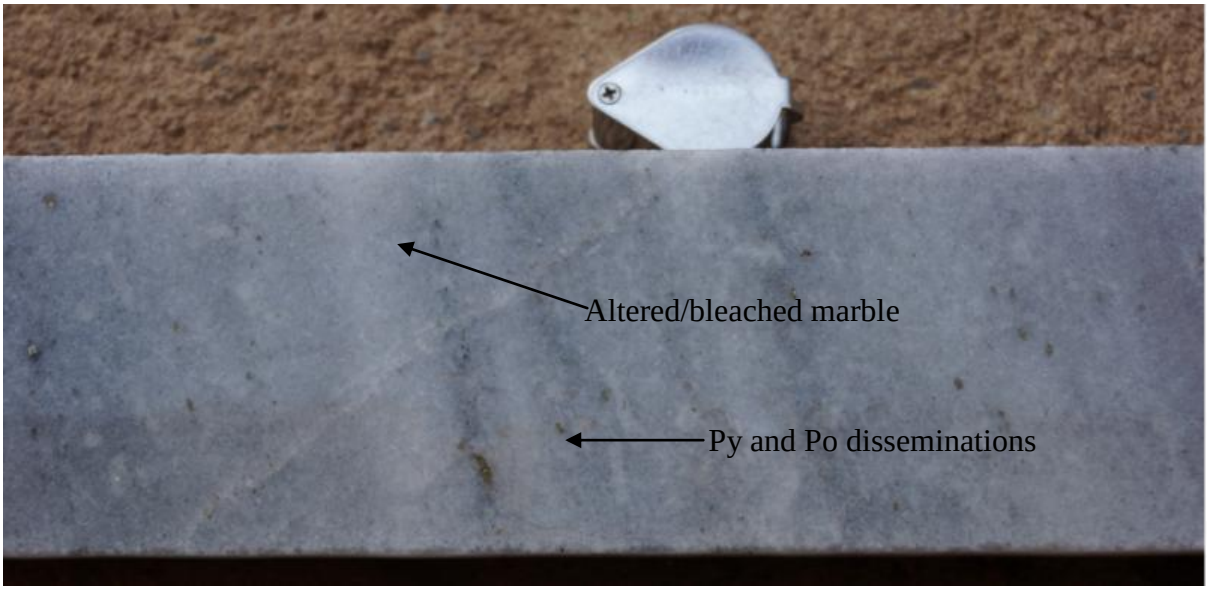

Figure 16. Photograph of Top Most Marble (altered/bleached) which is dominantly calcareous with disseminations of pyrite and pyrrhotite. (KRDD625, 137.7-142.55m)

4.2.5 Kansanshi Mine Formation (KMF)

This unit consists of five members, refer to figure 11. The members are further divided into closely related units that can be readily correlated throughout the deposit. The critical and economically significant units within the Formation are phyllites, knotted schists, biotite schist and marbles (Broughton et al., 2002).

4.2.5.1 Upper Mixed Clastics (UMC)

The UMC forms the upper unit of the KMF and consists of a sequence of phyllites, shales, knotted schists and calcareous horizons. The unit ranges in thickness to about 250m. The unit displays a slightly undulating, flat lying metamorphic foliation (Torrealday, 2000). The UMC is further subdivided into 12 units, some of which are repeated.

UMC1 consists of thin intercalated units of locally carbonaceous phyllite, calcareous phyllite and marble. This unit is characteristically brecciated and has secondary enrichment of Cu.

UMC2 is a garnetiferous mica schist (Knotted schist), figure 17 which ranges in thickness from 10 to 30m. The garnets are usually retrograded. This unit is usually barren.

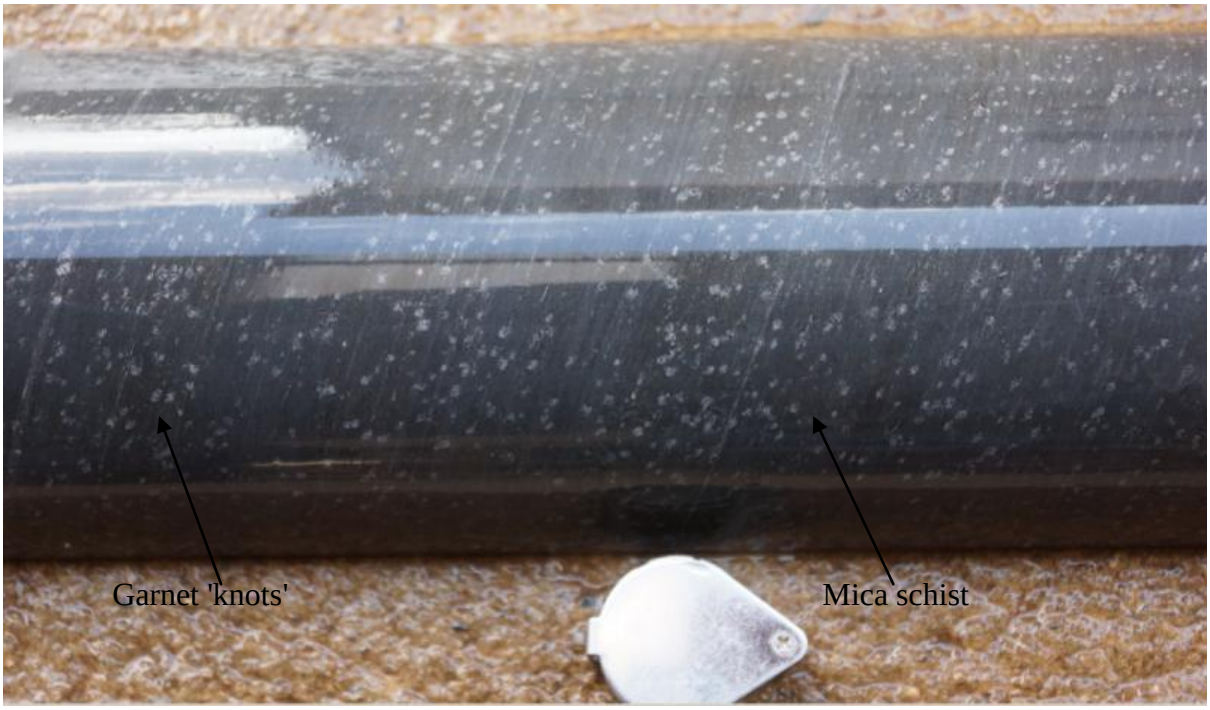

Figure 17. Photography of garnetiferous mica schist (Knotted Schist) of the UMC unit (KRDD704, 76-78.75m)

UMC3 is a black to grey carbonaceous phyllite (CBPH) which characteristically consists of 3-8% Po in unaltered and unmineralised zones, figure 18. A thin band of knotted schist indicates the transition to UMC4.

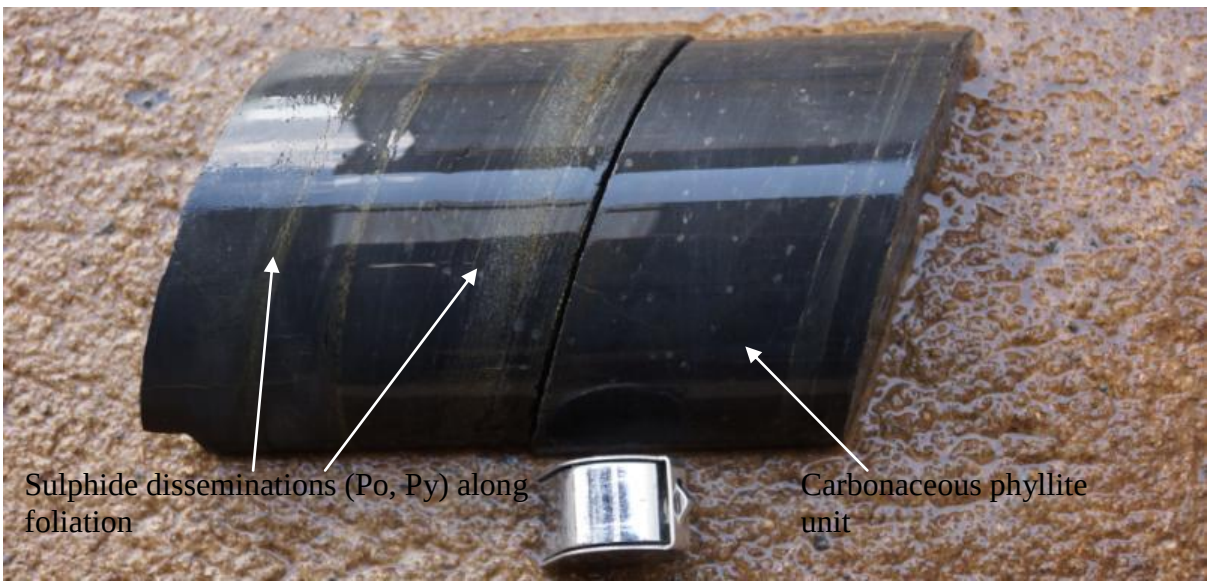

Figure 18. Photograph of carbonaceous phyllite (CBPH) of the UMC which characteristically consists of Po within the foliation. (KRDD704, 76-78.75m)

UMC4 is a mixed unit that consists of calcareous phyllite, biotite schists, calcareous and dolomitic sandstone and usually carries noticeable amounts of albite alteration.

UMC5 to UMC12 are repeated units of knotted schist and carbonaceous phyllite. The contact between the UMC and the underlying Upper Marble is the phyllite at the top of the marble unit.

4.2.5.2 Upper Marble (UM)

The Upper Mable unit comprises of a thick (10-80m) marble layer with minor remnant bedding, underlain by a transitional sequence of intercalated marble and phyllite. The UM is further subdivided into a marble dominated unit (UM1) and a lower phyllite dominated UM2. The UM1 horizon usually weathers to a brownish, often micaceous 'residual unit' within which relict mineralogical banding is preserved (Cyprus Amax, 2000). The UM2 characteristically consists of carbonaceous to calcareous phyllite with an underlying thin marble unit, figure 19.

Figure 19. Photograph of the marble unit of the UM horizon. (KRDD704, 153.6-156.2m)

4.2.5.3 Middle Mixed Clastics (MMC)

The MMC horizon consists of 30-80m thick sequence of knotted schists, biotite schists and phyllites, figure 20. The rocks of the MMC display similar metamorphic fabric to those of the UMC (Torrealday, 2000). The MMC is subdivided into five units detailed below.

The MMC 1 unit consists of carbonaceous phyllite/phyllite and biotite schist. The phyllite units in the MMC consists of 20-30% muscovite, 30-40% quartz, <15% biotite, <3% plagioclase and ca. 10% carbonaceous material (Torrealday, 2000). Where unaltered, the carbonaceous phyllite/phyllite contains 3-8% pyrrhotite as the back ground sulphide.

Figure 20. Photograph of biotite schist (BS) and knotted schist (KS) of the MMC unit. (KRDD704, 203.75-207.4)

The MMC2 unit consists of knotted schists defined by garnet porphyroblasts (usually retrograded to calcite and biotite). The unit is composed of 30% biotite, 20-30% garnet porphyroblasts, 20% quartz, 7-10% scapolite, <10% muscovite, <7% plagioclase and minor carbonaceous material (Torrealday, 2000).

The MMC3 unit consists of carbonaceous phyllite with minor biotite and knotted schist and calcareous schists, with narrow bands of calcareous sandstone in the middle.

The MMC4 unit consists of 5-10m thick layer of carbonaceous phyllite with a central thin band of knotted schist.

MMC5, the basal unit, consists of a sequence of dark biotitic and knotted schists which tend to become calcareous near the contact.

4.2.5.4 Lower Calcareous Sequence (LCS)

The LCS comprises of thick sequence of calcareous schists, calcareous biotite schists, marbles, knotted schists and phyllite which are divided into two units, a strongly calcareous portion, termed LCS1 and a lowermost weakly calcareous LCS2. The LCS is characteristically referred to the ‘Zebra rock’ due to the well developed compositional banding seen in the schist (alternating biotite and carbonate layers), figure 21.

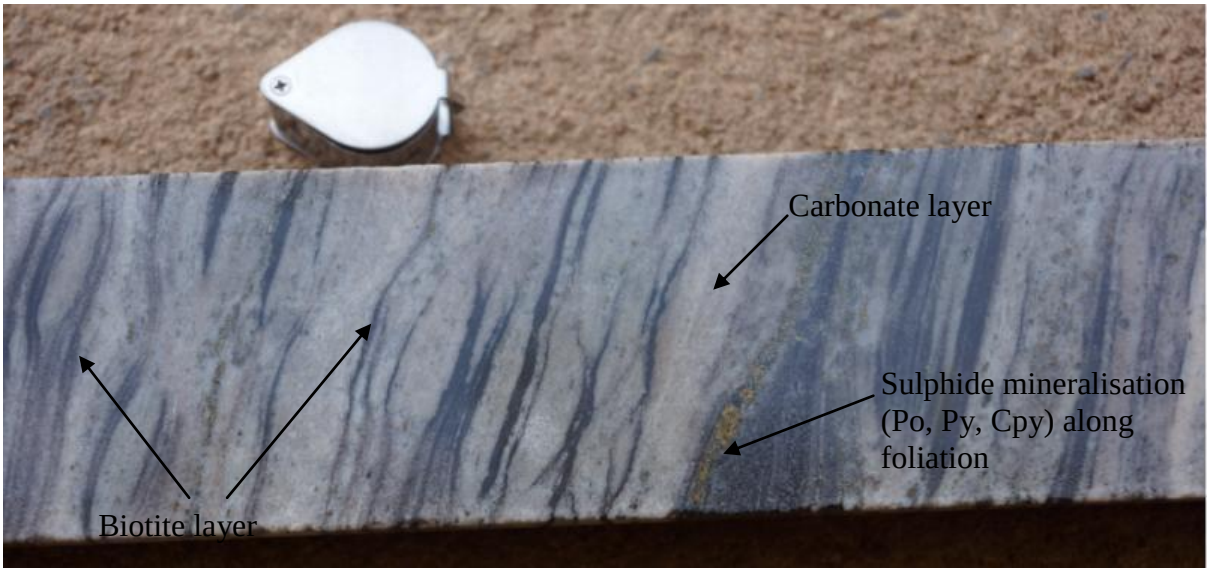

Figure 21. Photograph of calcareous biotite schist (CLBS) of the LCS unit showing compositional banding (Zebra rock) and sulphide disseminations. (KRDD535, 130.45-135.90m)

4.2.5.5 Lower Marble (LM)

The LM unit varies in thickness from 20-100m thick and is compositionally different from the UM in that it usually contains seams of dark brown crenulated biotite (Torrealday, 2000). The unit is subdivided into three units, the LM1 (uppermost and thick) which consists of marble with locally developed thin phyllite layers, the LM2 which consists of a discontinuous 10-20m thick carbonaceous phyllite/phyllite and is characterised by transposed bedding and narrow foliation bands (high strain), (Cyprus Amax, 2000), figure 22.

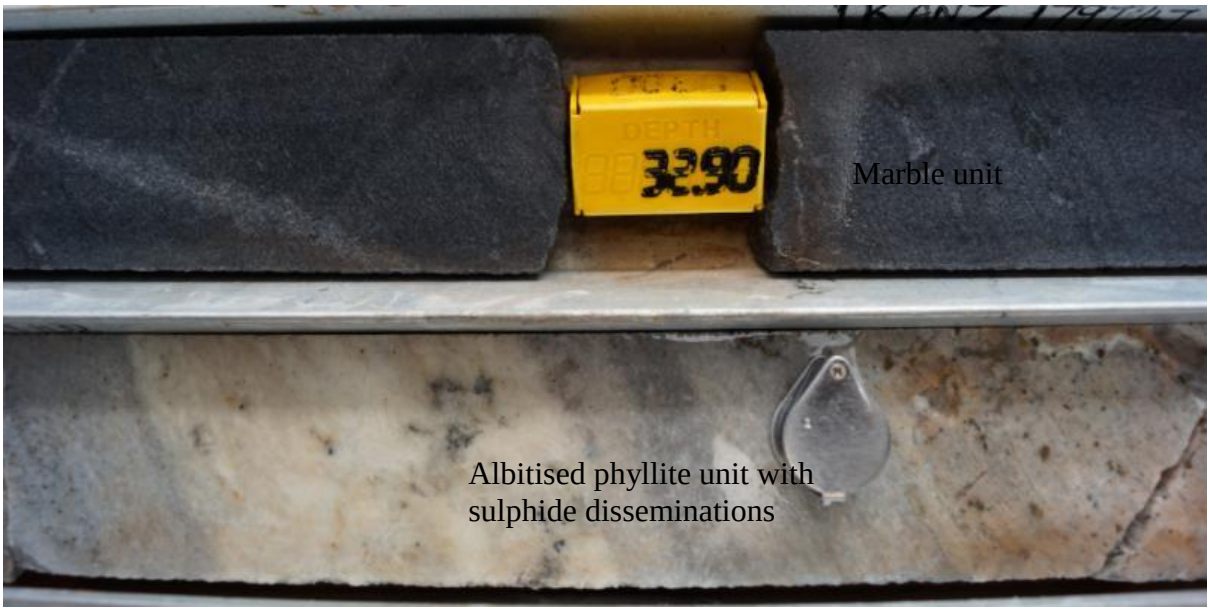

Figure 22. Photograph of marble and altered (albitised) phyllite of the LM unit. (KRDD609, 29.90-34.50m)

The LM2 unit generally consists of pyrrhotite, pyrite and replacive chalcopyrite in the Main pit. This unit is generally absent west of the 4800 zone in the Main pit. LM3 defines the marble unit underlying the LM2 phyllite. The lower contact of the LM and the Lower Pebble Schist (LPS) is strongly foliated with porphyroblasts of garnet, scapolite and carbonate material, this being parallel on either side of the contact (Cyprus Amax, 2000). Torrealday (2000) suggests that the contact maybe structural.

4.2.6 Lower Pebble Schist (LPS)

Underlying the LM is a unit referred to as the LPS that consists of calcareous biotite schist, biotite-garnet schist, scapolite-dolomite-biotite±chlorite schist and paraconglomerates or exotic clasts, which account for ca. 5% of the rock (Torrealday, 2000, Hitzman, 2013). This forms the primary marker unit in the area and is equivalent to the Grand Conglomerat on a regional stratigraphic scale, figure 23.

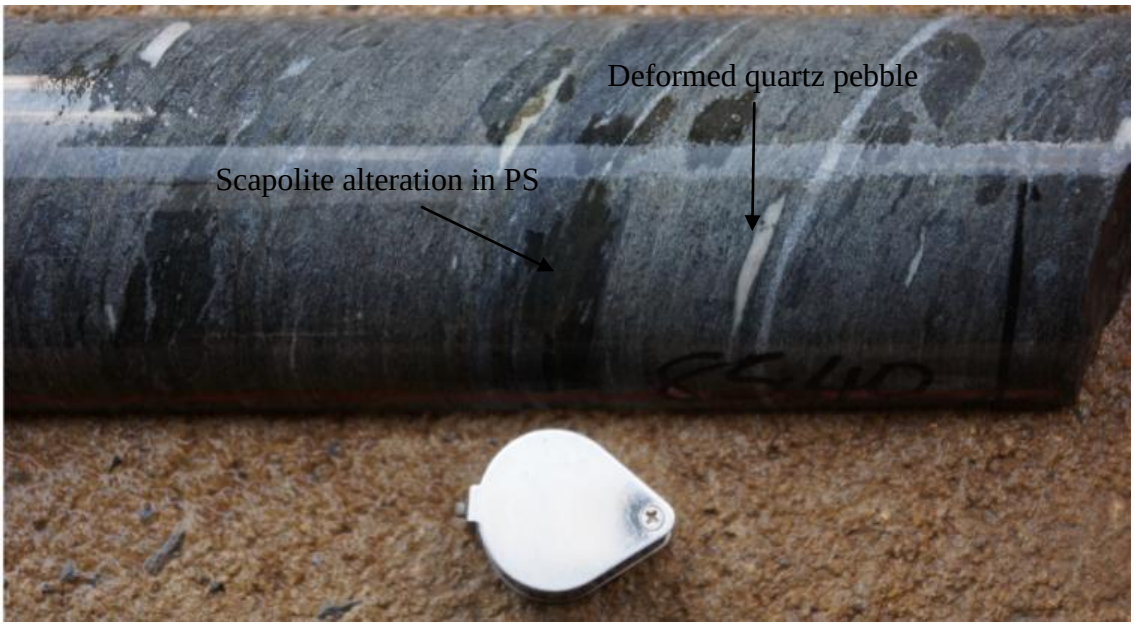

Figure 23. Photograph of PS unit of the LPS showing porphyroblasts of scapolite and ‘elongated quartz pebbles’ (KRDD609, 80.6-85.4m)

The contact with the LM varies from sharp to gradational, and is typically an area of intense concentration of albite-ferroan dolomite alteration. The exotic clasts typically consist of granitic material, intermediate intrusive rocks, quartzite, limestone and dolostone in a matrix of calcareous phyllite. As seen in core, the LPS unit is dominated by

diamictites which are poorly developed compared to other areas of the ZCB. Also evident in core logged, is a clear sequence of 'iron formation' consisting of iron carbonate with disseminated or thin magnetite bands near the base of the unit, figure 24.

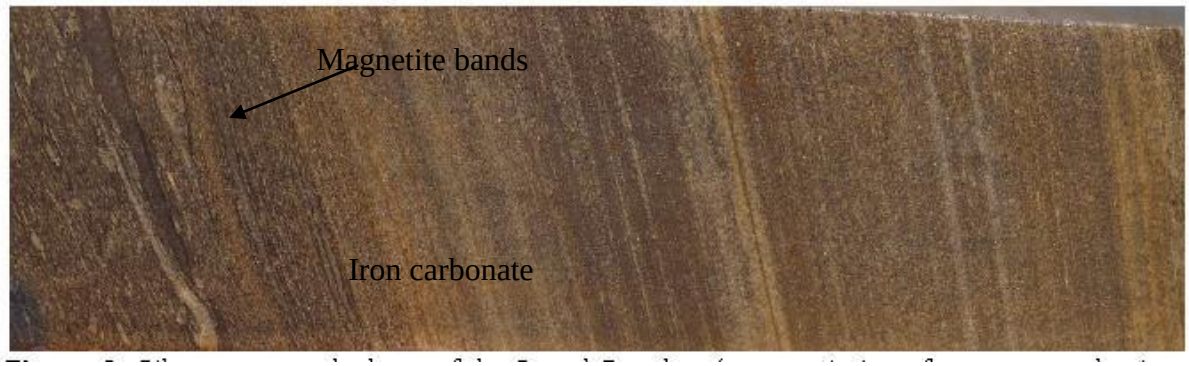

Figure 24. Siltstone unit in the LPS showing the presence of 'iron formation' and black magnetite, KRX 055 (820m)

The LPS varies in thickness from 100 to 400m in some areas. The thickening is attributed to structural complexities due either to fold repetition or stacking along low angle structures, or both (Hitzman, 2013). There are minor differences between the pebble schists of the UPS and LPS however; on the whole their similarities would allow them to be interpreted as the same unit.

4.2.7 Lower Dolomite (LD)

The LPS unit is underlain by the Lower Dolomite unit which consists of thick carbonate which transgress downward into grey marble sequence with minor biotite schists (garnet bearing at times) and dark grey phyllite, figure 25. These rocks are part of the shallow marine Mwashya subgroup sequence. Within the Kansanshi area, the carbonate rocks of the LD may contain disseminated scapolite or phyllite and schists (Hitzman, 2013).

Figure 25. Photograph of the carbonate unit of the LD with intercalations of biotite. (KRDD609, 335.35-339.8m)

4.2.8 Micaceous Calcareous Schist (MCS)

Underlying the LD is the MCS, which is part of the Upper Roan subgroup. The unit consists of dolomite-magnesite-biotite schists which tend to be rich in anhydrite, figure 26. These tend to be cyclical repeating beds of thick massive white granular textured dolomite-magnesite with biotite-dolomite beds and minor phyllite bands (Hitzman, 2013).

Figure 26. Dolomite-magnesite-biotite schists of the MCS. (KRX066, 930m)

4.3 Structures

The Kansanshi vein hosted deposit developed within a tectonised rock sequence and as such, structures play a critical role in paragenesis of the ore. Lithological layering within the phyllites and knotted schist is referred to as bedding (S_o). This is characteristically gentle dipping to sub-horizontal. Mapping of structures in the pit and core observations has defined four deformation events within the deposit area and is related to large scale structures.

The earliest deformation event, D_1 is characterised by S_1 mineral foliation, F_1 folds and L_1 mineral lineations. The S_1 foliation forms a distinct flat lying to gentle dipping metamorphic fabric that's parallel to S_o lithological contacts whereas the F_1 folds are recumbent and tight to isoclinal. (Broughton et al., 2002). These folds normally trend west-northwest to east-southeast. The L_1 mineral lineation which is defined by the preferred orientation of biotite or the intersection of S_o and S_1 foliation occurs parallel to the F_1 fold axis. Mineralised undeformed veins or vein swarms are usually orientated at a high angle to the F_1 fold axis (Broughton et al., 2002). In summary, the D_1 structures define a prolate strain ellipsoid with a subhorizontal plane of flattening, a WNW axis of maximum extension, and a NNE axis of maximum shortening.

The D_2 deformation event is characterised by F_2 crenulation folds (folded S_o and S_1). These F_2 folds are normally upright to inclined to recumbent, asymmetric and dip to the east. F_2 synforms trending north to northeast separate the different mineralised districts. These structures are associated with the regional antiform that is believed to have formed as a late stage broad folding that was coaxial with the D_2 event which produced small scale tight isoclinal folds (Torrealday, 2000). The D_2 are therefore believed to have developed due to west to northwest directed deformation.

The D_3 event is associated with development of north striking, steep to moderate east-west dipping conjugate F_3 kink bands. Mineralised veinlets with associated alteration can be seen in some of these bands (Broughton et al., 2002). This deformation event is poorly constrained to the next deformation event i.e. D_4.

The youngest deformation event, referred to as D_4 is associated with northwest trending folds (Kansanshi antiform). This deformation event is associated with mineralised veins and vein swarms which are distributed en echelon along the axis of the Kansanshi

antiform. This suggests a temporal and genetic relationship between formation of the antiform and mineralisation (Broughton et al., 2002).

4.3.1 Large scale Structures

One of the clearly interesting features of the Kansanshi geology is the consistent lateral continuity of the lithological layers ie phyllite, knotted schist and marble units can be traced over kilometres. The presence of preserved bedding and the pervasive bedding-parallel foliation, it is most likely that the lithological layers represent S_o that have undergone layer-parallel deformation. The lithologies are believed to control the distribution, type and intensity of alteration and mineralization.

North-south structures are a major structural element visible from drilling data and the aeromagnetic surveys as prominent lows. The most significant and economically important of these is the 4800 and 5400 structures which are believed to be major north-south zones of complex faulting, abundant vein injection, breccia development and down-dropped rock units. The 4800 zone in particular can be traced on the western side of main pit (11500N to 12700N) and becomes more complex toward the north. On the southern extreme of the (11850N) the zone tapers to a single asymmetric kink zone, subvertically dipping with the west side down. Faulting and vein injection are common along and adjacent to this structure, and in this southern portion occur over widths of more than 50 metres. From 11900N to its northern termination against the gabbro, it progressively develops from a box fold to a complex series of kink folds, faults and veins with a width of over 100 metres (Cyprus Amax, 2000).

The 5400 structure on the eastern side of the Main pit is not clearly understood but behaves similarly to the 4800 zone with less mineralisation intersected within the fringes of the structure.

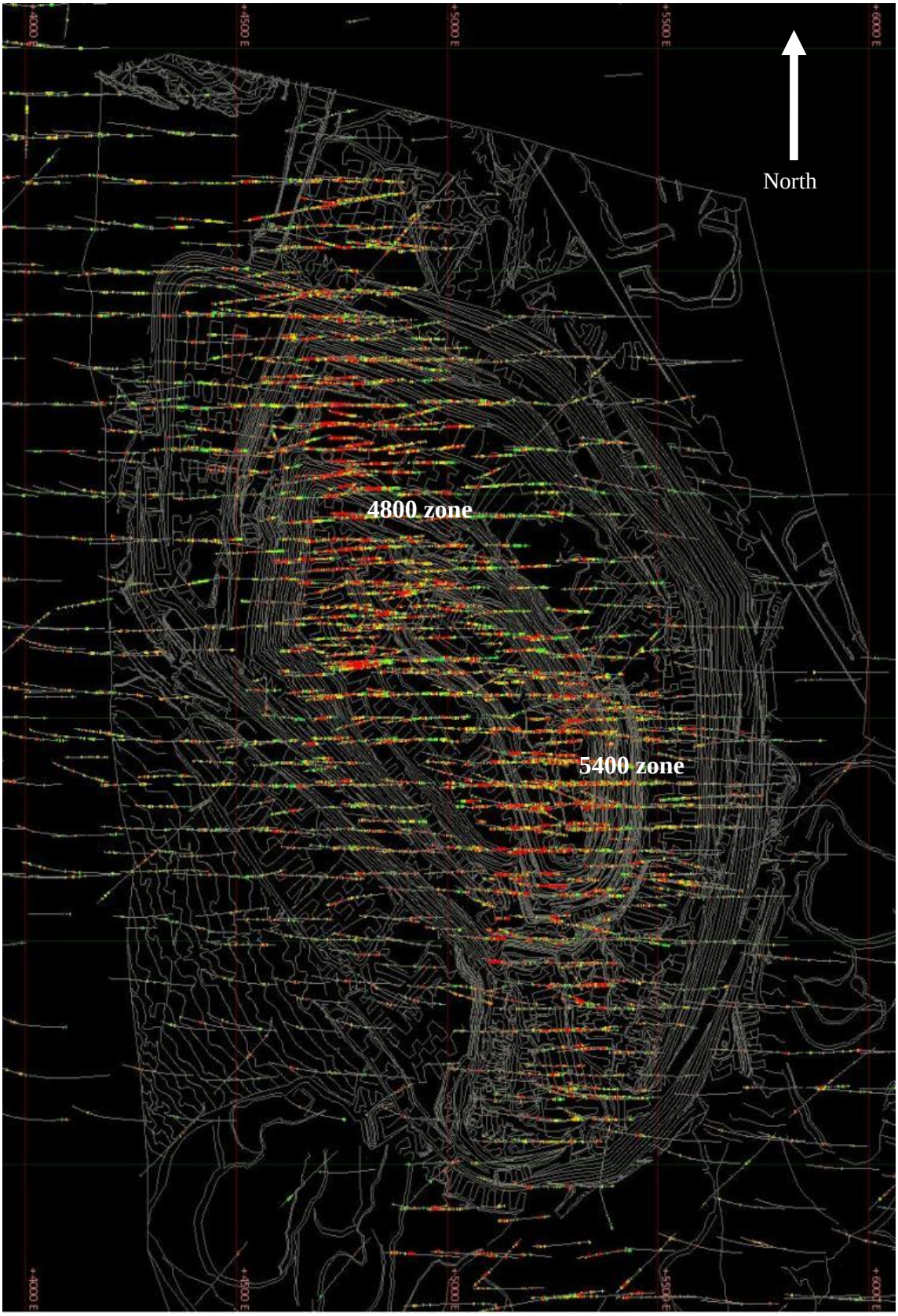

Figure 27. High grade Cu diamond drill intersections showing the 4800 and 5400 zones in the Main pit (plan view). Red zones indicate area with TCu > 1%. (Main Pit Leap frog model, 2013)

Recent structural finding through modelling of the major stratigraphic unit (Pebble Schist) and assay data, indicate that there are ductile-low angle structures (fluidised breccia) within the Main pit dome and are generally planar but displays an apparent ramp immediately under the "pimple" area of the Main pit and may have a minor inflection beneath the 4800 zone. There are generally associated with thickening of units such as PS. The low angle structure is believed to have acted as channel for hydrothermal fluids (feeders for mineralisation) during the mineralisation event as can be seen by the alteration along it's extents (Hitzman, 2013). Recent work on trying to understand the Kansanshi deposit, suggests that the 4800 zone represents intersection of low-angle thrust structures at the oxidation front and further highlights the compartmentalisation of low-angle thrust planes by the NW-SE trending, NE dipping normal faults. Increased brecciation occurs in the hanging-wall of the normal faults and increased grade is observed in the oxide at the intersection of the low-angle thrust and normal faults.

4.4 Metamorphism

Host rocks at Kansanshi have undergone regional metamorphism associated with at least two phases of deformation related to the development of the Lufilian fold belt (Torrealday, 2000). The UMC and MMC are essentially biotite-garnet schists, biotite schists and phyllite which have well developed micaceous fabrics. The biotite-garnet and minor chlorite mineral assemblage indicates that these rocks are within the garnet isograd, i.e. maximum temperatures of between 450 and 500°C. This represents a metamorphic grade of upper green schist to lower amphibolite facies, figure 28. Formation of garnets with calcareous units within the Kansanshi deposit is an indication that temperature the garnet isograd, however the majority of these garnets retrograded to calcite, quartz, muscovite, minor albite and chlorite.

The high carbon content of some of the original rocks seem to have inhibited growth of coarse grained muscovite, biotite and garnets, thus accounting for the interbedded nature of the phyllites, biotite schists and biotite-garnet schist. Scapolite is which dominantly found in carbonate units, occurs as a prograde mineral (Torrealday, 2000). Pebble schist units within the deposit represent the most variable metamorphic assemblage which is commonly retrograde and consists of chlorite after biotite, carbonate after scapolite, calcite, quartz, muscovite and albite after garnet. At least one foliation is evident in the pebble schist, indicating that metamorphism was associated with deformation

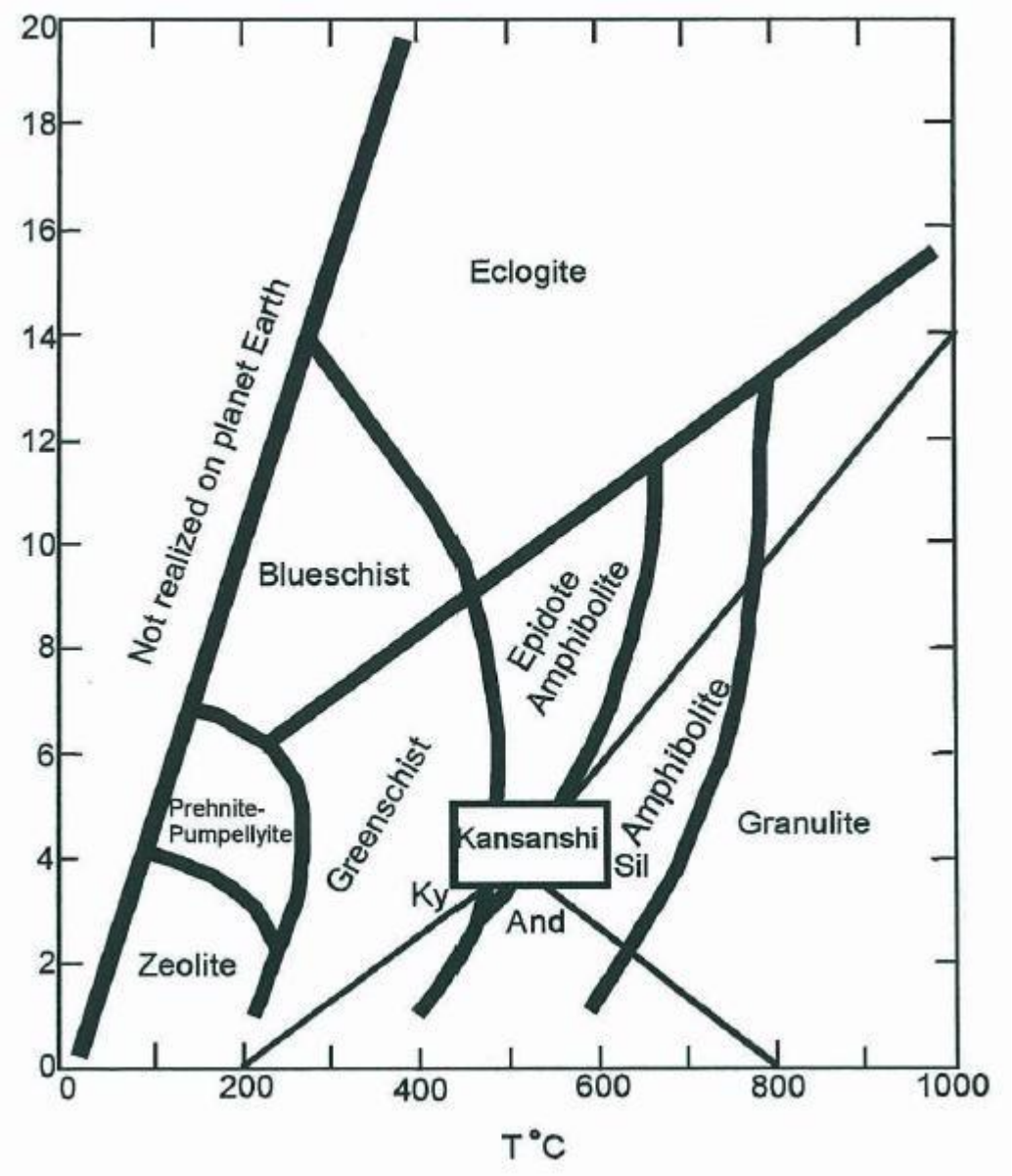

Figure 28. P-T diagram indicating metamorphic facies for Kansanshi metasediments (Torrealday, 2000)

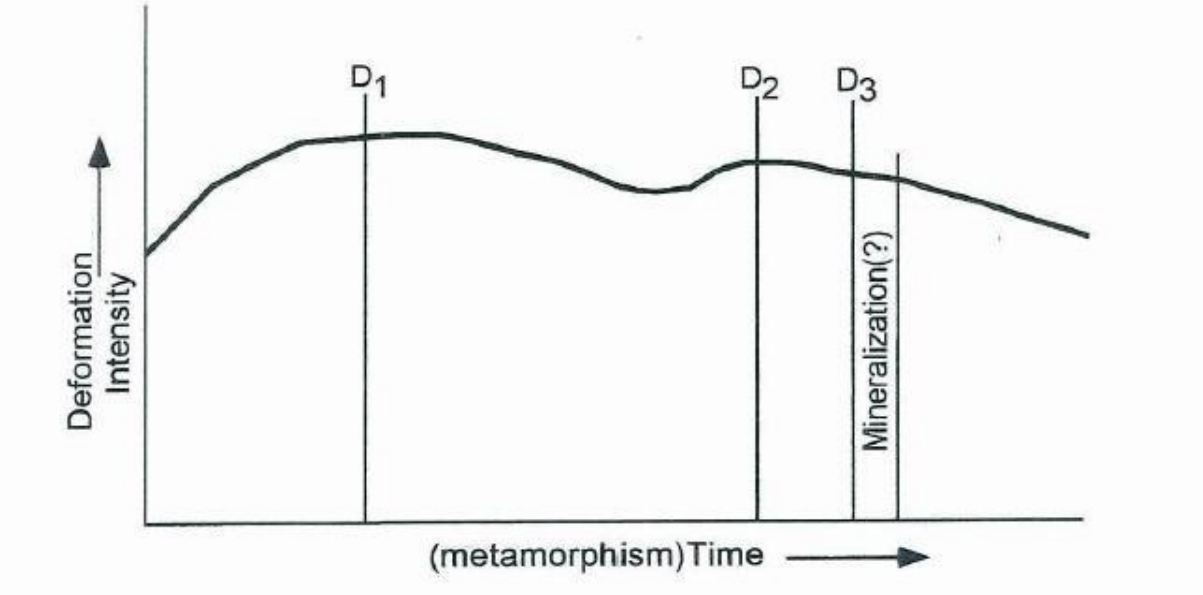

Figure 29. Progression of metamorphism associated with deformation and development biotite fabrics (Torrealday, 2000)

There does not appear to be any correlation between the distribution of metagabbro/diorite bodies and metamorphic grade, as their contacts generally lack metamorphic aureoles. These mafic bodies have been metamorphosed to the same greenschist facies as the adjacent sediments, and as well contain Cl^{-} in the amphibole, biotite and scapolite phases (Masaitis, 1998).

4.4.1 Age of Metamorphism

A widely accepted metamorphic age for the Katangan metasediments is between 666 and 305 Ma, which is based on K-Ar dating of biotite and muscovite (Cosi et al., 1992). However it is appropriate to note that age and timing of metamorphism of the Katangan sediments is based on limited dating of higher grade metamorphic basement rocks of the ZCB (Torrealday, 2000). Application of U-Pb dating techniques on the Hook granite which cuts metamorphic rocks of the Lufilian arc in the south of Zambia yielded an age of 566±5 Ma (Hanson et al., 1993). The timing of the main deformational and regional metamorphism within the inner portion of the Lufilian fold belt is thus constrained by this age. According to Torrealday et al. (2000), biotite samples collected from the pit area yielded ages of 499±2.9 Ma and 492±2.94 Ma using $^{40}Ar/^{39}Ar$ dating.

It is believed that metamorphism may have lasted for long period, but the achieved ages represent a separate younger metamorphic event associated with a separate phase of deformation.

4.5 Magmatism (Intrusive activity)

Granitic, gabbroic and potassium rich intrusives have been identified within the Solwezi area, however altered metagabbros are the only distinct igneous rocks encountered in the Kansanshi Mine area, figure 31ab The gabbros are tholeiitic suggesting they were formed during the advanced stages of continental rifting (Barron, 2003). They are also believed to have undergone alkali metasomatism related to Lufilian metamorphism which accounts for the variable degrees. In an unaltered state, the gabbros are dark green-brown to mottled grey-green, melanocratic and medium to coarse grained, however the majority of these intrusives within the study area have been metamorphosed to epidote and amphibolite facies and are locally scapolitised. Primary textures are rarely preserved owing to recrystallisation during metamorphism (Barron, 2003). The primary mineralogy for the unaltered gabbro is dominantly plagioclase, augite (cpx), enstatite (opx) and ilmenite-magnetite. This differs completely with the metagabbro which dominantly consists of amphibole (70% Hornblende), plagioclase, scapolite, epidote, sphene and pyrite.

A

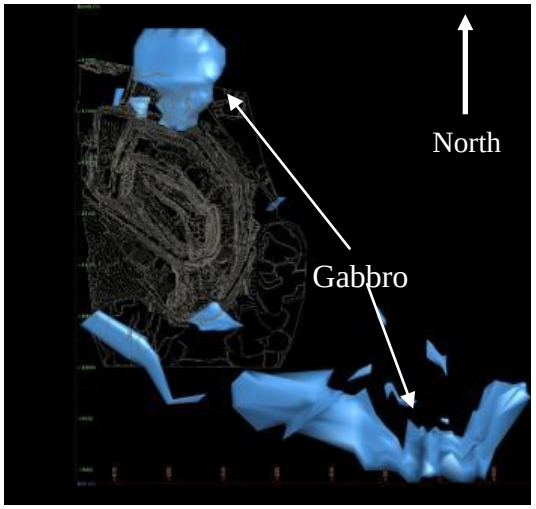

B

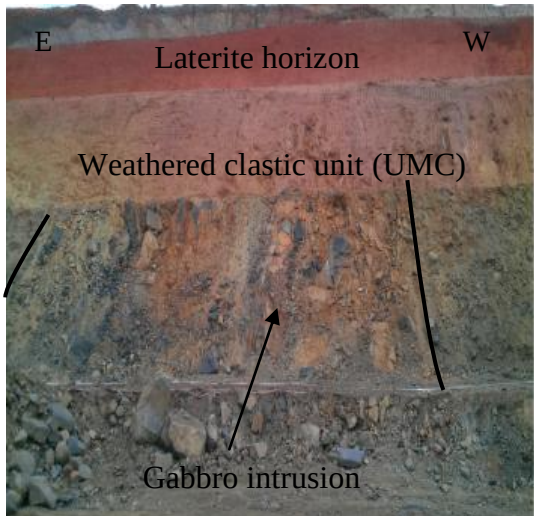

Figure 30: (A) Distribution of Gabbros within the confines of the Main pit area, plan view (Main Pit Leap frog model, 2013). (B) Gabbro intrusion as on the pit wall in Main 6, the body occurs as sill within weathered schists/phyllite, looking south.

The distribution and occurrence of these intrusives has not been clearly defined, however the majority of them have been identified and interpreted through drilling, mapping and airborne magnetic surveys flown over the Kansanshi area. These gabbro bodies are known to ring the domes and displace lithological units, refer to figure 31. According to Barron (2003), U/Pd SHRIMP dating of primary zircons from the gabbros gave ages between 742 and 753 Ma with a metamorphic thermal overprint at 511 Ma. These suggest

that the intrusives are pre-mineralisation and therefore could have had an influence on the mineralisation event(s). This however has not been confirmed.

CHAPTER 5: MINERALISATION AND ALTERATION TYPES

5.1 Introduction

Mineralized zones within the Kansanshi Cu-Au deposit contain steeply dipping, undeformed ~502 to 512 Ma quartz dolomite– calcite-chalcopyrite (pyrrhotite-pyrite–Molybdenite-uraninite-gold) veins, the earliest of which exhibits carbon and biotite-destructive, albite-ferroan dolomite alteration haloes (Torrealday et al., 2000). Other significant alteration types include carbonate, sericite and scapolite. Veins vary in thickness from several centimetres to over 2 m. The veins are most abundant in the vicinity of 100s m-scale domes, which form topographic features along the crest of the Kansanshi antiform. The Main pit deposit is characterised mainly by radial vein sets in the vicinity of the dome apex. List of minerals associated with the different mineral assemblages is detailed in section 5.2 and 5.3.

Supergene enrichment and subsequent partial oxidation of the upper parts of the deposit produced copper oxide and mixed copper oxide/chalcocite assemblages which have been the focus for oxide and transitional ore mining. The depth to primary sulphide mineralization is fault and fracture controlled and highly variable, ranging from 200 to 300 m to less than tens of meters (Hitzman et al., 2012).

The Kansanshi deposit has an exceptional high gold tenor which occurs in association with quartz sulphide veins. Redistribution of the gold through supergene processes has resulted in local enrichment in the oxide and mixed zones (Cyprus Amax, 2000).

5.2 Ore body and Mineralisation characteristics

The Kansanshi ore body which is associated with dome structures along the northwest trending antiform is characterised dominantly by vein-specific mineralisation, stratiform mineralisation in thin bands and veinlets parallel to bedding/foliation, and disseminated mineralisation associated with either plagioclase (albite) or carbonate alteration.

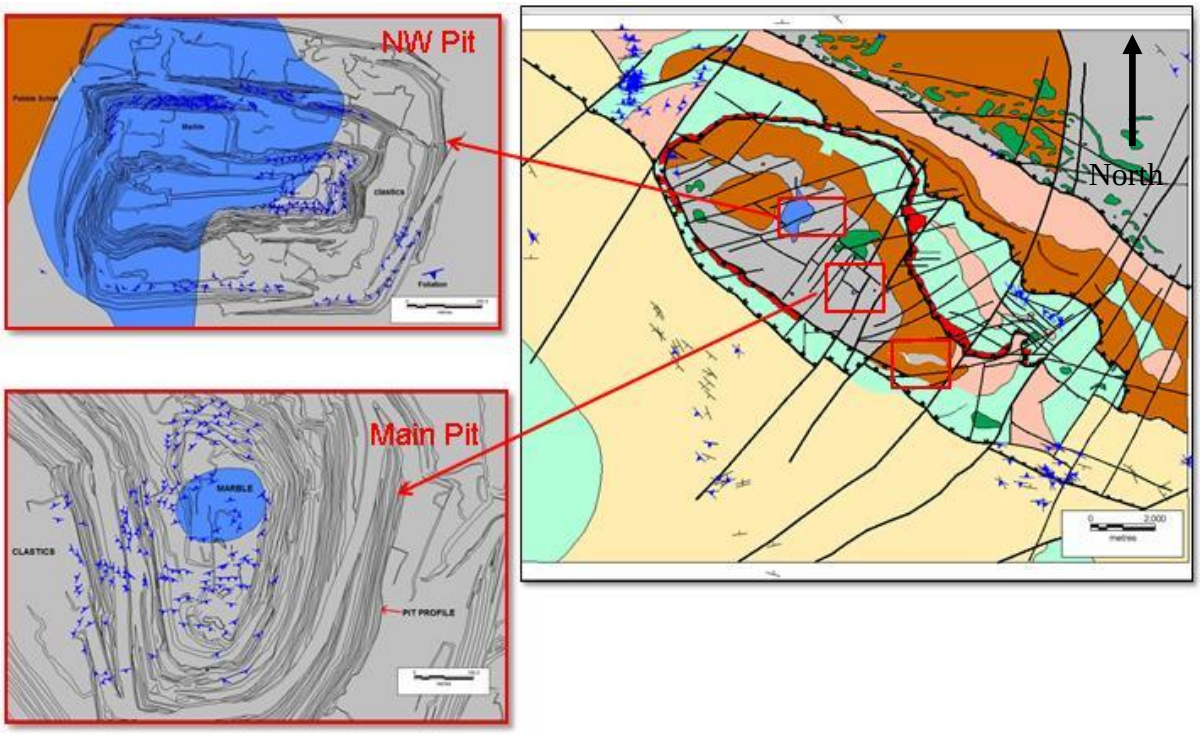

Figure 31. Kansanshi Orebody (Main and NW Pits) located along the crest of the antiform also showing associated domes along it. (Fourie et al., 2012)

Of relevance, the Main Pit deposit is hosted in strongly foliated and recumbently folded carbonaceous phyllite, schists and marbles. Mineralised zones contain steeply dipping undeformed quartz-dolomite (carbonate)-chalcopyrite veins with albite, ferroan dolomite alteration halos. Veins exhibit variable thicknesses (cm to metre scale) and increase in density towards the apex of the domal structures. The Main pit dome shows high amplitude and is associated with radial vein sets around the dome.

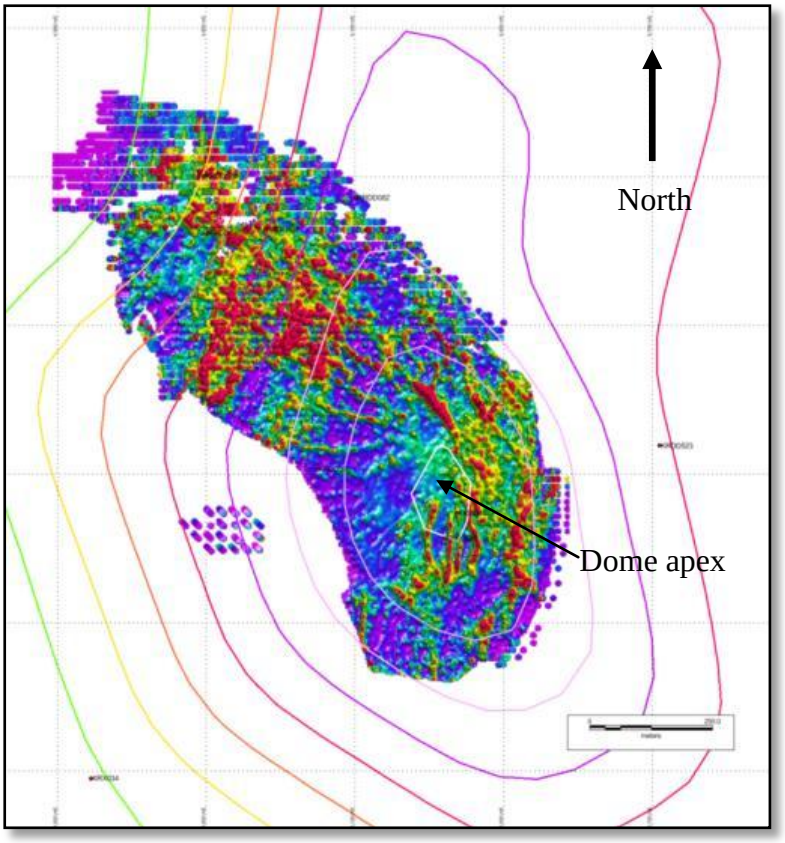

Figure 32. Graphical representation of the vein distribution in the Main Pit based on the total copper grade contained in the KMP Grade Control Model (constrained to an elevation of 1350m AMSL). Radiating veins illustrated around the 'pimple' area of the Dome.

Ore mineralogy within the deposit is dependent on the weathering profile which at Main pit has characteristically produced a zoned profile of leached, refractory, oxide-refractory, oxide, mixed and sulphide mineralization (Cyprus Amax report, 2000). These zones are controlled by depth and degree of weathering, with the major structural terrains such as the 4800 and 5400 E zones showing deeper and complex weathering profiles. The mineralization/ore type boundaries can be clearly defined in core and on the pit walls. They are usually associated with mineralogical changes at lithological, stratigraphic and vein contacts. It generally holds that carbonate is absent above the mixed zone, and furthermore that calcareous units and veins play a major role in controlling the depth and geometry of the oxide/mixed contact (Cyprus Amax, 2000). Brittle structures such as faults and shear zones have an influence on the depth of weathering owing to fluid movement along these structures, thereby affecting the oxide-transition-fresh (sulphides) contacts.

The upper leached zone of the weathering profile is rarely associated with copper mineralization. The saprolite zone consists primarily of cupriferous goethite, with minor black copper oxides (refractory mineralization). This zone shows total copper grades of between 0.5% and 1%, however the ASCu is usually less than 30% of the total Cu grade. This zone is characteristically found in much of the UMC, north of section line11600N in

the Main pit. Processibility of this material is a challenge due to the abnormally high clay content which affects floatation in the plant and is therefore being stockpiled.

At increased depth in the oxide-refractory zone, the cupriferous goethite becomes mixed with greater amounts of soluble copper oxides, and locally minor amounts of native copper. The mineralization is transitional to the underlying oxide zone, and is defined as having an ASCu/TCu ratio of 30% to 80%.

The oxide zone is classified as having an ASCu/TCu ratio > 80%. Its upper oxide contact is usually sharp and occurs at a lithological contact, residual within the UM. The oxide zone is produced by supergene enrichment and partial oxidation of the upper portions of the deposit. The main copper species include chrysocolla, malachite, tenorite, cuprite, and native copper, with minor amounts of chalcopyrite and chalcocite locally present. The contact between the weathered residual marble and the underlying fresh marble usually forms the base of the oxide zone, figure 33.

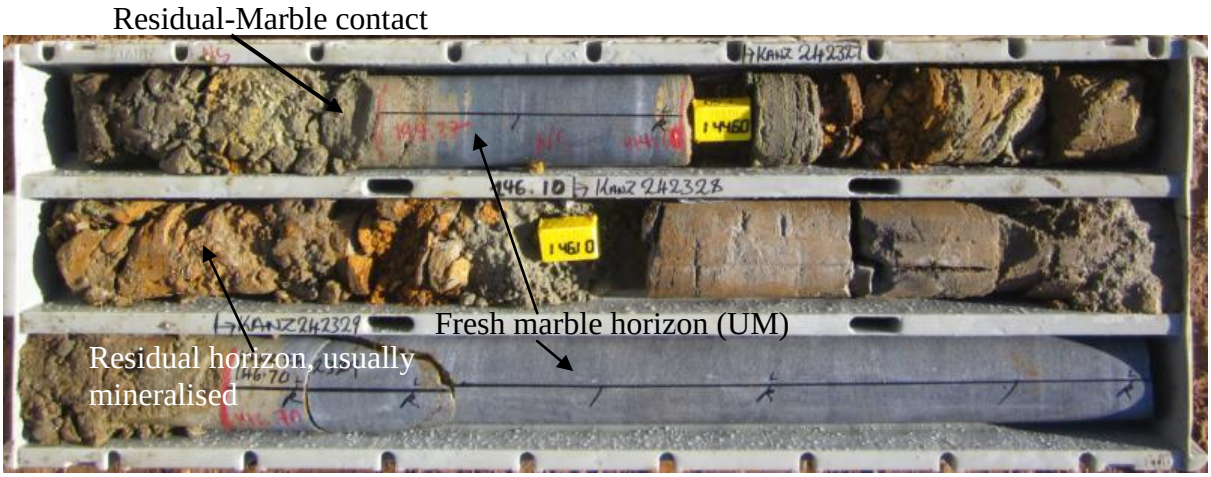

Figure 33. Residual and fresh marble contact as seen in core. KRDD 704 (144.05-147.45m)

The mixed or transitional zone contains 30 to 80% acid soluble copper, including some or all of the minerals of the oxide zone and is usually defined by the presence of > 0.1% total S, with a Stot/TCu ratio greater than 10%. Supergene chalcocite, native copper and cuprite are most common minerals in this zone, minor chalcopyrite can be observed. It is also characterized by the local presence of carbonate, within partially leached calcareous rocks and veins. The transitional zone may also develop vertically, due to fluid circulation along veins or faults such as the 4800 and 5400 structures. The base of the transitional zone is characterised by the lowermost occurrence of copper oxides and chalcocite, with an ASCu/TCu ratio of < 20%.

The sulphide zone is defined as chalcopyrite (and minor bornite) mineralization hosted in fresh rock. It is subdivided into sulphide (or low carbonate sulphide ore) and high carbonate sulphide ore based upon occurrence in phyllites and schists versus calcareous phyllites, schists, and marbles (Cyprus Amax, 2000).

5.2.1 Mineralisation controls

According to Unrug (1988), mineralisation in the ZCB is essentially controlled by two major factors i.e. stratigraphy and structure. This can be related to the Kansanshi deposit.

Stratiform mineralisation occurs in the entire Roan Group, whereas vein mineralisation is present in the Roan to the shales of the Nguba Group. As observed on the main Copperbelt, two impermeable stratigraphic units exert major control on the distribution of mineralisation i.e. the Pebble Schist unit of the Grand Conglomerat form the upper limit for stratiform mineralisation. With the exception of the Kansanshi deposit, with particular reference to the Main pit which occurs higher up in stratigraphy and is dominantly vein hosted, mineralisation is normally confined to within the marble units of the Kakontwe Limestone of the Nguba Group. This is evident in the pit, refer to figure 34.

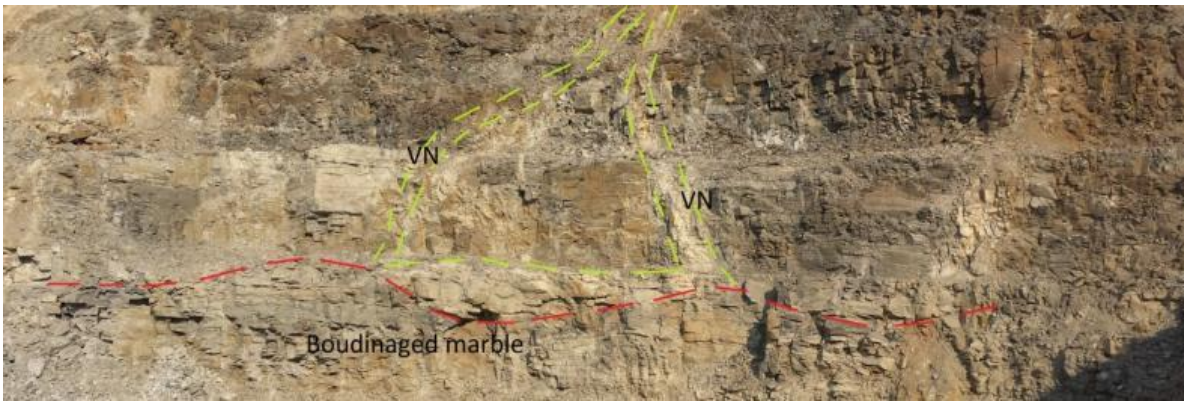

Figure 34: Vein mineralisation confined by calcareous units (UM/LM)

Foliation boudinage is characteristic of the lower contact of the MMC and the LCS in Main pit. Veins observed in the pit appear to start at the tops of the boudins. Structural controls on mineralisation occur in two forms, folding which determines the occurrence of units that host stratiform deposits similar to those of the main ZCB. Faulting also determines the location of major vein orebodies such as Kansanshi and Musoshi Mine in the DRC. As mentioned earlier, low angle fault structures in the Main pit of the Kansanshi deposit are believed to have acted as channel ways or feeders for mineralisation events (Hitzman, 2013). Polymetallic vein deposits are characteristically

located where faults cut across fold axes. Gold mineralisation in the CACB is associated with shear zones with W-SW and E-NE trends. (Unrug, 1988).

5.3 Types of mineralisation

Three mineralisation events have been identified through core logging and mapping of the Kansanshi deposit by Torrealday et al., (2000). These generally occur as vein–hosted, stockwork/breccia and disseminated sulphides. Mineralisation in the Main pit occurs predominantly within undeformed high angle veins with associated alteration halos (pale grey to white halos of replacive albite and ferroan dolomite). These tend to strike north-northwest and sub perpendicular to S_o/S_1. Veinlets and disseminated sulphides have been noticed within the marble, pebble schist and Lower Dolomite units of the Main pit. Disseminated sulphides also occur in association with hydrothermal halos adjacent to the veins. These are clearly evident within the clastic units of the UMC and MMC and calcareous units of the UM, LCS and LM. Veins are normally abundant in the MMC unit, but are known to cut the entire stratigraphy, meta-foliation, recumbent folds, crenulation and mineral lineation (Torrealday, 2000). Minor veining has been noticed in the intrusives (gabbros), but this is a minor occurrence in the Main pit. Veins in the Main pit formed in three overlapping stages (Broughton et al., 2002) and are highlighted below.

5.3.1 Vein Mineralisation

Mineralization occurs within simple gash or extensional veins that generally occur at a high angle to bedding and foliation, and are normally undeformed. Early deformed quartz veins are usually small and lack mineralisation. The mineralized veins formed in three overlapping stages ie, quartz-carbonate-sulphide veins, carbonate-sulphide-U-Th-bearing veins, and sulphide veins. There is considerable mineralogical overlap between the first two types, and chronological overlap amongst all three. Cross cutting relationships are uncommon, and a single vein may change type over short distances.

Age dating work on Molybdenite from the first two vein types confirms earlier work done by Darnley et al (1961) and constrained the the age at approximately 510 Ma (Torrealday, 2000). The veins form part of a late Cu-U-Au mineralization event that occured throughout the Lufilian fold belt. Carbonate breccia veins and breccias comprise a fourth hydrothermal event that post-dates the Cu-mineralized veins at Kansanshi, but probably forms part of the overall ~510 Ma event. Vertical zoning in vein mineralogy is clearly evident in the Main pit as shown by the different material types with depth, however no

lateral zoning has been recognized. This primary vertical zoning occurs as a result of the influence of weathering and oxidation of the original mineralogy.

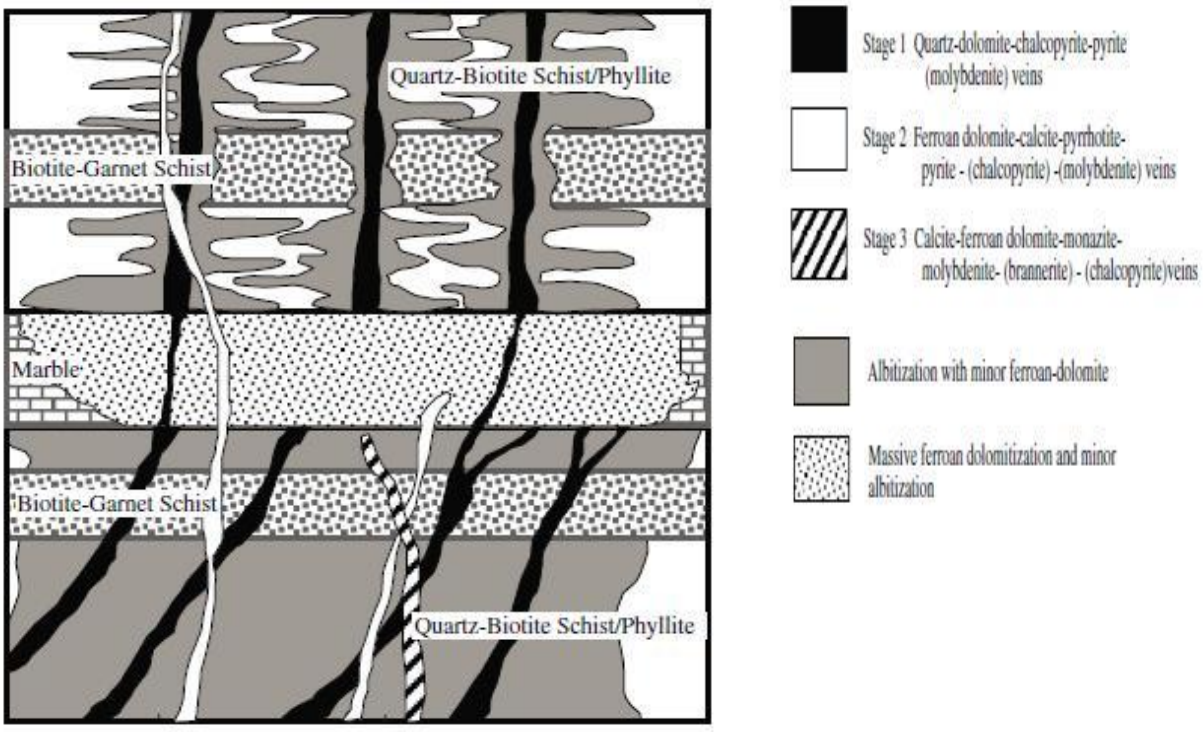

Figure 35. Schematic cross section through the Kansanshi vein system showing distribution of veins and alteration zones (Torrealday et al., 2000)

5.3.1.1 Stage 1: Quartz-Carbonate sulphide veins

Quartz-carbonate-sulphide veins range in width from less than one centimetre to more than five metres and occur as the dominant veins in the Main pit. These are generally north-south trending and steeply dipping over strike lengths of up to 400 metres, and dip lengths of more than 50 metres, figure 36.

Both ferroan calcite and ferroan dolomite occur within these veins. Sulphide mineralogy include chalcopyrite, pyrite, pyrrhotite, minor molybdenite and rare bornite. Rutile is a common accessory, and biotite is sometimes present, usually within pyrrhotite-rich veins. The radiometric U-Th bearing minerals common in the carbonate-dominant veins may occur, but are rare. Magnetite may form a significant phase in veins within the LM and LPS, in the vicinity of the Main pit dome. Bornite is also more common at depth in the dome. The veins also contain minor amounts of Au, Ag, and Ni (Cyprus Amax, 2000).

Figure 36: Quartz-carbonate-chalcopyrite vein in core from Main pit. KRDD273, 355m

Sulphide and carbonate are normally intergrown, indicating a similar cooling history (Cyprus Amax, 2000). Crack-seal textures are rare or absent, and the veins can be classified as syntaxial. The vein margins are usually diffuse and akin to alteration fronts, or grade into alteration, which is particularly true of veins associated with marble contacts and carbonate alteration bands. In the majority of instances, the contacts are usually sharp. Most of the veins are quite coarse-grained, even megacrystic, with locally occurring vugs. The morphology and mineralogy indicate that the veins are mesothermal, which is confirmed by preliminary fluid inclusion study done by Speiser et al, (1995) and Torrealday, (2000).

In other parts of the deposit particulary in the NW pit, the quartz-carbonate-sulphide veins show a crude change in mineralogy with depth, from quartz-carbonate in the upper part of the MMC to carbonate-rich in the lower units of the LCS and LM (Broughton et al., 2002). This is not evident in the Main pit and can be attributed to differences in CO2 content within the two areas. Throughout the Kansanshi deposit, Main pit included, it is common to observe quartz-carbonate-chalcopyrite veins emanating from alteration bands of carbonate-quartz-(albite) The LCS (and the UM) apparently acted as a reservoir for the formation of carbonate-rich veins during hydrofracture.

5.3.1.2 Stage 2: Carbonate-sulphide-U-Th rich veins

Stage 2 veins are distinguished by the dominance of carbonate over quartz, and the presence of an unusual suite of U- and Th-bearing minerals, figure 37. Chalcopyrite, pyrite, pyrrhotite and minor molybdenite occurs in association with trace to accessory amounts of brannerite, monazite, uraninite and pitchblende. Carbonate veins within the marbles may also contain gypsum and anhydrite. These veins tend to be relatively narrow, centimetre-wide structures, but still produce typical albite-carbonate-sulphide alteration haloes. Cross-cutting relationships with the stage 1 quartz-carbonate veins are not abundant, and sometimes contradictory, and hence the relative ages of these two vein stages are only broadly constrained.

Figure 37. Carbonate-sulphide-rich veins in the Main pit, dominantly consists of chalcopyrite, bornite and minor pyrite hosted in schists of the LCS (looking west).

The presence of U-Th in these veins forms a useful exploration tool in the search for similar deposits through radiometric surveys. Studies by Blair (1997) on seventy-five samples of wallrock (72) and veins (3) returned an average U content of 9.8 ppm, with a standard deviation of 20.4 ppm The U values of the three veins were low (average 0.6

ppm), which reflects the erratic distribution of the uraniferous phases in the veins. The larger database of wallrock samples shows a general increase in U content with increasing alteration, from an average of 4 to 7 ppm in unaltered to moderately altered wallrock (Blair's stages 1, 2, 3 and 3/4), to 23 ppm in strongly altered (Blair's stage 4) wallrock. Thorium values remain relatively constant at an average of 7 to 10 ppm, independent of alteration (Cyprus Amax, 2000).

5.3.1.3 Stage 3: Sulphide veins

Massive sulphide veins and vein stockworks generally occur on a local scale and appear not to form large, continuous structures. Chalcopyrite veinlets cross-cut albite-ferroan dolomite alteration in the UM, and narrow chalcopyrite or pyrite veinlets cross-cut the stage 1 and 2 vein types.

Figure 38. High grade chalcopyrite vein hosted in Knotted schist (KS) with no alteration.

5.3.2 Breccia/Stock mineralisation

Deeply weathered portions of the deposit are characteristically found in close proximity to brecciated zones especially in the 4800 zone. Breccias and breccia veins are invariably comprised of fine to medium grained carbonate, often intergrown with lesser quartz/albite and carrying minor to locally spectacular amounts of rutile. Presence of chalcopyrite is

often rare. The breccias typically contain angular to moderately rounded fragments of mineralized wallrock and veins, and are therefore considered to have formed from hydrofracturing event. Jigsaw-fit textures and locally derived fragments are common where the breccia is fragment-supported, and consists essentially of a stockwork. Wallrock fragments are often completely re-oriented, even within very narrow veins, and this characteristic is normal. More varied fragment types occur where the breccia veins are larger and weathering has caused dissolution and collapse within the structure.

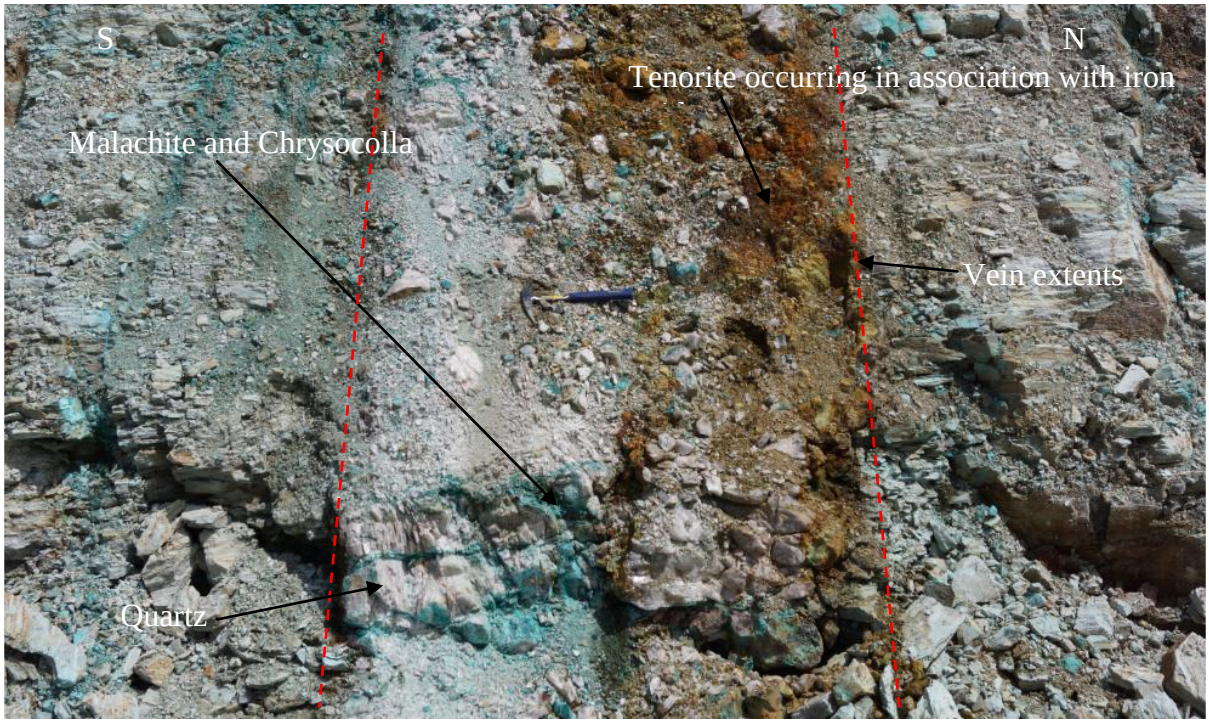

Figure 39. Oxide mineralisation consisting of malachite, chrysocolla, tenorite within a quartz rich vein in the 4800 zone of the Main pit (looking west).

All of the carbonate breccias observed in fresh rock follow earlier vein structures or occur within altered units adjacent to marbles. As mentioned earlier, the 4800 zone and the top of the UM north of the Main pit are characterized by weathered breccias.

5.3.3 Disseminated sulphide mineralisation

Disseminated sulphides are directly associated with alteration, predominantly albitisation, and are best developed in clastic units (phyllites) in the UMC and MMC, figure 40. The mineralisation usually occurs as chalcopyrite. Within the Main pit, disseminated sulphides are common in the higher levels of the MMC owing to stronger albitisation and increased vein density (Torrealday, 2000). This could be due to accumulation of hydrothermal fluid under the impervious UM unit.

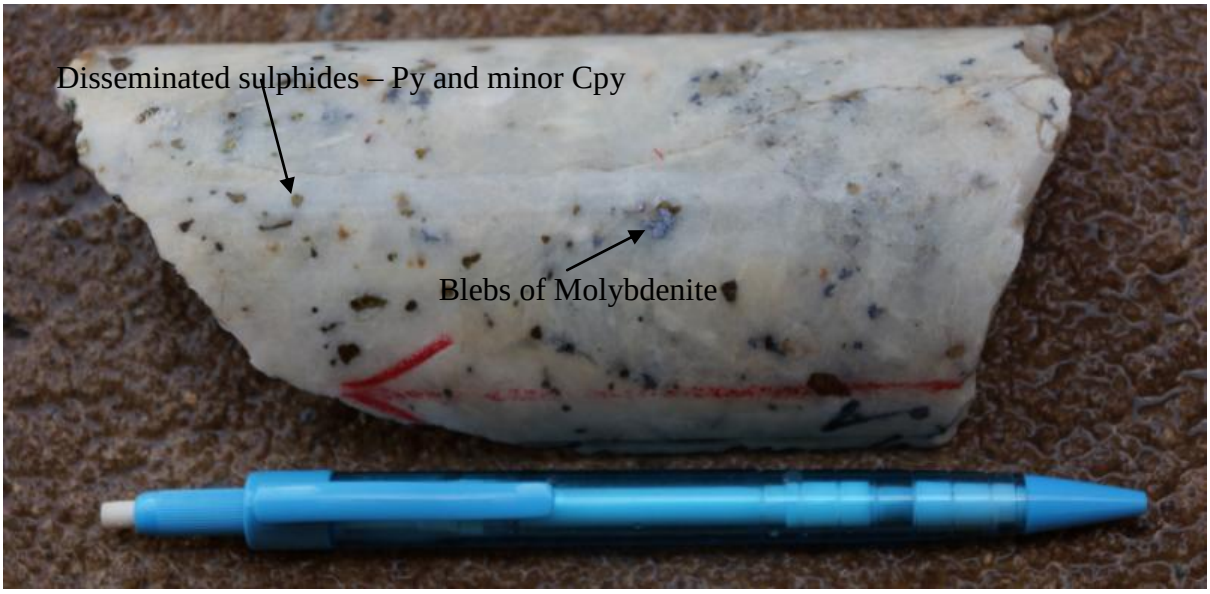

Figure 40. Disseminated sulphide (Py and minor Cpy) and blebs of Molybdenite mineralisation in core from Main pit showing albite alteration. (KRDD 609)

Disseminated sulphides also occur within calcareous units (LCS, LM) but less extensive in schists (Knotted Schist). The presence of disseminated sulphides in the LCS and LM is associated with alteration. This is also true for the deeper 'seated' mineralisation in the LPS and LD units which is characteristically found within the apex of the Main pit dome. This mineralisation seems to be structurally controlled (low angle structure under the dome) and is reduced in occurrence away from the dome. Vein density seems to follow the same trend.

5.3.4 Distribution and geometry of vein mineralisation

The veins are predominantly hosted within the phyllite units of the UMC, UM, MMC and LM which occur in association or contact with marbles. Veins are sparsely distributed in knotted schists and marbles, with the exception of the Main pit dome vicinity which is characterised by intense vein mineralisation and alteration. Pit mapping within the Main pit has confirmed that phyllite-hosted, mineralized veins pinch out at or near contacts with knotted schist or marble/dolomite (figure 35). The majority of veins are therefore interpreted to terminate or originate, as described for the LCS at marble contacts (Cyprus Amax report, 2000).

The veins essentially form extensional "ladder" structures within the stratigraphic units, figure 41. Exposures in the pit indicate that the local dip of the domed host rocks exerts a

strong control on the dip of the veins, which preferentially form at a high angle to the bedding (Cyprus Amax, 2000; Torrealday, 2000).

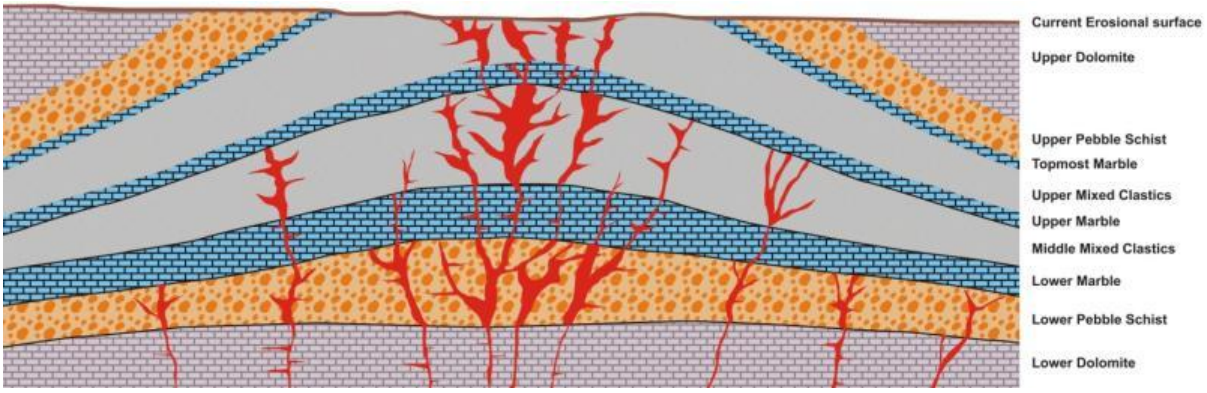

Figure 41: Sketch showing the prevalence of veins in the clastic units and higher vein density under the dome (associated with thickening of the strata, not to scale)

Radial veins are present in the dome area forming large swarms of 5 to 30 centimetre wide veins which are almost exclusively have high angle dip of ca. 70-90°. Refer to Appendix 4 showing mapped veins and lithologies for Main pit. Recent deep drilling in the Main pit indicates that the stratigraphic sequence including the LPS and LD is altered and veined within the dome, a notion that had previously been disputed owing to limited drilling information. Conformable centimetre-wide veins which are abundant in the LM may have formed by dilation during doming.

5.3.5 Age of mineralisation

No recent age dating data has been derived for the Kansanshi deposit. The only age of mineralisation data available was conducted by Torrealday et al., (2000) using a number of different geochronological techniques. Re-Os dating of Mo samples from stage 1 and 2 veins gave a date of 511±1.7 Ma and 503±1.7 Ma respectively. $^{40}Ar/^{39}Ar$ dating of metamorphic biotite gave ages of 492.9±2.9 Ma and 499.28±2.94 Ma. Alteration assemblage (muscovite intergrowth) associated with stage 1 veins yielded an age of 473±2.9 Ma.

U-Pb dating of monazite intergrowth from stage 2 veins yielded an age of 509±11 Ma which closely agrees with dating of brannerite from mineralised veins done by Darnley et al. (1961) which gave an age of 500±15 Ma.

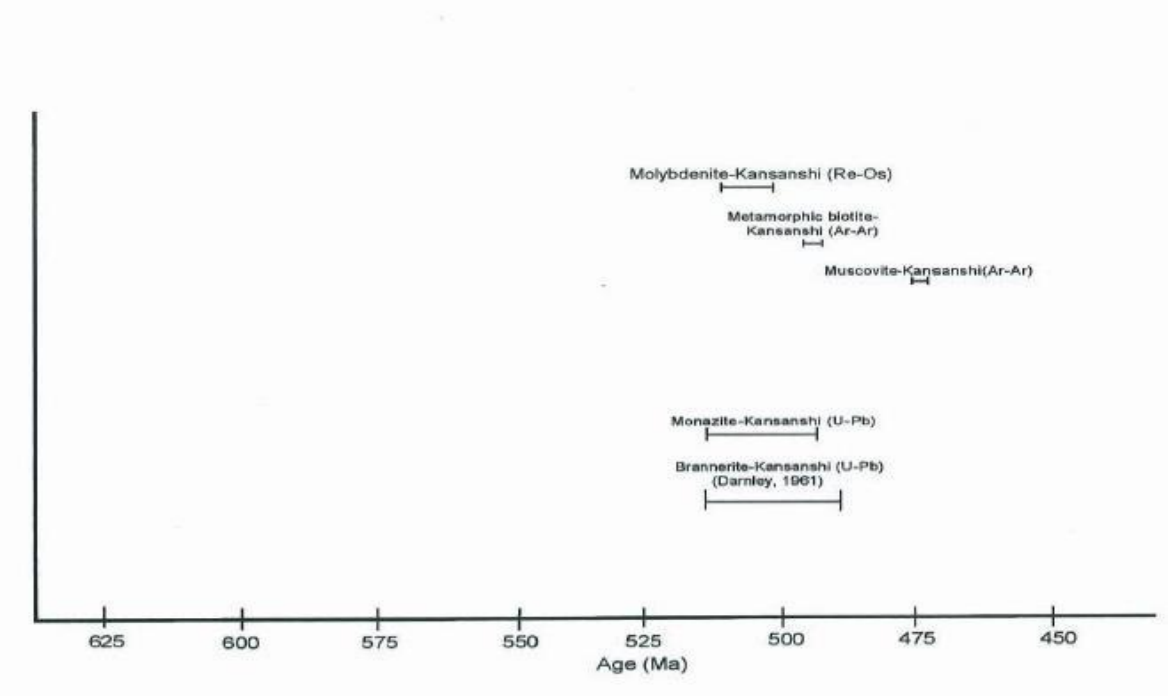

Figure 42. Range of mineralisation and metamorphic ages obtained for the Kansanshi deposit (adapted from Torrealday, 2000)

Geochronology, textural and fluid inclusion studies suggest that mineralisation and alteration within the Kansanshi deposit were temporally coincident with retrograde stages of regional metamorphism (Broughton et al., 2002).

5.4 Mineral Associations and zonation of Copper mineralisation

Characteristic mineral zoning is common in many sediment hosted copper deposits. In most deposits it is generally chalcocite (Cu_2S) - bornite (Cu_5FeS_4) - chalcopyrite ($CuFeS_2$) -pyrite (FeS_2) - pyrrhotite ($Fe_{1-x}S$), this relates to the higher solubility of iron-rich relative to the copper-rich sulphides during precipitation (Selley et al., 2005). Mineral vertical zonation within the CACB has been observed to occur at different scale i.e. regional or deposit. At deposit scale, a gross mineral zonation from hematite in oxidized rocks to a chalcocite-bornite assemblage in immediately adjacent reduced rocks, especially those adjacent to syn-sedimentary faults, is common. The chalcocite-bornite assemblage changes stratigraphically upward and/or laterally away from synsedimentary structures to a bornite-chalcopyrite assemblage, then a chalcopyrite-rich assemblage, a chalcopyrite-pyrite assemblage and, finally, pyrite (Hitzman et al., 2012). Mineral or metal zonation is less systematic and more complex on a regional scale. Deposits of the

Domes region (Kansanshi, Lumwana and Sentinel) generally consist of Cu-Au-Mo-U whereas those of the main ZCB and CCB are generally Cu-Co rich.

Veins within the Main pit are dominated by a simple mineralogy of exceptionally coarse-grained quartz-carbonate- chalcopyrite. Molybdenite has been observed as a sparse accessory mineral in the veins. The occurrence of pyrite in the veins is rare. Sulphide content is characteristically low in the wallrocks however disseminated chalcopyrite occurs with either pyrite or pyrrhotite, which is common occurrence in the carbonaceous phyllite.

5.5 Alteration types and characteristics

Alteration at Kansanshi with particular reference to the Main pit, occurs as discrete haloes around mineralized veins, and widespread replacement of selected lithologies and stratigraphic units. It is close to impossible to distinguish the latter two, because of their spatial and mineralogical overlap. The type and intensity of alteration is dominantly controlled by the lithological units. Alteration is texturally destructive and overprints the greenschist metamorphic minerals (Cyprus Amax, 2000).

Alteration within the Main pit characteristically consists of moderate to intense albitisation and weak to intense dolomitisation which is usually introduced during periods of vein formation. Albitisation dominantly occurs in phyllites and schists whereas dolomitisation is prevalent in calcareous units.

In general, the width of the alteration halo can be related to the width of the vein in a given lithology (Cyprus Amax, 2000). This suggests that the two are coeval. Alteration haloes can be absent in some cross-cutting mineralized veins. Alteration is abundant within phyllites but vein-specific in knotted schist except in the vicinity of the Main pit dome where alteration is pervavsive. This can be attributed to both higher vein density and greater lateral fluid flow (higher porosity in the phyllites) within the phyllites as compared to the schists. The scale of the alteration haloes is dependent on the width of the veins. It is normal to see an alteration-mineralization halo follow selected schistosity or bedding planes and persist laterally from a vein.

5.5.1 Albite-Carbonate Alteration

The most dominant type of alteration found within the rocks of the Main pit, inclusive of the LPS and LD, consists of pale grey to white haloes around individual mineralized

veins. The haloes characteristically consists of variable amounts of albite, ferroan dolomite, ferroan calcite, quartz, green muscovite (roscoelite), rutile, pyrite, chalcopyrite with minor Mo and brannerite (Cyprus Amax, 2000; Broughton et al., 2002). Carbon, biotite, metamorphic plagioclase (oligoclase) and muscovite are destroyed or replaced to form albite and sericite as an accessory mineral. Albite (An_{3-5}) which is usually fine grained forms the majority of the assemblage, whereas ferroan dolomite takes the form of fine-grained to millimetre-sized, ragged to euhedral rhombic porphyroblasts. Emerald green muscovite (V-rich roscoelite) forms porphyroblastic flakes, which are normally intergrown or in contact with chalcopyrite. Ferroan calcite and quartz are usually a minor occurrence (Broughton et al., 2002). Rutile is common but is usually erratically distributed, and locally occurs in dense clusters. In some places albite alteration appears as a slight pink colouration owing to 'haematite dusting'. Sulphides normally replace pre-existing platey pyrrhotite along foliation planes and in bedding/foliation-parallel veinlets, or form blebby grains. Refer to figure 43.

Figure 43. Albite carbonate alteration with chalcopyrite (Cpy) and molybdenite (Mo) mineralisation in the form of blebs and disseminations. KRDD559, 352m

Intensity and mineralogy of vein-specific alteration, and may be partially controlled by the host rock lithology (Cyprus Amax, 2000; Broughton et al., 2002). Narrow veins with an intensely bleached inner zone usually have 25 to 335 of the total halo carring a higher percentage of albite. In the wallrock, this zone is normally assocaited with molybdenite and brannerite. In phyllites this zone tends to have a low sulphide content, but in biotite

and knotted schists it may carry significant mineralization. This suggests that sulphur from early pyrrhotite is scavenged from the intensely altered wallrock and precipitated in the veins (Cyprus Amax report, 2000). The presence of carbon in the unaltered wallrock is usually minor because it is destroyed at the margin of the alteration zone. Pinkish-coloured alteration haloes are caused by minor very fine grained or dusty hematite, often associated with rutile. As seen in the pit, the majority of the sulphide veins carry chalcopyrite and produce chalcopyrite-pyrite haloes. In other instances an inner chalcopyrite-rich halo grades outwards to a pyrite-rich zone, which at the limit of the alteration grades to pyrrhotite. In other minor cases, there is only a chalcopyrite-pyrite zone grading outward to pyrrhotite.

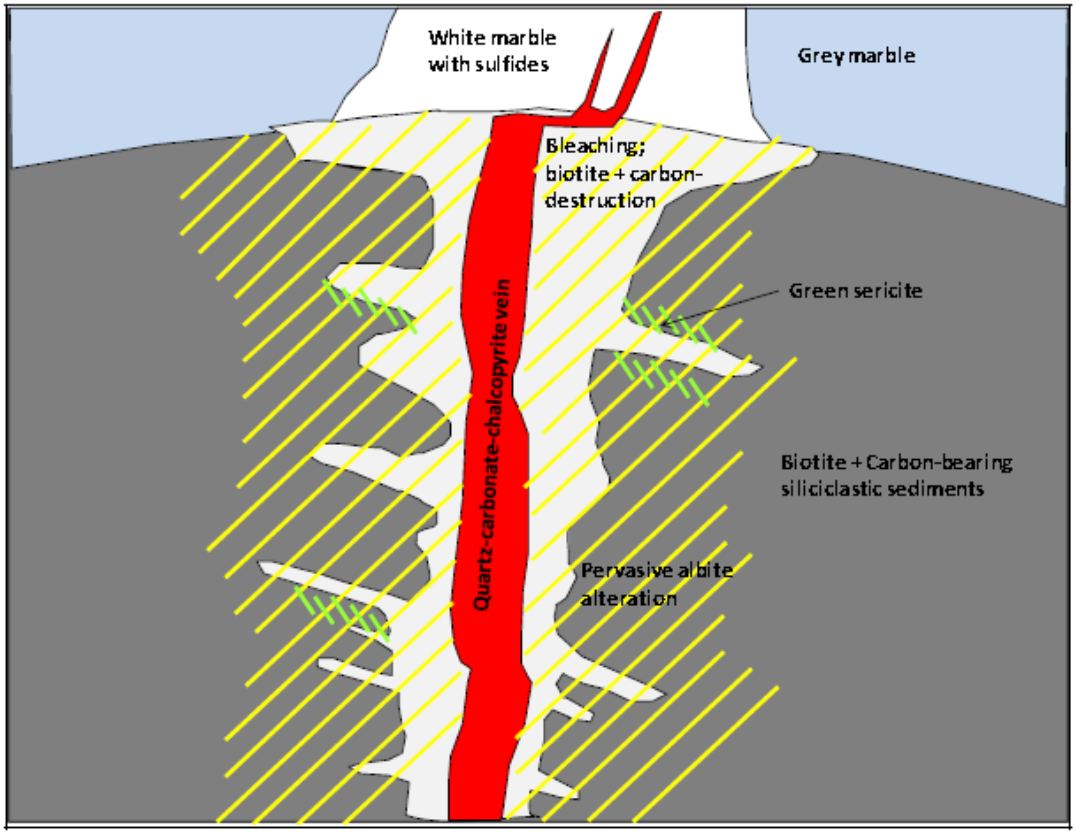

Figure 44. Zonation of alteration in different lithologies (Beeson et al., 2008)

Whole rock data done by Cyprus Amax, (2000) suggets that the onset of weak alteration is marked only by a modest increase in Na_2O and decrease in FeO, without any significant flux of the other major or trace elements. This coincides with formation of albite and the onset of biotite/chlorite destruction. Moderate alteration intensity is characterized by an influx in metals such as Cu, Au, Mo, V, U, Th, Ti. This influx is also characterised by growth of ferroan dolomite, roscoelite and rutile at the expense of biotite

and chlorite. Intense alteration adjacent to the vein shows further growth of albite and ferroan dolomite (Na, Ca, MgO, CO2), loss of K relating to complete destruction of biotite and the presence of a muscovite-depleted zone, and strong addition of Cu, Au and S as sulphide (Cyprus Amax, 2000).

A closer look at textures can be used to determine the relative age of vein-related alteration and deformation events. It is suggeted in the prefeasibility by Cyprus Amax (2000), that albite alteration follows low-angle microthrusts that produce or dislocate the F_1 folds and mineralized veins with alteration haloes cut across the F_1 folds. This suggests that alteration was introduced both prior and during the development of the D_2 folds and cleavage. The acceptable notion is that alteration occurred during progressive D_1-D_2 strain and culminated in a late brittle fracturing event.

The occurrence of the albite-carbonate alteration is a function of vein density and a combination of lithology and stratigraphy resulting in preferential development along specific lithological horizons. Alteration is is clearly developed and extensive in phyllites and biotite schist. Albite alteration within the UM occurs as small pod like bodies associated with stockwork veins. The scenario is different in the MMC, where alteration is more intense. In the LCS and LM, albite alteration is less obvious and extensive, occurs as 'bleached' zones, refer to figure 45.

Figure 45. Bleached Albite alteration zones in LM. KRDD (29.90-34.50)

Proportion of albite alteration reduces with depth as seen in core by the minor occurrence below the phyllite within the marble. Within the LPS and LD, albite alteration tends to be associated with veining.

Not all of the albitic alteration carries ore grades. An exercise was undretaken by Cyprus Amax (2000) where 44 samples of strongly albitized and unveined fresh MMC1 phyllite

and biotite schist assayed less than 0.2% Cu. Sixty-five percent of fresh unveined strongly albitized UMC4 assayed less than 0.2%. The association of alteration and calcareous units indicates that they were major fluid conduits, this is in particular reference to the marble units. The marbles consist of ferroan carbonates rather than dolomite, and contain significant amounts of silicates including scapolite, a well-developed foliation and are coarser-grained making them a suitable fluid conduit. The vein-specific and stratigraphically controlled albite-carbonate alteration possess enough fundamental attributes to conclude that they formed from the same fluid system, at more or less the same time.

5.5.2 Carbonate alteration

Carbonate alteration (Dolomitisation) is characteristic of the marble units and biotite rich schists. The resultant products are ferroan dolomite, which accounts for ca. 90% of this alteration type, normal dolomite, minor albite and rutile. The alteration primarily occurs at the top 10-15m of UM, forming an irregular massive replacement of marble. It is usually associated with Cu mineralisation. The intensity of dolomite alteration decreases significantly downwards through the MMC and LCS and has minor occurrence in the LM, LPS and LD horizons.

Figure 46. Dolomitisation alteration in LCS. KRDD475, 301m

Dolomitisation can be seen as enveloping zones of dark grey ferroan calcitic marble and is always juxtaposed between albite alteration and calcitic marble. Zoning can be seen north of the pit, where pervasive albitization of the UM grades laterally into intermixed dolomite-albite alteration which also grades laterally into ferroan calcitic marble. This zoning is distributed along the Kansanshi antiform which forms the locus of veining, alteration and mineralization. The interaction of albite and ferroan dolomite alteration clearly shows overlap in time and association with mineralization, however the albite-rich stage began a little earlier and the ferroan dolomite stage persisted a little longer.

5.5.3 Other significant alteration types

Other significant alteration types intersected in the Main pit include sericite and scapolite.

Sericite alteration occurs in association with albite and is not abundant in the system. It usually occurs at the margins of the albite bleached zones. Dark green sericite is normally observed close to the mineralised veins. This was interpretated in Cyprus Amax (2000) as the V-rich mica called roscoelite. Sericite and carbonate have been shown to occur as replacement products of garnets.

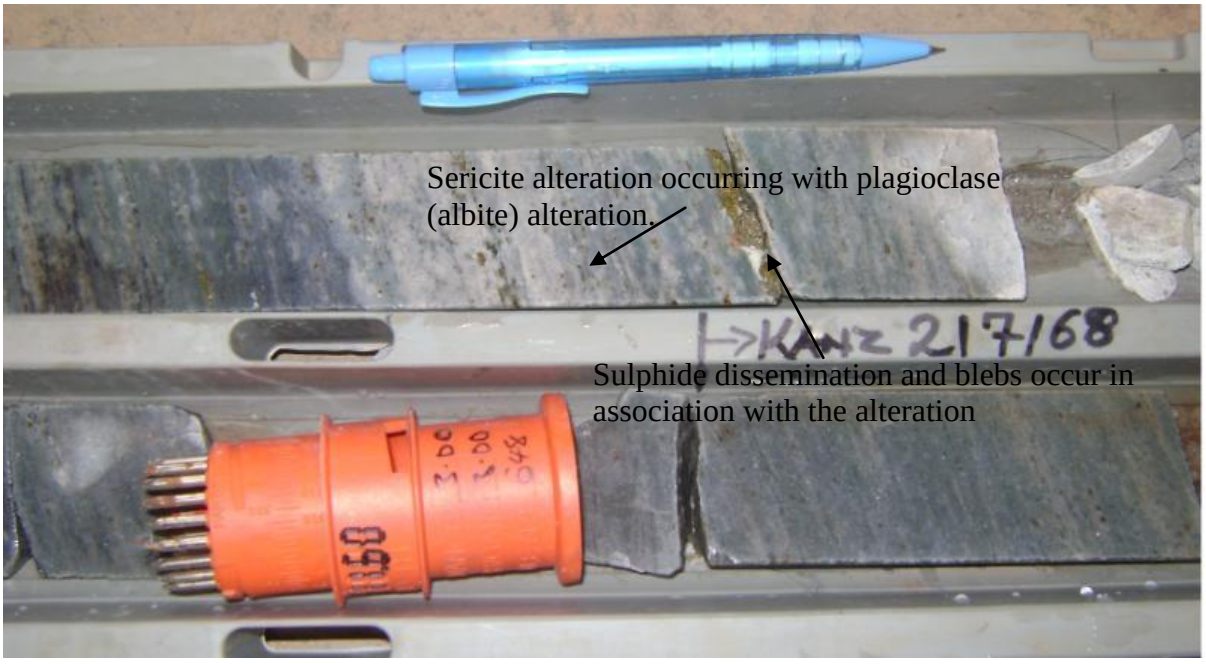

Figure 47. Sericite alteration in core. KRDD 648 (309.90-311.60)

Scapolite occurs as subhedral to euhedral crystals, dark grey in colour with a grain size range for 0.5 to 2 cm. The alteration is usually observed at marble and calcareous biotite schist contacts. Scapolite is affected by albite-dolomite alteration which is associated with

mineralisation. Petrographic work by Cyprus suggests that scapolite overprints metamorphic minerals such as biotite, feldspar and quartz (Beeson et al., 2008). This therefore shows that scapolite formed after peak metamorphism and late or post-D_1, but prior to mineralization-alteration (Cyprus Amax report, 2000).

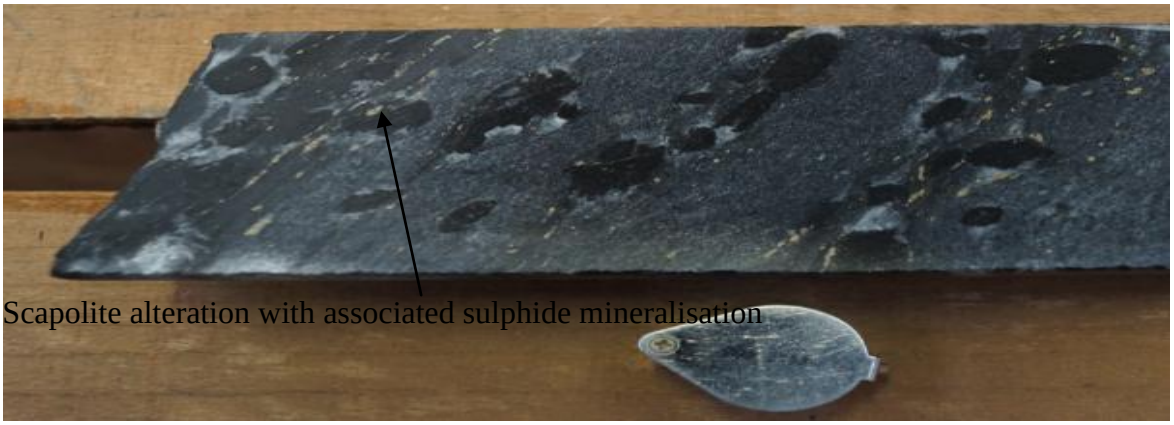

Figure 48. Scapolite alteration associated with sulphide dissemination (Py) in marble. KRDD455, 326m

5.6 Gold mineralisation

The Kansanshi deposit is exceptional in that it has a higher gold tenor than the deposits on the Copperbelt, where gold contents are generally negligible. Gold mineralisation is suspected to dominantly occur within the sulphide and quartz dominated veins and veinlets, throughout the deposit. This is supported by the interaction of Au mineralisation with sulphides. Gold also occurs within stratiform mineralization in carbonaceous phyllites, for instance the LM2 unit that contains relatively few cross-cutting veins. Supergene redistribution of gold, which is leached in the refractory and oxide-refractory zones and locally enriched in the oxide and mixed zones is evident in most parts of the deposit. This has been confirmed by the fact that oxide and mixed ore accounts for the bulk of the gold produced from the plant (72% of the total 'bullion' produced in 2012). Not much work has been done in terms of characterisation of Au mineralisation except for a MSC project done by Goodship in 2010 and various internal reports on deportment studies done.

Goodship (2010), utilised four analytical techniques to understand the occurrence of gold within the Kansanshi deposit. These included optical microscopy, x-ray diffraction, scanning elctron microscopy and elctron microprobe analysis. Scanning electron and

microprobe analysis revealed that gold occurs as free grains in association with melonite ($NiTe_2$) and microfractured pyrite intergrown with chalcopyrite.

Work done by Beeson et al. (2008) on gold trends and distribution in the main pit suggest that gold is leached from oxidised material and undergoes supergene enrichment in the transition-oxide-sulphide zone thereby giving a weak subhorizontal supergene blanket. Looking at the gold grade distribution, there is a clear indication of gold concentration along the major north-south trending structures like the 4800 and 5400 zones, refer to figure 49 below.

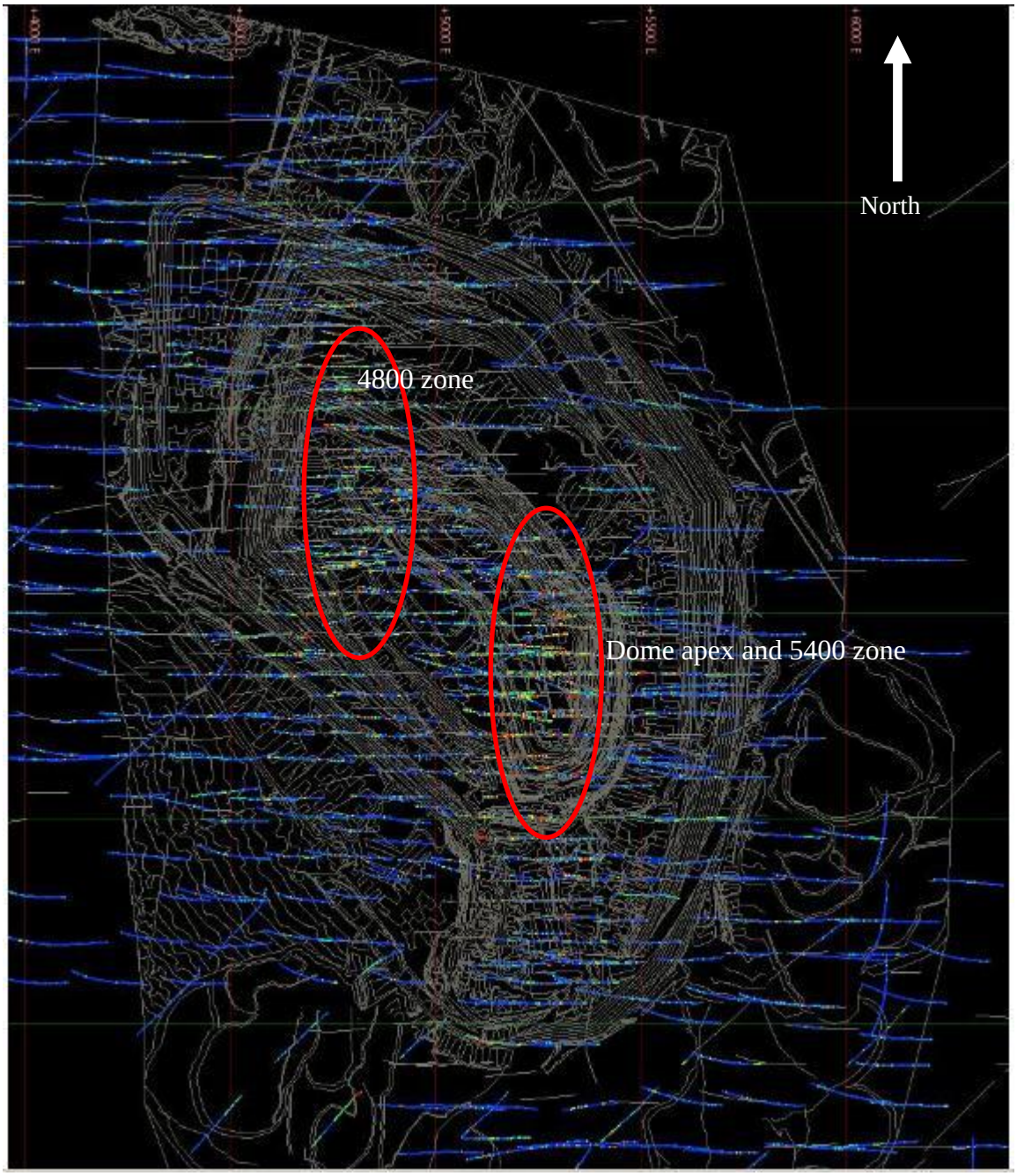

Figure 49. Gold grade trends in Main pit as represented by Au grades above 0.2g/t (red coloured areas). Blue represents areas with no Au grade. There's a clear concentration of Au along the major structural zones and the 'pimple' of the dome.

Gold is evident in selected high angle structures that cross-cut the dorminant copper trends, this is supported by the presence of a subtle east-west domain of elevated Au:TCu north of the apex of the Main pit dome, figure 50.

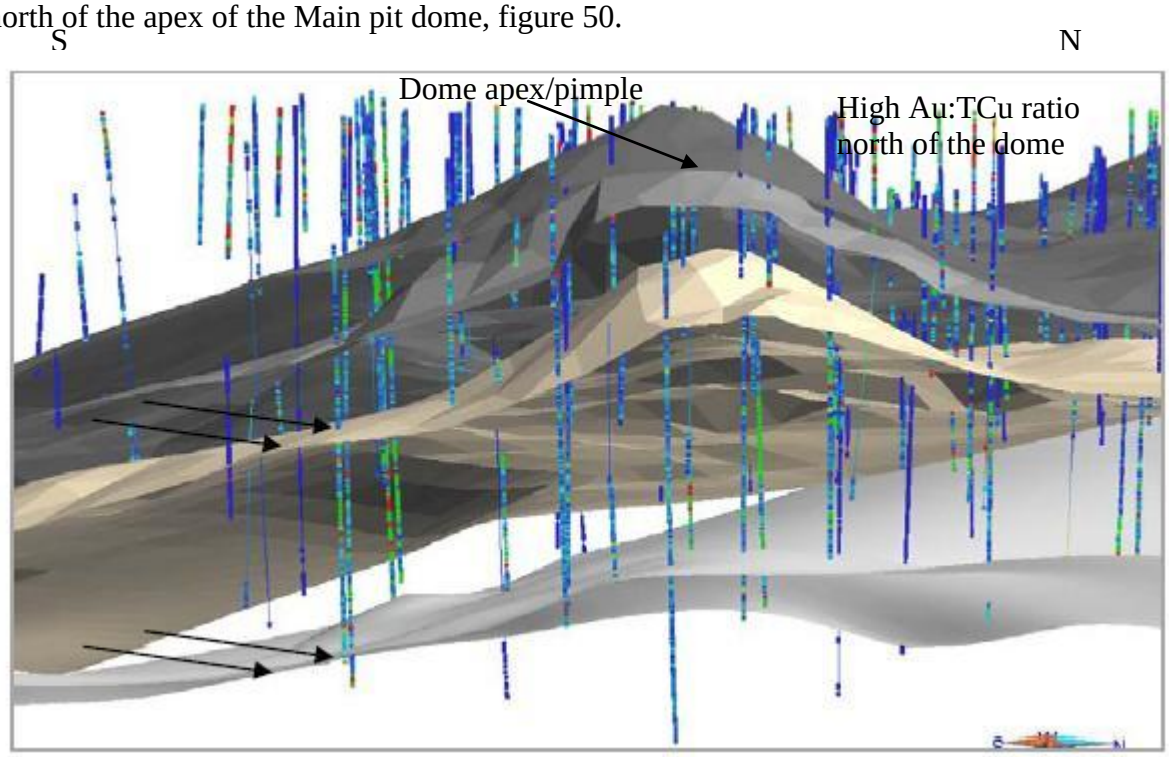

Figure 50. Section of the Main pit dome apex/pimple showing domain with high Au:TCu in the north. Looking west. (modified from Beeson et al., 2008).

Further work done by Cyprus (2000) suggests that host lithologies show a relatively consistent Au to Cu ratio of about 0.21, which compares with the known historical data. Previous suggestions that veins in UM2 and MMC1 units have higher ratios (~0.35) than do the veins lower in the section (~0.15) have been disapproved as averages for veins in all the stratigraphic units show a similar Au/Cu ratio. It can therefore be concluded that every percent of sulphide copper will carry in the order of ca. 0.2 grams of Au (average run of mine (ROM) grades of between 0.2 and 0.3g/t). This relates to the back calculated Au grades achieved on the processing plant. Correlation coefficients done during the prefeasibility study , between Au and Cu grades are reasonably good throughout the majority of the mineralized section ie UMC, UM and MMC where they range from 0.5 to 0.65. Au is more poorly correlated with Cu in the LCS and LM2 units within the lower part of the section (Cyprus Amax, 2000). Metal enrichment for Au and Cu does not

largely depend on stratigraphic horizon, except in certain portions of UMC and UM where the vein data sets are statistically too small. Metal partitioning occurs between knotted schists and phyllites, where veins in the MMC2 knotted schist characteristically show 3 to 4 times the Au and Cu enrichment over host rock, as compared to the phyllites in the other stratigraphic units. In knotted schists the mineralization is concentrated in the veins and the wall rock alteration-mineralization halo is sparse (Cyprus Amax, 2000). No recent work has been done to disprove this. These observations from the Cyprus Amax (2000) suggest that Au and Cu were mutually introduced during mineralization.

CHAPTER 6: GENETIC IMPLICATION FOR THE DEPOSIT

6.1 Introduction

The formation of sediment hosted stratiform deposits and the source of mineralisation in particular the CACB are topics of contention. Various genetic models have been put forward to explain their origin. It is recognised that these deposits generally consists of 3 lithostratigraphic units, continental red beds which act as the source of mineralisation, evaporites which act as transport and seals and reducing strata (hydrocarbons) which facilitate precipitation of the metal sulphides. Basin architecture is also critical in the formation of these deposits.

The widely accepted model for the formation of sediment-hosted stratiform deposits was proposed by Unrug (1988) which looks at hydrothermal fluid circulation. Vein-hosted deposits such as Kansanshi are believed to have formed from remobilisation of hydrothermal fluids through later stage metamorphism, compression and deformation in the Katangan basin. Work done by Hitzman (2000) on the CACB suggests that there's insufficient thickness of red beds to justify a viable source. Numerical modelling by Koziy et al. (2009) tends to suggest that high-salinity sedimentary brines, generated beneath a halite seal, develop convective hydrothermal plumes that penetrate into the crystalline basement, which could be a source for the metals.

6.2 Formation of Sediment hosted Copper deposits

Sediment hosted stratiform or stratabound copper deposit are defined as occurring within sedimentary basins, at the contact between sub aerial redbed sequences and overlying marine shales, siltstones, sandstone and carbonate rocks (Hitzman et al., 2010). These deposits generally consists of sulphide bearing zones (generally 3m thick) that are almost parallel to lithologies, however there're a few deposits that are dominated by undeformed high angle veins such as Kansanshi and Musoshi. There are typically three basins in the world that contain supergiant deposits which contain >24Mt of Cu (Singer, 1995) i.e.

- The Palaeoproterozoic Kodaro-Ukodan basin of Siberia (Udokan deposit),
- The Neoproterozoic Katangan basin of Central Africa (CACB deposits),
- The Permian Zechstein basin of Europe (Kupferschiefer deposit).

The origination of these deposits seems to occur after the oxygenation of the atmosphere at around 2400 Ma. This is represented in the graph below adapted from Hitzman et al. (2010) that compares metal Cu content and age of host rocks.

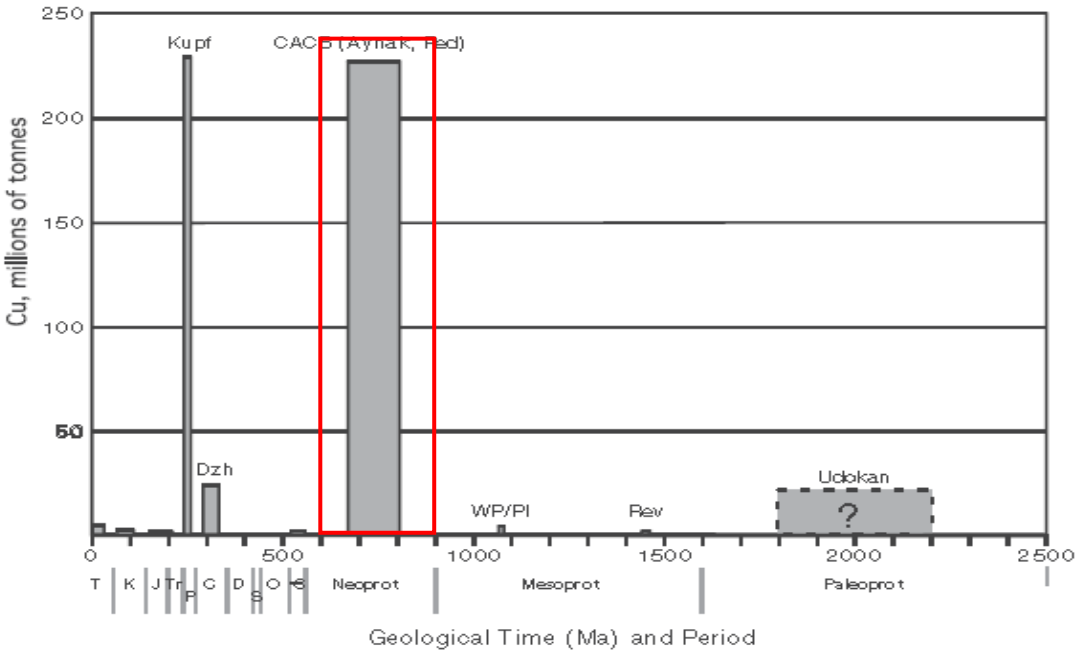

Figure 51. Metal content of sediment-hosted deposits plotted against age of host rocks. (modified from Hitzman et al., 2010)

Basin evolution is critical for ore-genesis within the sedimentary basins; therefore sediment-hosted stratiform deposits formed as a result of evolving basin or sub-basin scale fluid flow systems. The deposits evolved through process involving initial source of metals and S followed by presence of metal transporting fluids and transport paths and finally precipitation or 'trapping' of sulphides. The basin architecture for these deposits involved deposition of specific sedimentary sequence within an intracratonic basin that became hydrologically closed (Hitzman et al., 2010).

The stratigraphic sequence for these sediment hosted deposits consists of a basal sequence of synrift red beds with mafic volcanics that serve as a source of oxidised fluids (potential source of metals). This package is overlain by marine or lacustrine sediments deposited during rifting phases of sedimentation and is associated with an aerially extensive zone consisting of large amounts of reductant in the form of in situ organic matter or hydrocarbons (Hitzman et al., 2010). These units are overlain by thick, laterally extensive evaporate strata which act as seals to the underlying permeable units.

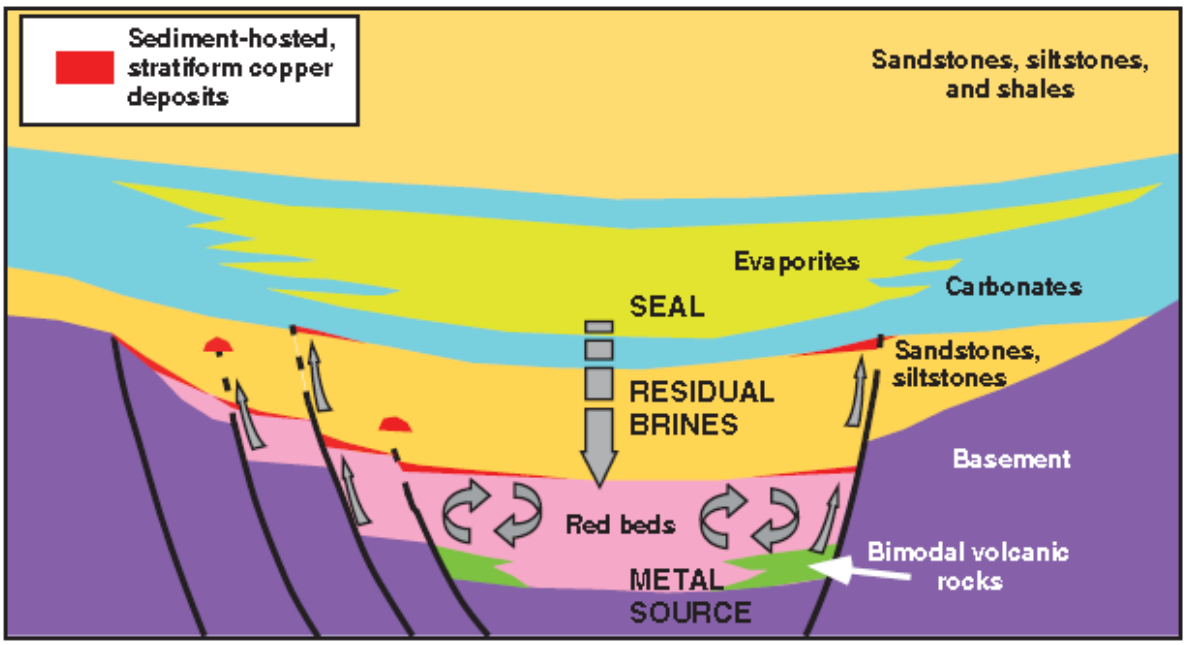

Figure 52. Schematic section of an intracratonic basin, host to sediment-hosted stratiform Cu deposits. (Hitzman et al., 2010).

In essence, sediment hosted stratiform deposits form when evolved basinal fluids leach significant amounts of Cu and other metals from the basinal synrift sediments. Structurally controlled fluid pathways form within the upper portions of the basement and fluid moves upwards to the evaporites (anhydrite). The fluids then interact with oxidation-reduction interfaces in marine sediments resulting in precipitation of metal sulphides.

Sediment-hosted stratiform deposit generally consists of 3 lithostratigraphic units i.e.

- Continental red beds (metal source)
- Evaporites (seal)
- Reducing strata (trap)

Formation of suitable basin through continental breakup (rift basin) has been observed as a critical factor in the formation of 'non-leaky' intracratonic basins capable of accommodating moderate-high salinity basinal fluids for long periods. Evaporite deposition is important for the formation of dense high salinity residual brines capable of leaching metals from the basal oxidised red beds and also to act as regional aquiclude/seal (Hitzman et al., 2010). According to Hitzman (2005), breaking of the evaporite seal during basin inversion allowing upward escape of potentially mineralising basinal brines to higher stratigraphic levels resulting in cross stratal sulphide. This concept has been

applied to the origin of higher stratigraphic deposits such as Kansanshi (Zambia) and Frontier (DRC).

6.3 Regional Genetic Models

Ore systems in sediment-hosted deposits are related to flow of fluids in sedimentary basins. According to Person and Garven (1994), two flow systems can develop in a sedimentary basin. The first type involves gravity driven fluid flow caused by early phases of rifting whereas the second type is through compaction of sediments. The latter fluid flow is characteristic of post-rift subsidence.

The formation of the CACB deposits is still a controversial topic and various models have been suggested. The mineral zonation model by Garlick (1961) and Fleischer et al (1976) proposed that mineral zonation occurred from shore to sea with Cu sulphides precipitating near shore (Cc, Bn, Cpy) whereas Py precipitated deeper in the anoxic waters. These deposits were later capped by evaporites upon desiccation of the basin (Pirajno, 2010). However this model has two major setbacks i.e. metal zonation requires that transgression of the sea should have occurred and that the highly soluble metals occur in the most basin wide position and that the metal bearing horizons extend into the overlying evaporites and oxidised layers.

The Sabkha model proposed by Renfro (1974) takes into account the presence of evaporites and fossil algal mats in sedimentary successions that host mineralisation. By definition, a sabkha is a coastal evaporite flat bordering a lagoon (Pirajno, 2010). The model utilises the presence of blue-green algae that normally forms algal mats which produce H_2S, CO_2 and CH_4 upon decay. The landward flowing marine water is usually enriched with the latter whereas the terrestrial meteoric waters tend to have high concentrations of the metals. The model therefore postulates that the metal bearing ground waters combine with S derived from the decay of the algal mats to precipitate sulphides; Mg in the sea water is responsible for dolomitisation of carbonate rocks (Pirajno, 2010).

The widely accepted model for the formation of sediment-hosted stratiform deposits was proposed by Unrug (1988) which looks at hydrothermal fluid circulation and combines with work that was done by Jowett (1986) on diagenetic brines and deep-seated fluids. The proposed model by Unrug (1988) takes into account a unified framework of rift

tectonics, associated basin evolution and hydrothermal fluid development (Pirajno, 2010). The model looks at formation of stratiform and vein mineralisation separately.

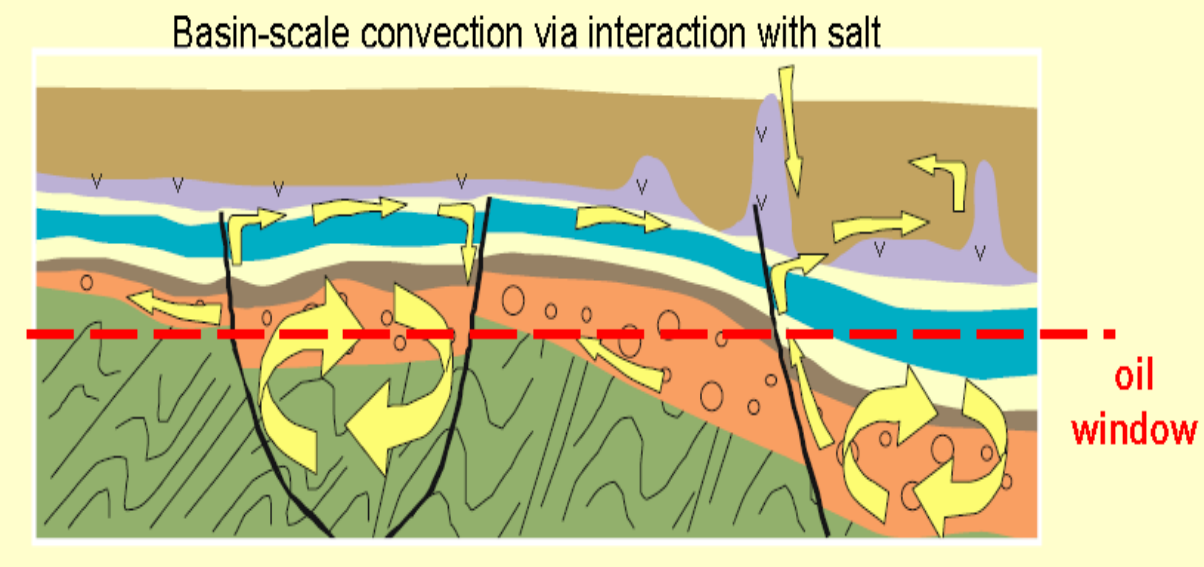

Figure 53. Regional genetic model for CACB deposits involving widespread circulation of residual brines and/or dissolution of evaporites. Basin-bounding faults provide cross-stratal permeability and the Basement is a potential metal source. Organic rich portions of stratigraphy pass into oil window and result in precipitation of sulphides at multiple REDOX interfaces throughout basin. (Hitzman, 2005)

Stratiform mineralisation within the Katangan basement, dominantly occurring below the Grand Conglomerat, was emplaced in early Kundelungu time by convection recirculation of basinal brines driven by thermal gradient across the basin (Unrug, 1988). Numerical modelling studies done by Brown (1984) and Jowett (1986) indicate the necessity for head and thermal gradients across the basins which are critical for brine recirculation. The interaction of the early diagenetic primary pyrite mineralisation with metal rich brines acted as a metal trap and experienced replacement of pyrite with Cu and other metal sulphides. Unrug (1988) suggests that the polymetallic nature of the CACB deposits can be attributed to igneous and volcaniclastic activity during rifting as being the source of the metal. This is supported by the occurrence of metasomatic alteration on clasts of volcanic rocks owing to hydrothermal processes. The second rifting event which was associated with rapid subsidence and faulting in the basin gave rise to compactional dewatering which was responsible for the second pulse of metal rich brines in the basin (Unrug, 1988). An elevated heat flow owing to a regional thermal event based on basin evolution resulted in fluid recirculation within the Roan Group and emplacement of stratiform mineralisation. It is believed that the mineralisation was emplaced prior to

folding and metamorphism and that the metals (Cu, Co, U, Au, and Mo) were introduced into the basin at a later stage of diagenesis (Pirajno, 2010). Later stage metamorphism, compression and deformation of the Katangan sequence gave rise to renewed hydrothermal activity (metamorphic fluids). This could have been responsible for the vein-type mineralisation found in some deposits of the CACB e.g. Kansanshi.

Vein-hosted deposits of the CACB are characteristically associated with metamorphism and deformation of the Pan African/Lufilian Orogeny, late faults that postdate folding and thrust sheet formation. Vein deposits occur higher up in the stratigraphy owing to fault systems that enabled ore fluids to be transported beyond the impermeable Grand Conglomerat. Fluid inclusion studies done on the two types of mineralisation indicate the mineralisation pulses were different (Unrug, 1988).

6.4 Localised Genetic Models

The simplified genetic model for the Kansanshi deposit involved the three key processes of source, pathway/conduits and traps refer to figure 54.

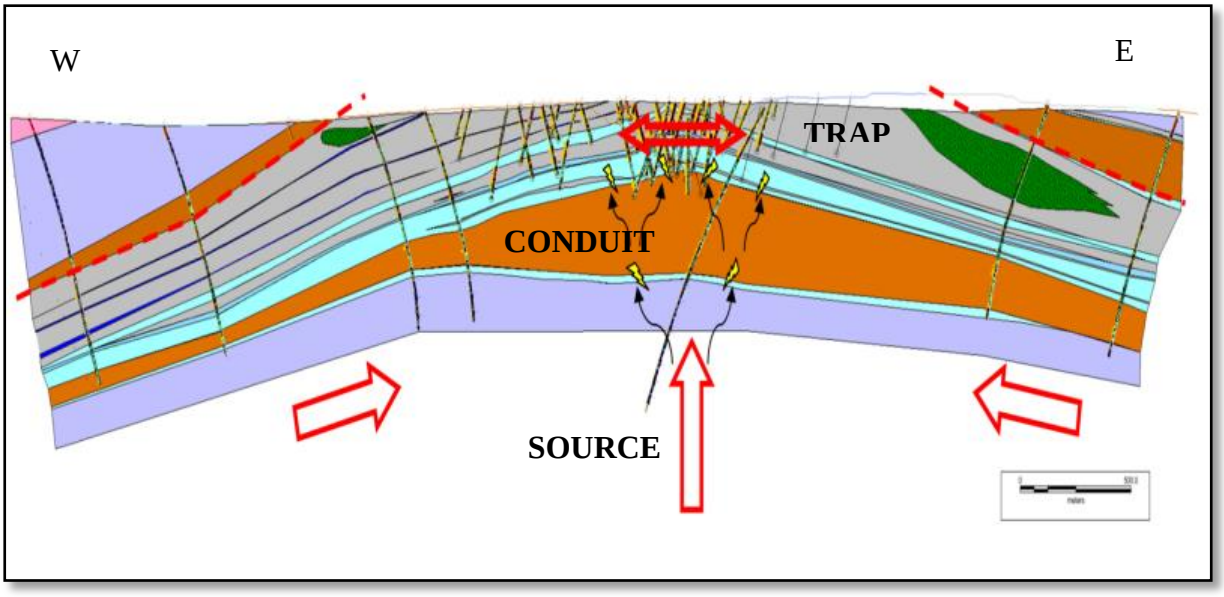

Figure 54. Simplified Genetic model for the Main Pit (modified from Fourie et al., 2012)

The model envisages an oxidising Cu enriched fluid source at depth. This is followed by fluid migration through overlying stratigraphic units. Redox reactions at the highest point of the domal structure resulted in precipitation of Cu.

Work done by the Jigsaw team in 2008 which involved pit mapping, relogging of core and 3D modelling, managed to come up with an understanding on the mineralising

system in the Kansanshi deposit in particular the Main pit. Two models were proposed based on structural work that was done.

6.4.1 Fold-Thrust belt model

This model looks at evidence for compressional deformation and suggests that north-northeast-directed thrusting is the primary cause for folding, faulting and mineralisation.

The model proposes that fluid mixing is primary for mineralisation. Secondary permeability through thrusting enabled the migration of Cu-enriched sulphate fluids from the basal units upwards into the Nguba Group. Interaction of these fluids with hydrocarbons within stratabound domains resulted in precipitation of Cu (Beeson et al., 2008). The fault systems and domal architecture provide suitable trap sites for mineralisation.

According to Beeson et al. (2008), the model consists of the following critical components;

- Moderately-gently southwest dipping thrust fault exhuming basement rocks to the southwest.
- Several synthetic footwall escape thrusts penetrating northeast into the Kundelungu Group.
- Anticlinal folds developed hangingwall to thrust faults with axial planes trending northwest-southeast. Doming of the anticlinal folds reflecting either gentle refolding about northeast axes or differential movement along basal thrust zones.
- Steeply-dipping transfer faults trending northeast-southwest that act to compartmentalise stratigraphy, strain and fluid flow.
- A thick and inhomogeneous sequence of Kundelungu Group rocks, including reduced sedimentary sequences (carbonaceous shales with connate methane-bearing fluids), non-carbonaceous clastic rocks and dolomitic carbonate units

- Basal ‘red bed’, locally evaporitic sedimentary sequence containing connate sulphate-bearing fluids. These fluids are assumed to be enriched in copper.

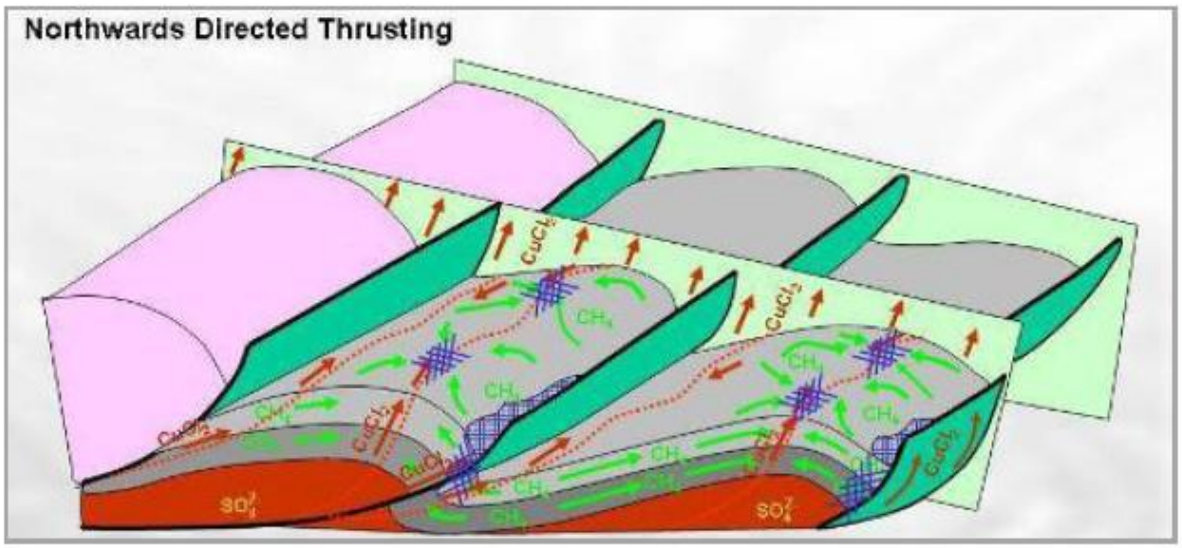

Figure 55. Sketch of fold-thrust model for mineralisation at Kansanshi (Beeson et al., 2008)

6.4.2 Extensional Fault-fold model

This is an alternative mineralisation model based on extensional fault-fold systems. The model considers the absence of upright fabrics, recumbent folds, crenulation cleavage and sub-vertical veining to infer a dominantly extensional environment for both ductile and brittle events.

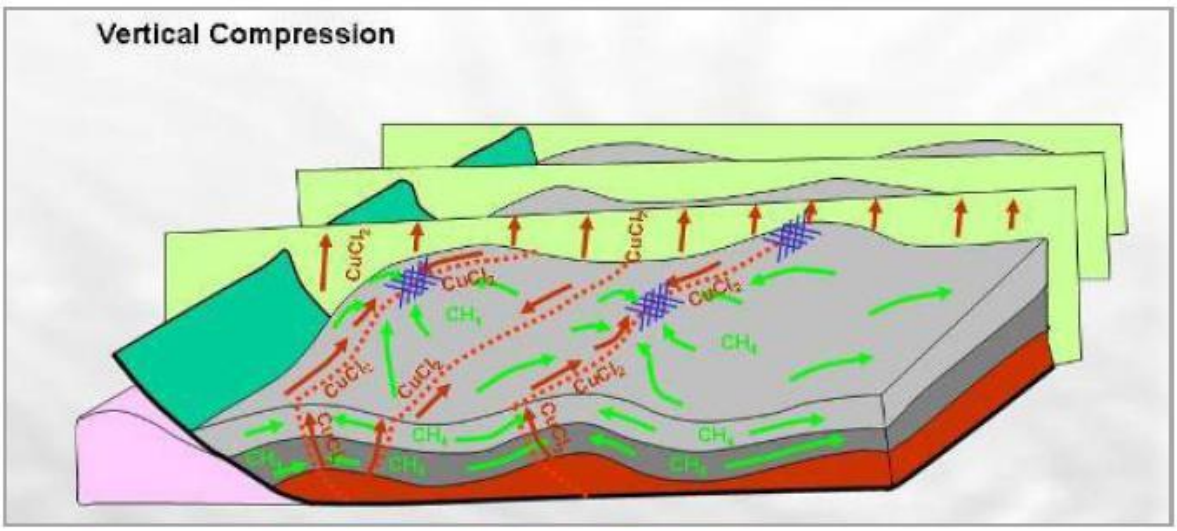

Figure 56: Sketch of fault-fold model for mineralisation at Kansanshi (Beeson et al., 2008)

The model also accepts that fluid mixing is critical for mineralisation. Secondary permeability during extensional faulting enabled the migration of Cu-enriched sulphate fluids from the basal units upwards into the Nguba Group. Interaction of these fluids with hydrocarbons within stratabound domains resulted in precipitation of Cu (Beeson et al., 2008). The fault systems and domal architecture provided suitable trap sites for mineralisation, based on fluid migration initially into fault system and then into anticlinal domes.

Recent work on the Kansanshi deposit by Beeson et al. (2013) has unearthed interesting findings and has brought better understanding or alternative ideas of controls on mineralisation especially in the Main pit. The findings suggest that the structural architecture of the Main pit consists of major low angle structures that are controlling distribution of mineralisation beneath the pit. Low angle faults were discovered which are suspected to have served as major fluid pathways during mineralisation of the pit.

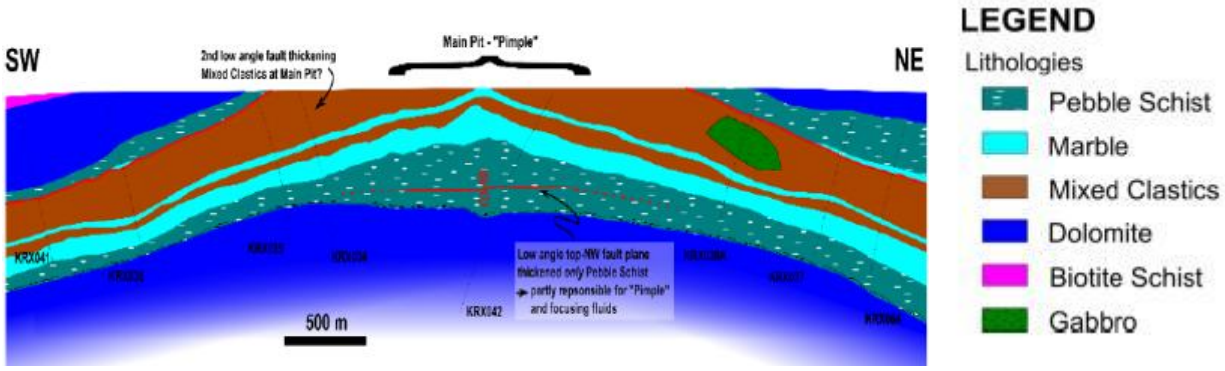

Figure 57. Section through the Main pit showing thickening of the PS and clastic units (Beeson et al., 2013)

Thickening of the Pebble Schist around the dome apex owing to the low angle structure (figure 57) is believed to have an influence on the mineralising fluids as evidenced by the reduction in Cu grade from the dome apex to the fringes of the pit. Recent findings by Beeson et al. (2013) identified drag folds and related low angle shear/faults as being responsible for thickening of favourable units (PS, clastics) and also acting as conduits for mineralising fluids. Ductile shear failure within the units through supra-lithostatic pressure led to the omni-directional distribution of veins, however larger veins are suspected to have formed in a steeply dipping orientation, perpendicular to foliation and bedding (Beeson et al., 2013). Permeability parallel to foliation and bedding allowed

mineralising fluids to migrate along many different planes resulting in smaller veins and disseminated mineralisation. On the other hand, large steep veins were formed either through fluids following few and short steep structures or fluid was able to create its own pathway. This however depended on the fluid pressure.

6.5 Source of Metals

The presence of widespread mineralisation within the CACB requires justification for a source for all the abundant metals. However this issue has not been fully addressed. Various schools of thought have been proposed and will be highlighted below. According to Unrug (1988), the metals especially Cu and Co were introduced into the basin at a later stage of diagenesis and replaced the earlier formed pyrite. Fluid inclusion studies done on dolomites of the Kamoto deposit in the DRC, suggest that there was circulation of dense brines during diagenesis. The temperature of the mineralising brines was estimated at between 200 and 250°C (Pirmolin, 1970). However fluid inclusion studies on the Kansanshi deposit by Torrealday (2000) suggest that the Kansanshi inclusions were derived from deep circulating, highly saline fluids in excess of 350°C, which is consistent with fluids, derived from greenschist-amphibolite facies of metamorphism experienced within the Domes region.

The source of Cu and other metals in the sediment-hosted stratiform deposits is generally considered to be red bed clastics located stratigraphically below the deposit, however work done by Hitzman (2000) on the CACB suggests that there's insufficient thickness of red beds to justify a viable source (Koziy et al., 2009). Numerical modelling on the CACB deposits suggest that high-salinity sedimentary brines, generated beneath a halite seal, develop convective hydrothermal plumes that penetrate through the red beds, deep into the crystalline basement, despite its low permeability and regardless of the availability of cross-stratal conduits (Koziy et al., 2009) . This proposes that the deep seated basement could be a potential source for metal in the Katangan basin.

CHAPTER 7: EXPLORATION IMPLICATION FOR THE DEPOSIT

7.1 Introduction

Exploration for Kansanshi-type deposits within the CACB will require the systematic use of magnetics, geochemical surveys, radiometrics and an understanding of weathering and soil profiles (Broughton et al., 2002). Aeromagnetic studies are critical for stratigraphic correlation and for identifying structural traps, figure 61 and 62. U and Th bearing minerals in the veins at Kansanshi make radiometrics a very suitable technique for delineating the veins. Geochemical and geophysical studies identify targets or anomalies which can be tested with drilling. This is followed by interpretation of structures and geology to form models which are in turn used in the calculation of mineral resource estimates (MRE).

7.2 Historical and Current exploration considerations

With the inception of full scale mining on the Kansanshi deposit by First Quantum Minerals in 2004, exploration has been fairly limited to drilling. However, minor pilot geophysical studies were carried out. Earlier exploration work included both geochemical and geophysical programmes by Cyprus Amax. An initial detailed airborne geophysical survey, sanctioned by Cyprus Amax Zambia was flown over the Solwezi area in 1997; the results and interpretation are found in a PhD report by Barron (2003). FQM has since done a number of geophysical surveys from 2007 to 2010 as a follow to the work done by Barron (2003).

Current exploration activities (brown fields) around the Kansanshi deposit have been focussed on the following key objectives;

- To understand and clearly define the Kansanshi antiform structure,
- To determine extents and controls on mineralisation,
- To determine and apply effective geophysical methods,
- To investigate the possibility of related domes along the Kansanshi antiform,
- To investigate the link between trace geochemistry and mineralisation.

Information from the brown field exploration activities feeds into targeting and further delineation of the Kansanshi resource (Main and NW pits, South East and Rocky Hill targets).

Geophysical techniques such as magnetics and radiometrics have been applied to identify structural traps for mineralisation and as a means for correlating stratigraphy. Uranium (uraninite, brannerite, zircon, sphene and apatite) and thorium (monazite, zircon, thoranite, uraninite, sphene and apatite) bearing minerals in the mineralised veins form a prominent radiometric anomaly. This property has been applied in recent investigations on vein characteristics. Generally the mineralised zones within the Kansanshi deposit are characterised by a positive U-Th anomaly and a negative K anomaly (Broughton et al., 2002), refer to section7.3.3.

In 2007, FQML undertook a time domain airborne electromagnetic (EM) survey over 107 km² of the Kansanshi Mining lease area. The EM exercise managed to pick out anomalies that coincided with domes. In September 2009, a Controlled Source Audio-Frequency Magnetotellurics (CSAMT) survey was conducted to image the sulphide veins that trend N-S in the Main pit. The survey did not pick out the veins; however it managed to define the carbonaceous phyllite units. In November 2010 a high resolution aeromagnetic and radiometrics survey was flown over 110 km² of the Kansanshi lease area. These surveys generated high resolution magnetic and radiometric images that have been used to refine the surface geology of the mining lease area.

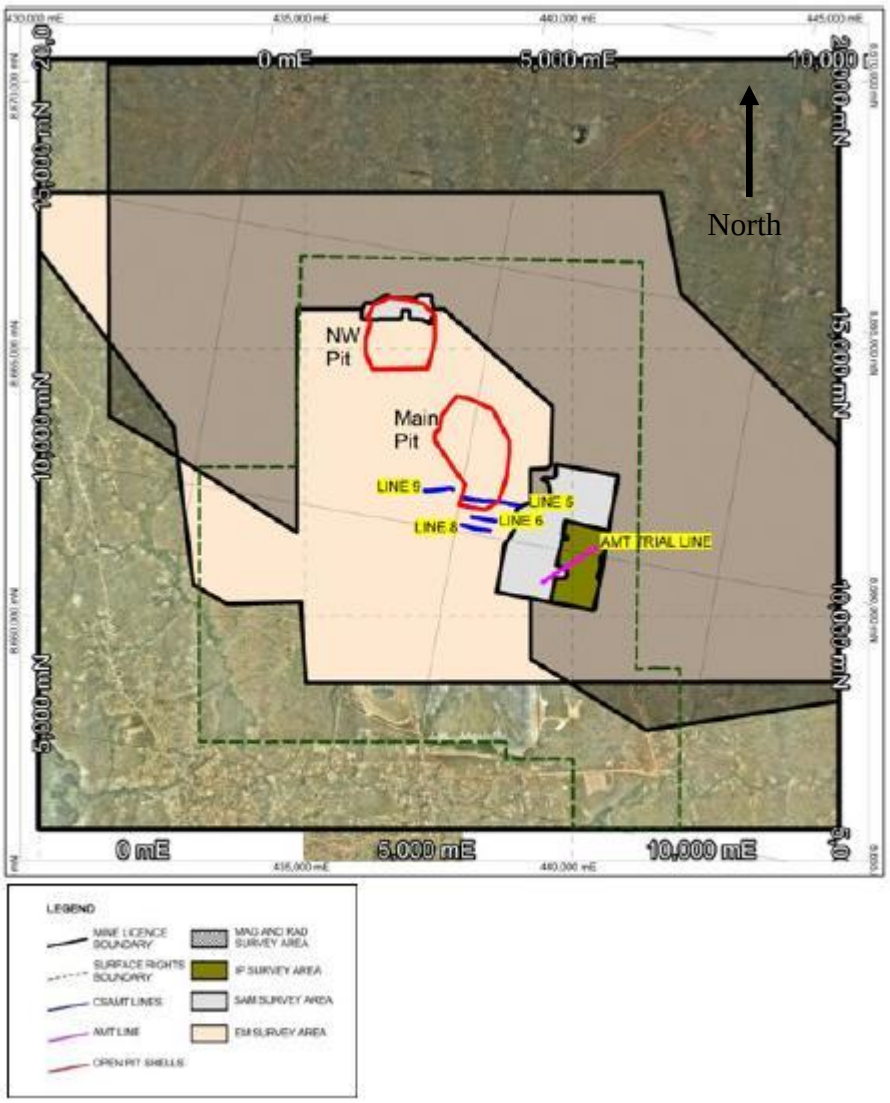

Figure 58. Location map of Geophysical surveys done in the Kansanshi Mining lease area (Titley, 2012)

Not much geochemical surveys were conducted post 2000. A geochemical sampling programme consisting of 5,170 samples on 800m x 100m centres on EW sample lines covering approximately 417km^2 was completed by Cyprus Amax in the late 1990s. Prior to that, ZCCM carried out a geochemical survey consisting of 5,518 samples on 30m x 300m centres on EW sample lines covering approximately 50 km² (Hanssen, 2010).

7.3 Geophysical Techniques

A number of geophysical techniques have been applied to the Kansanshi deposit as stated above. These will be reviewed in more detail below.

7.3.1 Electromagnetic Surveys

Electromagnetic systems can be broadly divided into two categories i.e. Time-domain (TEM) where measurements are done as a function of time and Frequency-domain where measurements are done at one or more frequencies. EM systems have a wide range of application not necessarily in mineral exploration. These include environmental studies (ground water contamination), mapping geology and or soil profiles, locating buried objects or cavities. EM systems have been applied at Kansanshi predominantly for exploration purpose but can also be applied to other facets of mining such as hydrogeology studies and rock mechanic evaluations. Electromagnetic surveys are based on induction of primary magnetic fields; detection is on secondary magnetic fields from near surface conductors. EM surveys do not require electrodes in the ground, so can therefore be done faster and cover more ground. They can also be applied in down hole geophysics logging. This technique however has limitation on the depth of investigation depending on the frequency used and requires technical expertise for interpretation of results.

The general principles for EM surveys involve;

1. Generating an EM field by passing an alternating current (AC) through a wire coil (transmitter) generates a primary field which is applied in pulses of 20-40 milliseconds.
2. The EM field propagates above and below surface.
3. In the presence of conductive material in the ground, the magnetic component of the EM induces eddy current in the conductor.
4. The eddy currents produce a secondary EM field which is detected by the receiver.

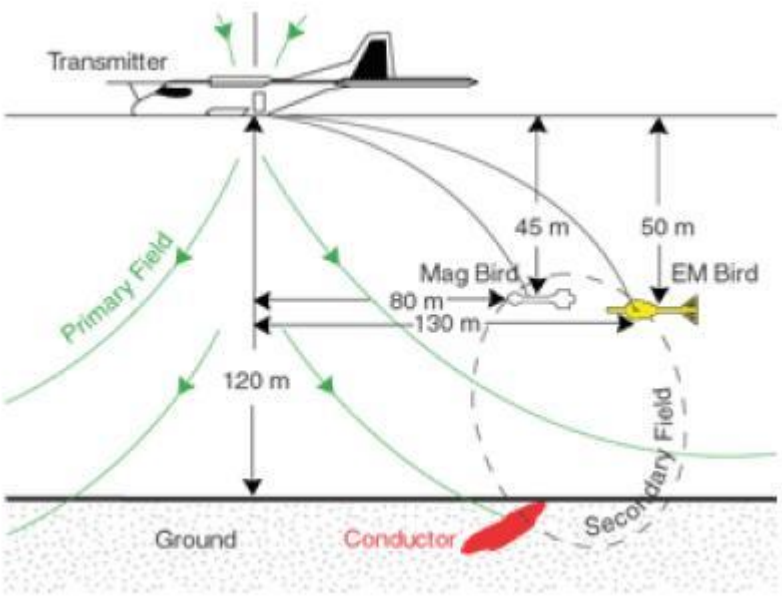

Figure 59. Generalised EM survey setup (Geophysics 424: Time domain EM)

The image of the EM survey that was done over Kansanshi is represented in figure 60 below;

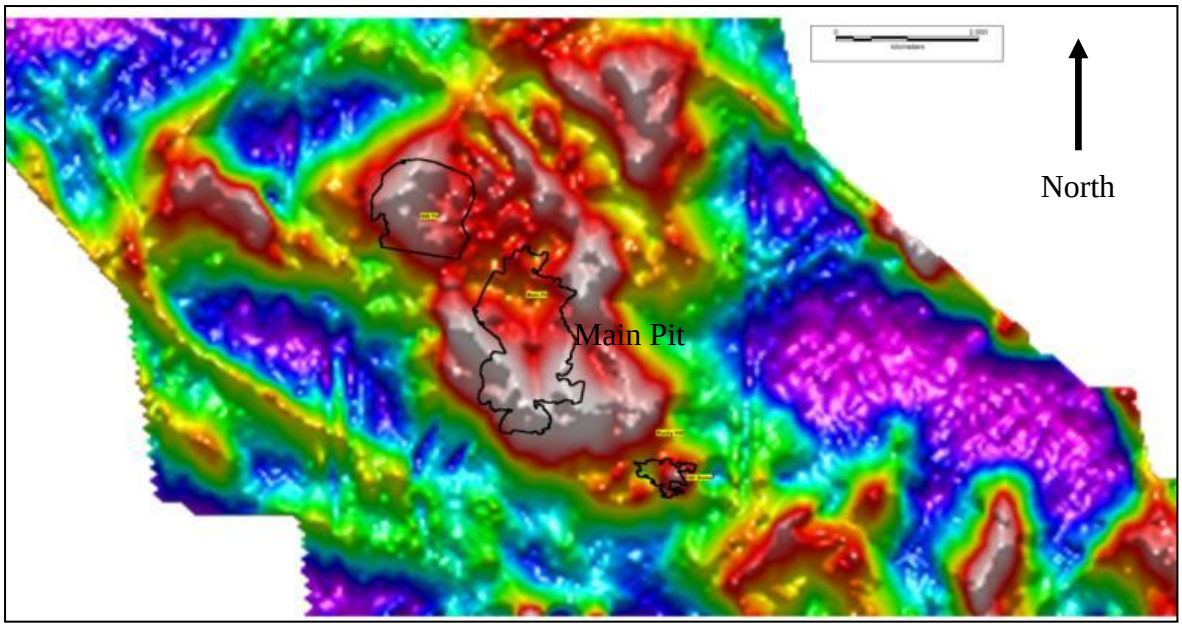

Figure 60. Image of electromagnetic survey done on the Kansanshi Mining Lease area (Fourie et al., 2012)

The image represents highly conductive units within the bounds of the main Kansanshi deposits i.e. Main and NW pits. The highly conductive units are represented by thick carbonaceous phyllite.

7.3.2 Aeromagnetic Surveys

The primary purpose of aeromagnetic surveys is to investigate the subsurface distribution of various lithological units based on measured anomalies in the earth's magnetic field due to variations in magnetic properties and geometry of underlying rocks (Barron, 2003). The fundamental principal of aeromagnetic surveys is that they reflect almost exclusively the distribution of magnetite and pyrrhotite in rocks. Magnetic anomalies are as a result of contrast in magnetic properties in adjacent geological units. Total Magnetic Intensity (TMI) data can therefore be used to infer the geometry and magnetic properties of the underlying magnetic bodies, figure 62. The latter data is used to construct a TMI map as represented below;

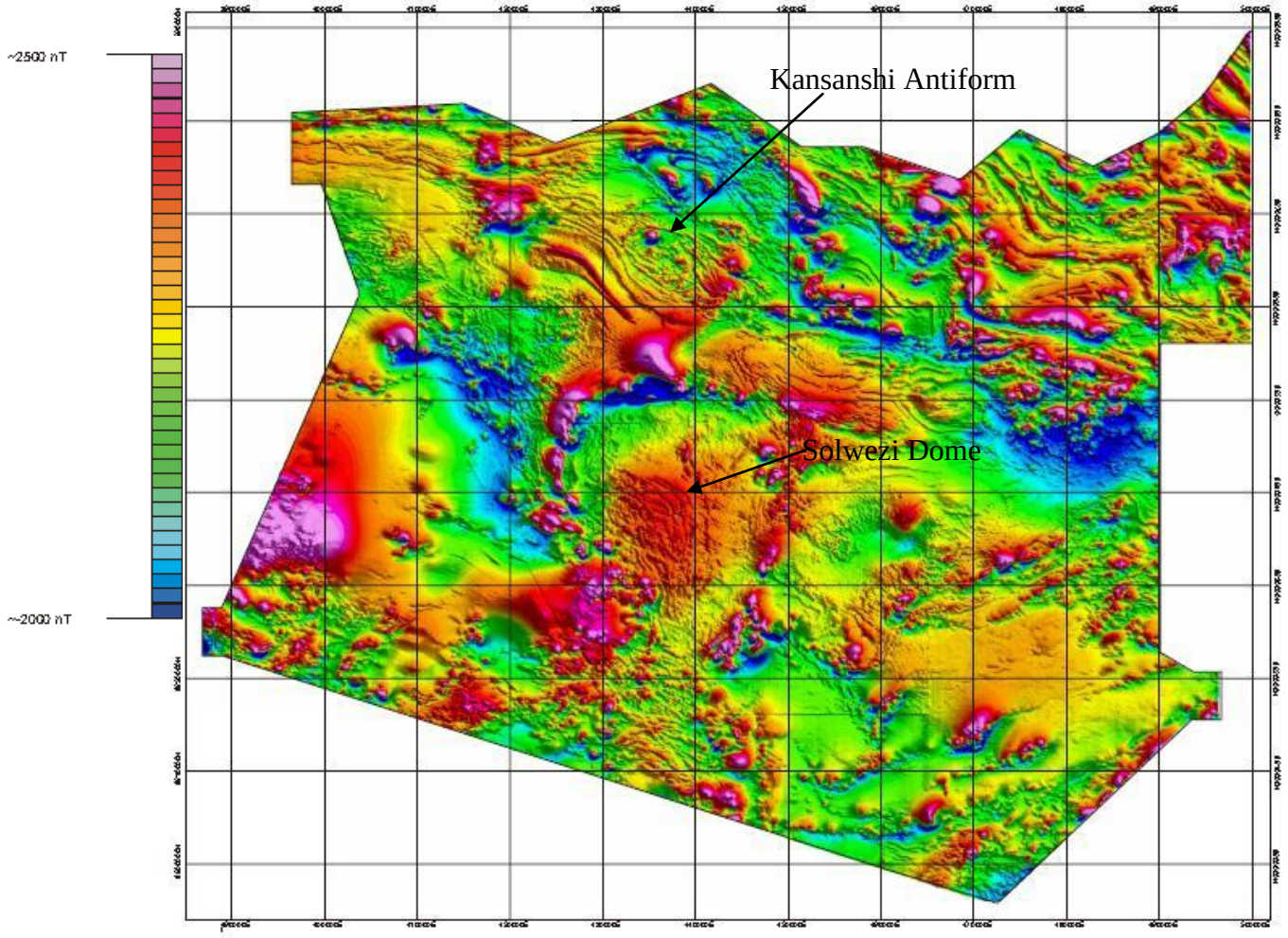

Figure 61. Total Magnetic Intensity image of Solwezi area showing Kansanshi Antiform and Solwezi Dome (modified from Barron, 2003)

In essence the TMI image represents high magnetic anomalies as hot magenta and red colours and low values as dark to blue colours (Barron, 2003). Barron (2013) highlights

that TMI images are good first approximation of the magnetic signature and don't reflect the complex relationship between the total field intensity magnetic anomaly and the corresponding magnetic bodies. Therefore TMI cannot be used for interpretation but just as a guide. Application of mathematical algorithms on the TMI data results in a Reduced to Pole (RTP) image which represents readjustment of the shape and location of the magnetic anomaly to a position directly over the magnetic bodies, figure 63 (Barron, 2003).

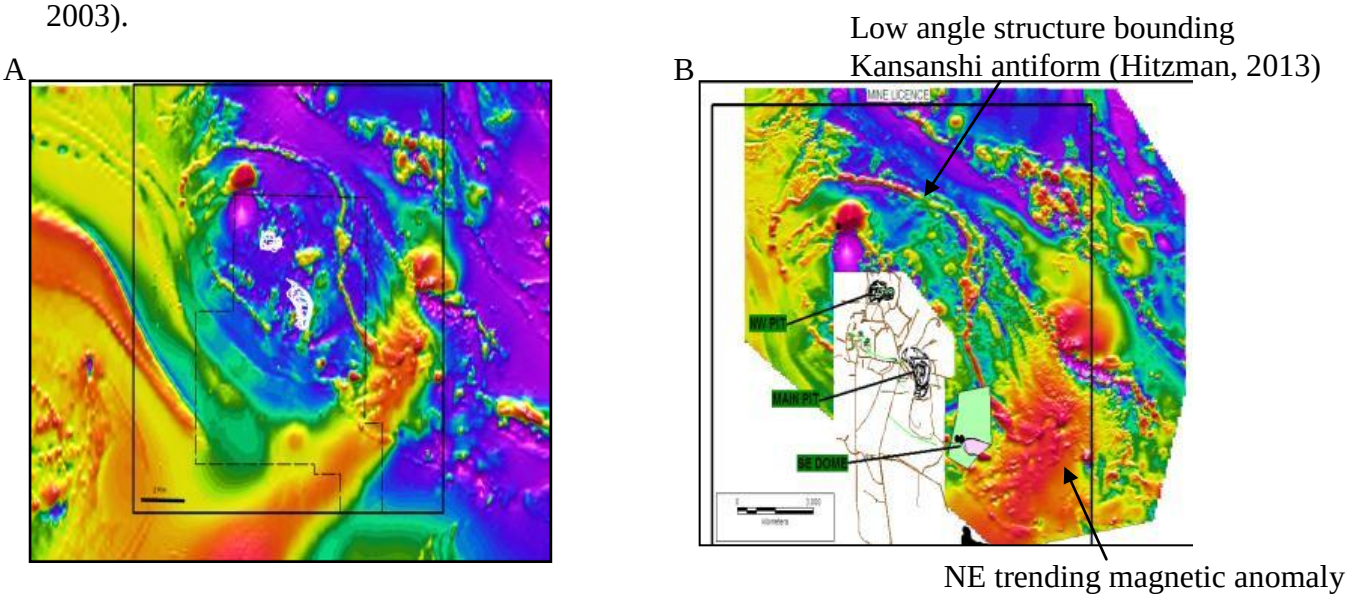

Figure 62. RTP images from (A) 1997 survey and (B) 2010 survey (modified from Fourie et al., 2012)

The images represent more or less the same features. The 2010 survey give better resolution, possibly due to better flight controls and interpretative technology. The images basically outline the trend of the Kansanshi Antiform (represented by current deposits being mined). Hitzman (2013) has interpreted the NE trending magnetic anomaly as a possible result of a deeply buried gabbroic (mafic) intrusive rock that intruded along an early normal fault zone.

As highlighted above, aeromagnetic surveys are ideal for mapping geological attributes such as lithology, structure, alteration, metamorphism and mineralisation. These surveys can be applied to poorly exposed terrains to interpolate between outcrops and in covered areas to provide some geological control.

7.3.3 Radiometrics Surveys

The presence of K, U-Th bearing minerals in the Kansanshi makes radiometrics surveys ideal as an exploration technique. The three isotopes of ^{40}K, ^{238}U and ^{232}Th are capable of

emitting gamma ray with enough intensity to be detected by can be airborne detectors. This property can therefore be used to map the variation in levels of K, U and Th in rocks and weathered material.

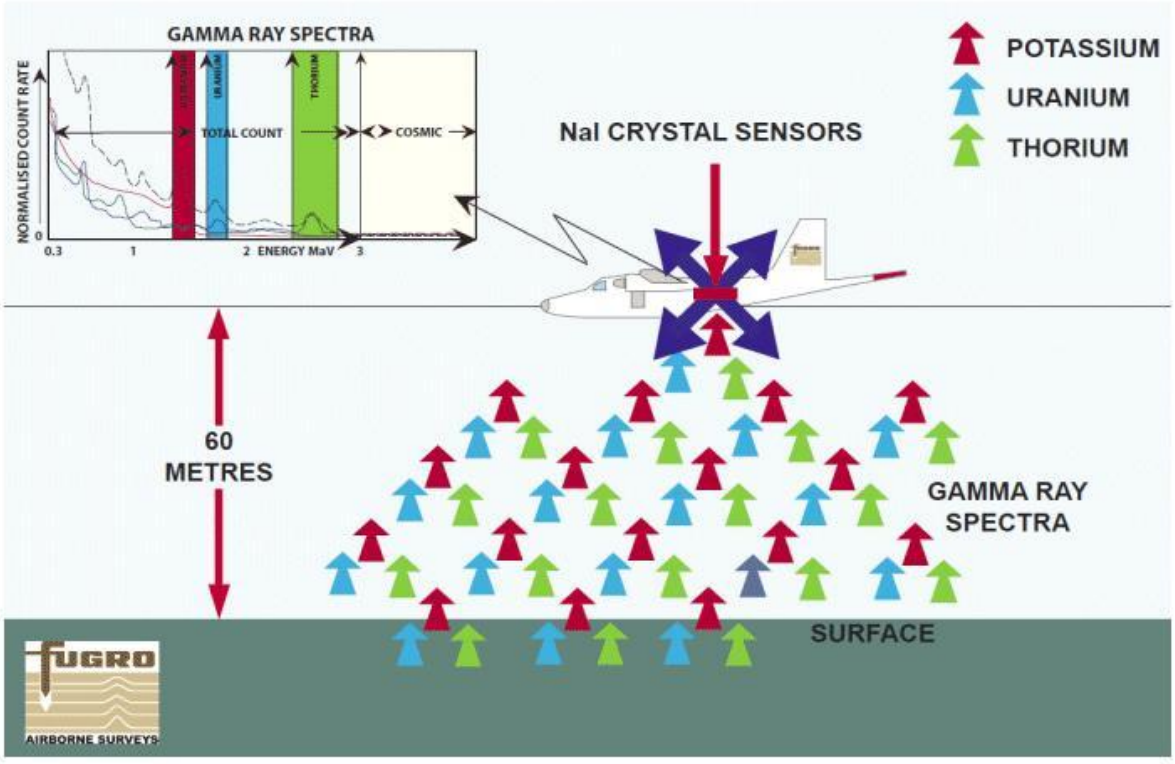

Figure 63. Schematic of airborne radiometric surveys (http://spatial.agric.wa.gov.au/geophysics/radiometrics.asp)

Radiometrics is primarily used for determining lithological domains based on the radioactive element composition (K, U, and Th) of surface geological materials. This results in a ternary image (generated by assigning values for K, Th and U to the red, green and blue bands of a colour image) which is used to produce a pseudo lithology map. Within the Solwezi area, K bearing minerals (biotite, muscovite, orthoclase, microcline, hornblende and scapolite) are associated with biotite/muscovite schists, biotite/muscovite gneiss, phyllites, granite and biotite ±hornblende calcareous quartzite. U bearing minerals (uraninite, brannerite, zircon, sphene and apatite) on the other hand indicate areas of granite, CBPH, schist, migmatitic biotite gneiss. Th bearing minerals (monazite, zircon, thoranite, uraninite, sphene and apatite) are associated with areas with granite, carbonates, QFMS and micaceous quartzite.

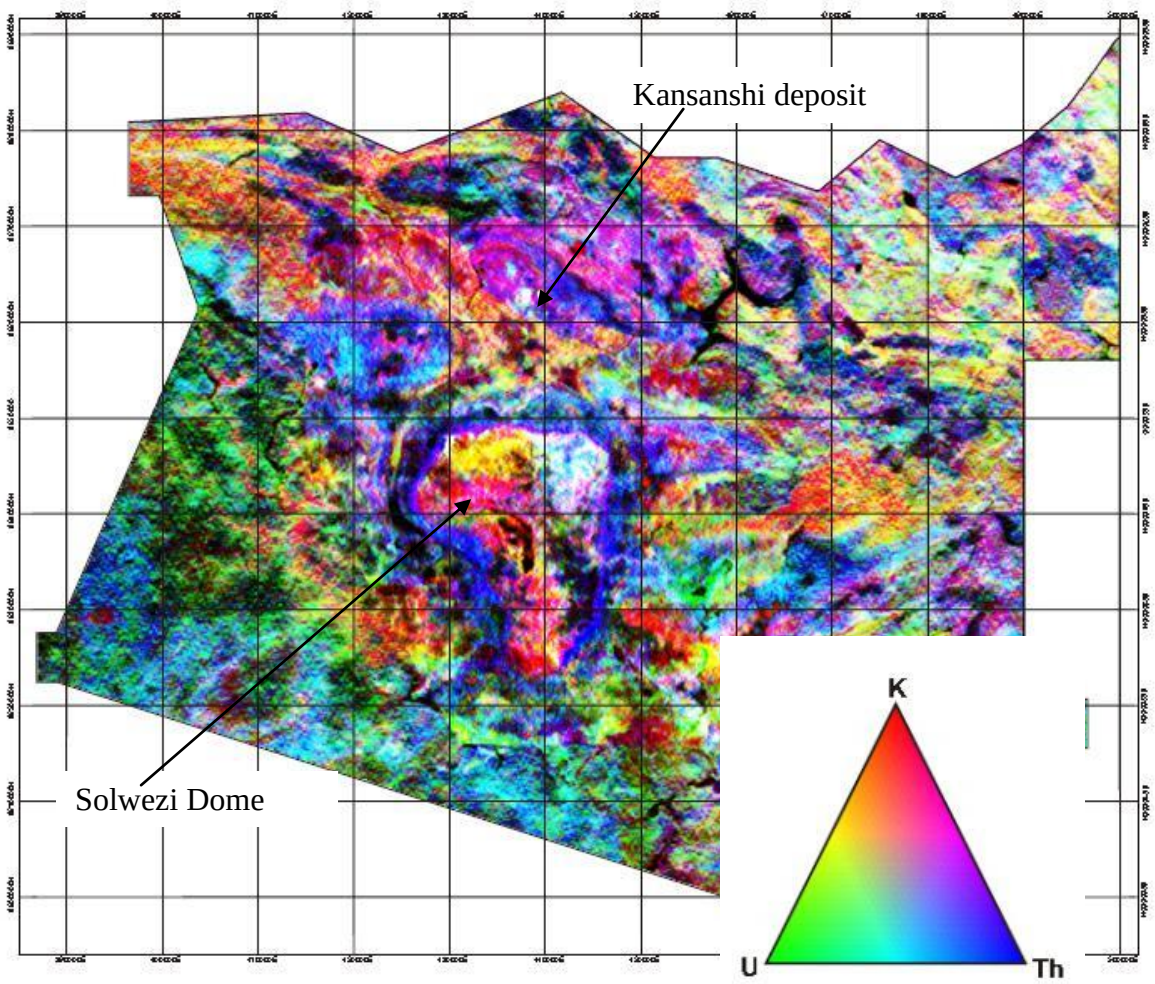

Figure 64. Ternary image of K, U, Th of the Solwezi area showing the Kansanshi deposit and the Solwezi dome, reds are potassium rich areas, green are uranium rich areas and blue are thorium rich areas. (modified from Barron, 2003).

The area around the Kansanshi deposit shows an accumulation of K, U and Th, however there is a dominance of thorium and potassium, figure 64. This is supported by Barron, 2003 findings of a Th high around Kansanshi Mine.

Radiometrics as an exploration technique has it's shortcomings as it is not effective when bedrock is covered by thick soil, laterite, alluvium or water. Vegetation and wet weather has a negative impact on the effectiveness of the technique, therefore will not be adequate in tropical-semi tropical terrain (Barron, 2003).

7.3.4 Other geophysical techniques applied to the Kansanshi deposit

A Controlled Source Audio-Frequency Magnetotellurics (CSAMT) survey, which essentially is a deep-seeing electromagnetic method with uses a distant electromagnetic

source, up to 10km away, and a moving receiver to image the two-dimensional conductivity (or resistivity) of the shallow crust beneath the receiver. The exercise was conducted so as to confirm whether the method is capable of imaging the semi-massive (to blebby) sulphide vein swarms which strike N-S though the main pit and their extension to the south (Selfe, 2009). The technique was not able to pick out the veins as anticipated owing to the nature to the veins which were not massive enough to facilitate flow of induced electric current (Selfe, 2009).

A gradient array Induced Polarisation (IP) survey was done in August and September 2010 on the south east of Main pit. The primary objective of the exercise was to test the suitability of the technique in identifying veins which host copper mineralisation. The exercise was therefore designed to test the the potential of resistivity to map the slightly more conductive weathered zones as much as the ability of IP to detect the mineralisation directly. The main outcome of the survey was the ability of resistivity to map the outline of the SE dome as conformation of the airborne EM survey done in the area (Selfe, 2011).

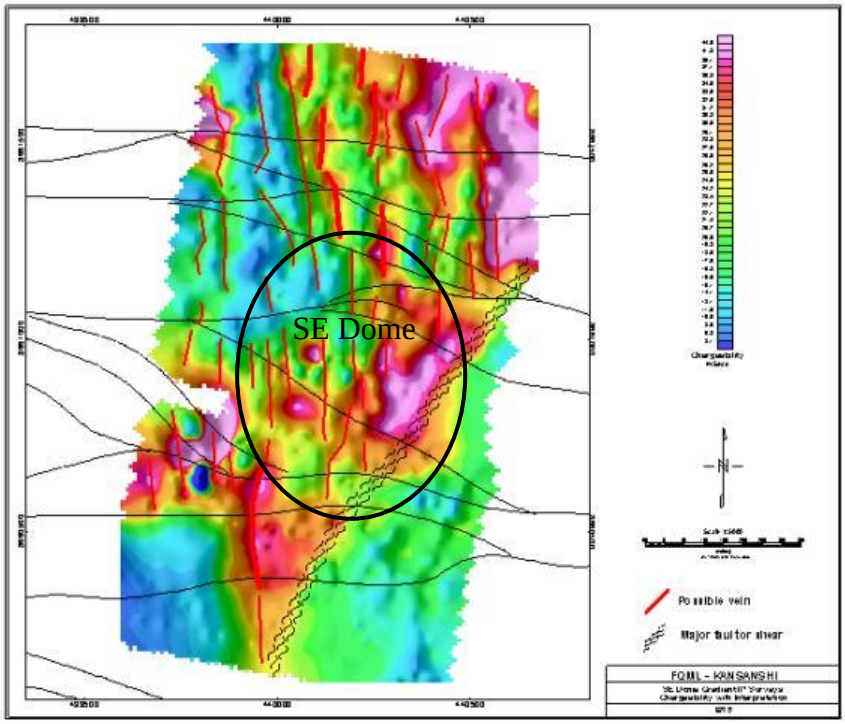

Figure 65. Chargeability image of the SE Dome area showing fault/shear zones (black) and possible mineralisation trends in red. (Selfe, 2011).

Downhole geophysical logging was done on 6 holes from south of Main (SE Dome). The purpose of this exercise was to measure and record physical properties for the various rock-types present and to ascertain which surface geophysical techniques would be most suitable for direct detection of the mineralised veins (Selfe, 2010). It was observed from this exercise that carbonaceous phyllite responds strongly in terms of both IP and

conductivity where ca. >2% disseminated sulphides are present. IP seems to respond well in the presence of pyrite as opposed to pyrrhotite (Selfe, 2010). It was also observed that large veins tend to have a positive response to EM as opposed to IP.

7.4 Geochemistry

Earlier exploration work around Kansanshi mine involved geophysical surveys (prediction) and to a lesser extent geochemical studies (detection). Geochemistry involves the systematic measurement of one or more chemical elements or compounds on naturally occurring material such as rocks, stream sediments, soils etc. Mineral deposits like Kansanshi, Sentinel, Nchanga or Kamoa (DRC) etc are essentially geochemical anomalies which represent unusual concentrations of elements in the earth's crust. The objective of any geochemical exercise is to:

- Identify an anomaly of economic interest,
- Delineate drill targets,
- Locate mineralisation and eliminate barren ground,
- Optimise target identification and maximise geochemical contrast.

The process of geochemical sampling involves the identification of pathfinder/indicator minerals which are chemically mobile elements associated with the element being looked for. These elements provide an indication of mineralisation. This information very useful for any exploration programme especially at the reconnaissance stage. In general, the chemical signature for sediment hosted Cu deposits is associated with the following elements; Cu, Ag, Pb, Zn, Mo, V, U, Co and Ge (AusIMM, 2011).

Earlier work on soil geochemistry around the Kansanshi district resulted in a large database from many sampling campaigns through the exploration history of the deposit. Results of these surveys indicate that Kansanshi is an obvious anomaly which 7km long and 3km wide with an assay value of 200ppm (0.02%), which is four times the average earth's crustal abundance for Cu, figure 67.

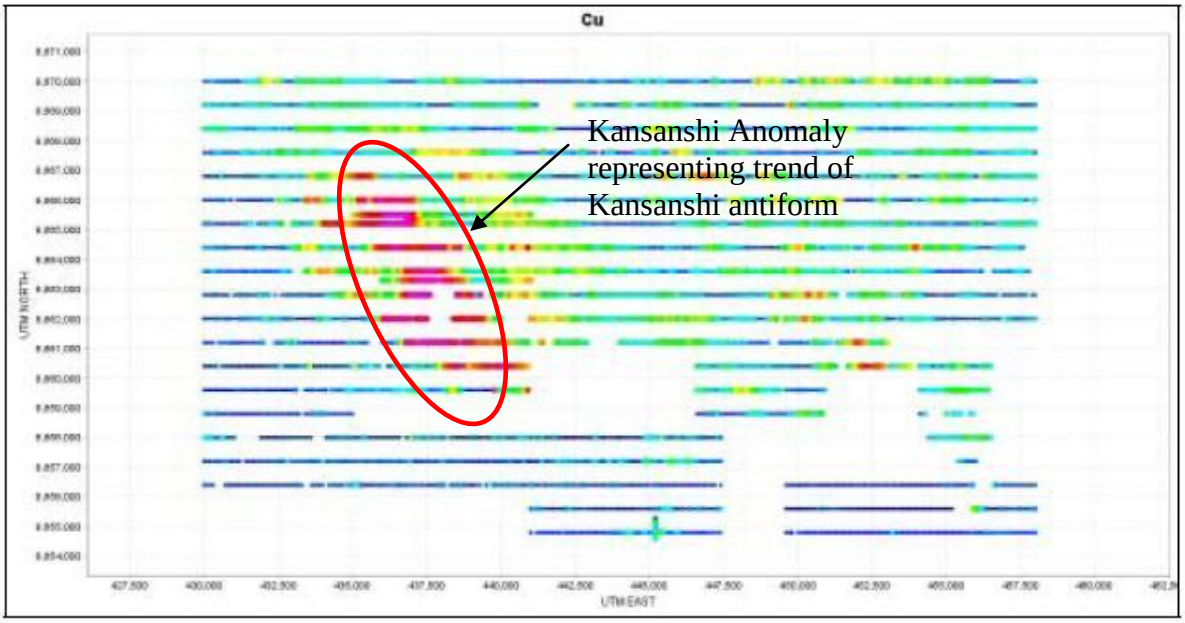

Figure 66. Results of soil sampling geochemical survey showing the Kansanshi anomaly. (modified from Beeson et al., 2008)

According to Beeson (2008), Kansanshi is surrounded by an anomaly of Mn. The 2 elements are transported by fluids in different states i.e. Cu is transported in an oxidised alkaline fluid whereas Mn is transported in a reduced acid fluid. The Mn anomaly is associated with siliciclastic marble and could suggest flow of reduced basinal fluid within the basin Beeson et al., 2008).

Lithogeochemical studies were done by Beeson et al. (2008) with the objective of characterising the geochemical composition of the host rocks, determine which major components are lost or added with alteration, identify which chalcopile (affinity for S) and silicate hosted pathfinders are anomalous in the system and to determine the effect of weathering on the anomalous signature.

7.5 Drilling, estimation and ore body modelling

Drilling at Kansanshi has taken place over a number of campaigns. As of the 2012 MRE at total of 1,455 holes have been drilled amounting to 333,701m, refer to table 3 below.

Table 3. Historical and Current holes drilled within the Kansanshi deposit for the MRE

Period	Client	BHIDs	Type	# of holes	Metres
1973-1980	ZCCM*	KML01 – KML73 KPR01 – KPR35	DD	110	19,420
1998	Cyprus Amax	K001 – K309A	DD	311	66,222
	Cyprus Amax	KRC001 – KRC032	RC	17	2,740
1999	Cyprus Amax	K310 – K379	DD	67	13,887
2001	FQML*	K380 – K412	DD	34	4,281
	FQML	KRC035 – KRC104	RC	66	5,880
2003	FQML	KRC105 – KRC149	RC	45	3,337
2005	FQML	KRC002A – KRC005	RC	3	262
2006	KMP*	KDD0001 – KDD0048 KSTD0002 – KSTD0013	DD	34	5,063
	KMP	KDW0002 – KDW0007 KE0006	RC	7	891
2007	KMP	Prefix KDD, KRDD, KSTD, NWD	DD	46	6,514
	KMP	NWRC0001 –NWRC0153	RC	124	15,680
2008	KMP	KRDD001 – KRDD031	DD	31	7,236
2009	KMP	KRDD031A – KRDD141	DD	119	29,256
	FQMO*	KXD001A – KXD015	DD	14	4,911
Total 1980 - 2009				**1,028**	**185,581**
2010	KMP	DCDD001 – 006 KRDD142 - 203	DD	77	22,468
2011	KMP	KRDD204 - 405	DD	195	61,013
	FQMO	Prefix KRX	DD	10	5,880
2012	KMP	KRDD407 - 552	DD	134	51,676
	FQMO	Prefix KRX	DD	11	7,083
Total 2010 - 2012				**427**	**148,120**
Total				**1,455**	**333,701**

* denotes

ZCCM – Zambia Consolidated Copper Mines FQML – First Quantum Minerals Limited

KMP – Kansanshi Mining PLC FQMO – First Quantum Mining Operations

Current drilling around the Kansanshi Mine lease has been done under three drill programs by two geological teams. The focus in the last couple of years has been on resource development in and around Main and NW Pits, resource definition targeting the South-East Dome and regional exploration targets.

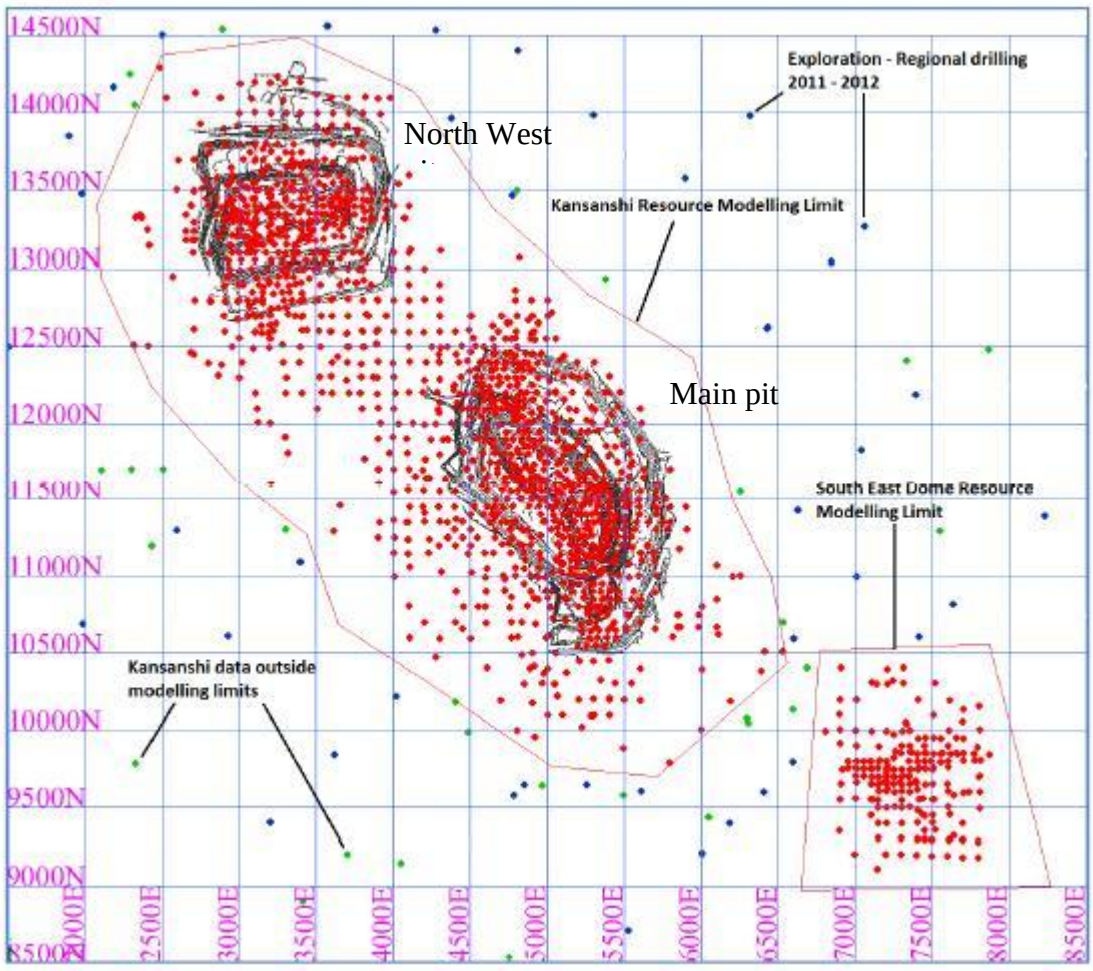

Figure 67: Kansanshi and SE Dome drilling showing drill holes in and around the NW and Main pits and the SE Dome. (Titley, 2012)

Drill spacing is 100x100m in the majority of the areas drilled; there is however limited closer spaced drilling of 50x50m in some of the areas e.g. central Main pit. Drilling orientation in the main pit which is dominantly east – west is designed to intersect the N-S orientated veins and structural domains. Regional drilling within the mining lease is orientated NE-SW targeting the Kansanshi antiform.

Geological domains (strata, weathering) within the deposit are updated or modelled based on recent drill data and pit mapping. 3D modelling is done in Surpac, working through the 50/100m W-E sections with an overlap of 25m either side. The result of the modelling is either a wireframe (e.g. weathering, redox, and stratigraphy) or 3D solid (e.g. veins, phyllite). Modelling of veins within the Kansanshi deposit is critical as these are the host of the bulk of the Cu and Au mineralisation. This process is important in minimising the amount of internal dilution. The veins are modelled based on the distribution of vein logged intercepts and associated alteration haloes. Owing to the wider drill spacing in resource and exploration programmes, grade control RC drilling (close spaced drilling) is often used to define or refine the vein model.

In any estimation process, there is need to define the domains that will be used in the estimation based on geology and ore types (REDOX) i.e. refractory, oxide, transitional and sulphide. The simplified flow of steps involved in the estimation process requires that basic statistics is applied on raw data within the estimation area. This is followed by application of top cuts/caps on the data, so as to remove outliers. The process essentially involves resetting any abnormally high composite data by domain to the appropriate top cut value. This is followed by basic statistics on the top cut data. The latter process is followed on by variography by domain. This involves comparing samples according to distance and orientation between the samples to produce parameters to be used in the estimation process. For the variography exercise to be representative of the domain/deposit it must be guided by geology. The process is followed by the development of the block model whose dimensions will depend on the geology (veins, lithology and stratigraphy) and the smallest mining unit (SMU). The 2012 MRE had the following block model parameters;

Table 4. Block model extents for Kansanshi Mine (adapted from Titley, 2012)

Easting		Northing		Elevation	
Min	Max	Min	Max	Min	Max
2,080m	6,560m	9,700m	14,500m	900m	1,470m
Block Dimensions					
10m	20m	10m	20m	2.5m	5m

- Parent cells – 20m x 20m x 10m

- Daughter cells (sub-blocking) – 10m x 10m x 2.5m

Table 5. Block model attributes for Kansanshi Mine (adapted from Titley, 2012)

Attribute	Description
ESTZON	Estimation zone code
REDOXN	Redox code (3 Oxide, 2 Transitional, 1 Sulphide)
WEATHN	Weathering Code (4 Laterite, 3 Saprolite, 2 SapRock, 1 Fresh)
GEOLN	Geology number based on stratigraphy or Vein type
STRATN	Stratigraphic position code
VEIN	Vein grouping code
PIT	If material is mined or not (0 Not mined, 1 Main Pit, 2 NW Pit)
DENSITY	In situ dry bulk density used to estimate tonnage
GAC	Gangue Acid Consumption based on lithology
DIPDIR	Direction of stratigraphic dip
DIP	Inclination of the stratigraphy from the horizontal plane
ORE	Probability of exceeding 0.2% Cu
CU	Total Cu% estimated grade
ASCU	Acid soluble copper % estimated grade
AU	Gold in ppm estimate grade
CLASS	Resource classification (1 Measured, 2 Indicated, 3 Inferred)

The Cu and Au values are then estimated into the block model using OK. Finally, once the model is created and populated there's need to validate it. The process of model validation as applied to the Kansanshi MRE of 2012 is highlighted below;

- Visual comparison of composite grade vs. block grade.
- Swath plots comparing grade on a more local scale looking at composite grade vs. model grade by bench, northing and easting.
- Mean grades - tabulation of mean grade to assess the percentage difference in the mean grade between the composites and the block models.
- Histograms of population data for key domains for both composite grade and block model grade.

Once the model has been validated and is sound, the mineral resource is then classified as Measured, Indicated and Inferred based on guidelines specified in the Canadian National Instrument 43-101 ('NI43-101'). Classification was based on a number of criteria including assessment of the reliability of the geological model, sampling, survey control, bulk density data, drilling grid, and OK confidence indicators during grade estimation.

The following parameters were considered in determining the classification of the Kansanshi 2012 MRE update;

• Adequate validation of drilling, sampling, and geological process completed during site visits by the Competent Person (CP).

• Adequate geological evidence for continuity of mineralization at the cut-off grade used in the estimation of the mineral resource.

• Adequate analytical evidence of copper, acid soluble copper and gold mineralisation.

• Adequate QAQC controls in place to validate the copper and gold grades.

• Adequate diamond core sampling to determine the dry in situ bulk density in order to estimate the tonnage of mineralisation.

• Reconciliation of production data with the MRE.

• Review of the Ordinary Kriging slope of regression as an indicator of relative confidence of the grade estimate.

The modelling and estimation process resulted in the MRE as represented in table 6 below.

Table 6. Kansanshi and SE Dome Mineral Resource Estimate as at 30th November 2012 (Titley, 2012)

KANSANSHI and SOUTH EAST DOME MINERAL RESOURCE ESTIMATE as at 30th November, 2012 at >= 0.3 Cu% cut-off						
Area	**Resource Classification**	**Million Tonnes**	**Cu Grade %**	**ASCu Grade %**	**Au Grade ppm**	**Cu metal kt**
KANSANSHI Main and NW Pits	Measured	88.9	1.10	0.48	0.17	974
	Indicated	601.1	0.83	0.19	0.14	4,967
	Total M+I	**690.0**	**0.86**	**0.23**	**0.15**	**5,942**
	Inferred	344.4	0.70	0.04	0.11	2,401
SE DOME	Measured	-	-	-		-
	Indicated	54.2	0.90	0.04	0.15	486
	Total M+I	**54.2**	**0.90**	**0.04**	**0.15**	**486**
	Inferred	20.8	0.91	0.03	0.16	188
TOTAL	Measured	88.9	1.10	0.48	0.17	974
	Indicated	655.4	0.83	0.18	0.14	5,453
	Total M+I	**744.3**	**0.86**	**0.21**	**0.15**	**6,427**
	Inferred	365.2	0.71	0.04	0.12	2,589

7.6 Exploration Ideas for CACB deposits

Most of the deposits within the CACB have been located by prospecting for outcrops (Cu oxides-malachite), vegetation anomalies due to poisoning and geochemical surveys. Exploration for Cu deposits in Zambia successfully pioneered many exploration techniques such as aerial photography, geochemical and electrical surveys (Hitzman, 2012). The success of systematic drilling of soil anomalies led to the discovery of concealed deposits such as Chibuluma (ZCB), Frontier and Kamoa (CCB).

Geophysical methods, mainly magnetic surveys are critical in understanding stratigraphy and structures but have not been used effectively in delineating ore deposits. EM and IP methods have worked well on the Kansanshi deposit to delineate lithological unit (carbonaceous material) and structures. These methods have proved ineffective on the traditional Copperbelt deposits. Not much gravity studies have been done on the CACB, as the technique is not suitable for detecting orebodies, but ideal for delineating structural basins. Alteration assemblages who are characteristic of CACB deposits have failed to provide a means of determining pathways for mineralisation. Fluid and isotope studies have not been systematically used as routine exploration tools on the discovery of CACB deposits. Studies by Annels (1989) and Selley et al. (2005) suggest that they may have

been a shift to lower O_2 and C isotope values in the carbonates that were affected by mineralisation relative to the unaltered.

Hitzman (2012) believes that, in conjunction with geochemical and geophysical studies, understanding of the geology of an area to identify the three lithostratigraphic units (red beds, evaporites and reducing strata) which are critical for the formation ore deposits. Exploration of CACB deposits shares similarities with exploration for petroleum, therefore seismic, inverse potential fluids and electrical data to constrain subsurface geology are anticipated to be popular techniques in the near future.

CHAPTER 8: Discussion

8.1 Introduction

The occurrence of a large vein hosted copper system within the Kansanshi deposit can be attributed primarily to structure in the form of low angle fault systems. Mineralisation within the deposit is believed to be associated with deformation events during the emplacement of the Lufilian fold belt. These mineralisation events are believed to have resulted in the accumulation of Cu and associated elements such as Au, U and Mo. Veins within the Main pit and other mineralised localities (NW and SE Dome) are stratabound and thus dominantly occur within the clastic units. Investigation the of the deposits characteristics has predominantly been done through drilling, however other exploration techniques have been applied in the last couple of years to better understand the deposit in terms of extension of current mineralisation trends and exploration of Kansanshi-type deposits in the CACB.

8.2 Controls on mineralisation

Mineralisation within the Main pit of the Kansanshi deposit is dominantly in the form of undeformed high angle veins that straddle the entire stratigraphy but are constrained by the calcareous units. Mineralisation within the Domes region is suspected to be associated with formation of the Lufilian fold belt. This is supported by fluid inclusion studies done by Torrealday (2000) that suggest that hydrothermal fluids responsible for the mineralisation events were influenced by regional metamorphism and deformation as shown by high CO_2 levels in the veins.

Varied schools of thought have been proposed concerning controls of mineralisation at Kansanshi. One of the main considerations has been structure(s). It is evident that structure in the form of folding, faults or thrusts play a critical role in the mineralisation events within the deposit and has influence on the occurrence and distribution of veins. The series of domes along the Kansanshi antiform have major influence on mineralisation as can be seen by an abundance of mineralisation under the Main pit dome within the clastics and calcareous units. This trend drops sharply with increase in distance from the ‘pimple’ or apex of the dome. Work done by Torrealday (2000) and others such as Broughton et al. (2002), Barron (2003) suggest that veins originated during hydrofracturing associated with formation of the series of domes in the North West province of Zambia. Their models don’t seem to relate mineralisation to regional fault or

thrust structures or systems which could have originated during deformation brought about by formation of the Lufilian arc. Stages of veining i.e. progression from quartz to carbonate rich veins is apparent in the Main pit, mainly towards the contact with carbonate or calcareous units (UM/LM). This is believed to indicate retrograde metamorphism which is associated with an increase in carbonate/calcite solubility and a reduction in quartz solubility (Torrealday, 2000). Folding, which is suggested by Unrug (1988) to have influence on the occurrence of rocks (Roan Group) that host stratiform mineralisation is characteristic of the main copper belt deposit. These deposits consist of tight to isoclinal folds and major recumbent folds formed as a result of the Lufilian deformation and early normal fault. Work done by Hitzman (2013) suggest that these are absent in the Kansanshi ore body.

Recent detailed structural mapping in the Main pit and logging of deep regional holes by Beeson et al. (2013) and Hitzman (2013) indicate that the dominant structures at Kansanshi are complex array of reverse and normal faults which are associated with underlying low angle faults (fluidised breccias) and drag folds, suspected to have control of mineralisation especially in the Main pit. The low angle structure is believed to originate below the LPS. At this stage, the low angle structure is not clearly understood, however there's evidence that these structures were pathways for hydrothermal fluids as shown by alteration along their extents (Hitzman, 2013). This alternative model will need to be investigated further with more drilling. As mentioned in Chapter 7, thickening of the PS around the dome apex owing to the low angle structure is believed to have control on the mineralising fluids, refer to figure 58 (chapter 6).

The influence of intrusive (gabbro bodies) on mineralisation is not clearly understood at Kansanshi. These gabbro bodies which normally occur as sills form a stark rheological contrast to the softer sediments of the mine sequence. It is possible that the gabbro bodies are responsible for focussing deformation at their margins due to this high rheological contrast, potentially giving rise to low-angle faults or fractures that serve as fluid conduits. This is evident from recent drilling in the SE Dome area (south east of Main pit) where these gabbros cause displacement (inflection) of the surrounding lithology. These inflection areas are usually associated with 'blow out' of mineralisation, refer to figure 68 below.

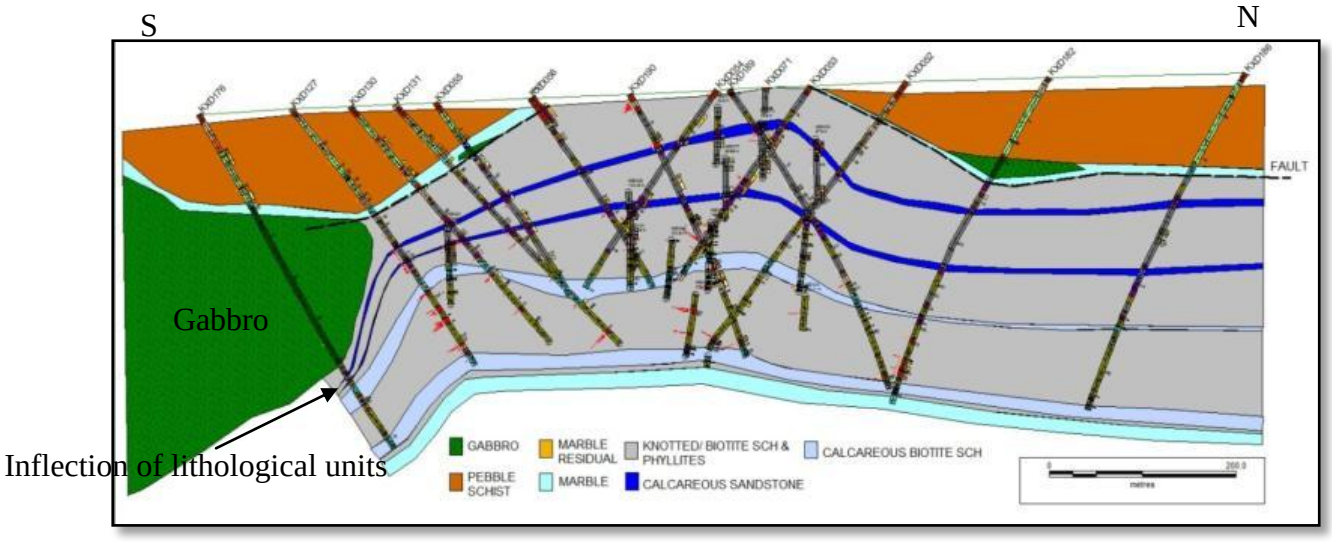

Figure 68. Section showing the impact of intrusive on lithological units along section line 7500E (SE of Main pit). The gabbro takes advantage of the detachment fault and causes inflection of lithological units (Fourie et al., 2012).

This is supported by Barron (2003) that the gabbros are pre-mineralisation. The majority of these bodies have been defined by aeromagnetic survey and to a limited extent through drilling. There's need to understand the position and size of these intrusive bodies which might be important for understanding the architecture and mineralisation at Kansanshi.

8.3 Relationship of mineralisation and stratigraphy

Vein hosted mineralisation is confined to certain stratigraphic units within the Kansanshi deposit. The veins form near vertical cross cutting structures whose extents are bound by the upper and lower marble units. The veins and stratiform mineralisation (mainly confined to the wall rock and associated with alteration) is dominantly found in the clastic units (upper and middle mixed clastics – phyllite and knotted schist). Due to the ductile nature of the clastic units, it is highly likely that mineralising fluids will find it easier to penetrate as opposed to the carbonates. Thickening of lithological units under the Main pit dome is now understood to have an influence on the density and distribution of vein mineralisation. This has been confirmed by deep drilling in Main pit that intersected mineralisation in the LPS and LM units, figure 69.

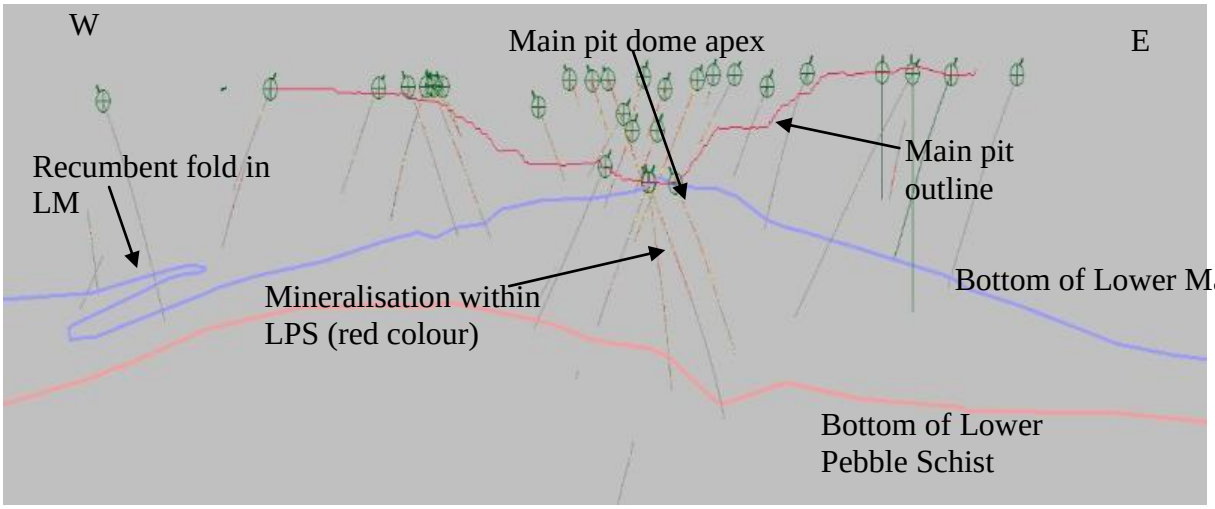

Figure 69. Section 11400N showing the Main pit domal structure, thickening of the LPS and deep 'seated' mineralisation in the LPS and LD (looking North).

The deep seated mineralisation occurs as veinlets and sulphide disseminations within the latter units. It was also observed that there is preferential occurrence of mineralisation in the MMC compared to the UMC. This could be attributed to mineralising fluids not having adequate pressure to 'punch' through the UM unit and therefore precipitating in the clastic units of the MMC. This also explains the absence of mineralisation in the bulk of the UM. Mineralisation within the marble units, if present, is characteristically in the form of low grade sulphide disseminations which are associated with carbonate alteration. Stratiform mineralisation is closely associated with carbonaceous phyllites, which act as reducing strata to the mineralising fluids. Common minerals found in this type of mineralisation include, Cpy, Py, Po and minor Mo. The abundance of Po increases with increase in distance from the vein.

8.4 Cu and Au mineralisation

The interaction of Cu with Au in the Kansanshi deposit is not clearly understood as its occurrence is sporadic. Studies done on Au mineralisation have not assisted in understanding the relationship between the two elements; however it is clear that Au mineralisation is associated with the vein mineralisation. Work done by Cyprus Amax during the prefeasibility suggests that there is correlation between Cu and Au. One question that needs to be addressed is the timing of Au mineralisation in relation to the Cu. The current understanding is that the Au and Cu were mutually introduced during mineralisation; however this has not been proved. As highlighted in Chapter 5, Au seems to follow similar mineralisation trend as Cu. This is shown by higher Au grades within

the major structural zones such as the 4800 and 5400. Au grades tend to sharply diminish outside these structural regions. The positive correlation of Au and Cu could be explained by the work done by Goodship (2010) where Au was found to be in association with Cpy in fractured pyrite grains.

The primary existence of gold in the presence of pyrite seems to suggest a link with the mineralising fluid. The composition of pyrite and structural deformation owing to metamorphic events within the basin are suspected to be controlling factors in mineralisation. Early-mineralising fluids may have included Au; therefore as hydrothermal fluids cooled and became enriched in sulphur, conditions for re-mobilisation of gold could have occurred allowing diffusion of native gold along fractures and grain boundaries (Goodship, 2010). As can be derived from work done by Goodship (2010) and Coetzee (2011) the occurrence of Au in the deposit could be associated with later stage deformation events, after the initial precipitation of sulphides such as Py.

Currently it is difficult to confidently relate Au and Cu grades owing to the limited assay information available. There is need to carry out an assaying campaign for Au on old or historical holes using coarse rejects or pulp from the lab. This will assist in increasing the confidence for gold modelling. One thing that needs to be highlighted is that Au is mainly found in its native form and therefore highly nugget. Disseminated sulphide mineralisation which is associated with alteration i.e. albite or carbonate, but as far as gold mineralisation is concerned; there's no evidence from work done previously to suggest an association with alteration.

8.5 Ore Genesis at Kansanshi

Ore genesis within the Kansanshi deposit is believed to have been facilitated by the tectonic activities within the Domes Region; however the source of the mineralising fluids is still not clearly understood. The Cu enriched solutions or fluids are suspected to originate from depth possibly the basement with remobilization owing to tectonism with the Domes region (Koziy et al., 2009). Fold and thrust structures are known to have created pathways for hydrothermal fluids rich in Cu sulphates to move upwards through overlying strata, refer to figure 54. These fluids then interacted with carbonaceous units (CBPH), through redox reactions to precipitate Cu. These processes were focused in highest point of the domal structures, which acted as trap sites for mineralization. This is supported by the concentration of mineralization in the vicinity of the domal apex and

sharp reduction of mineralization away from the dome as illustrated in figure 57. This has resulted in mineralization within the Kansanshi deposit to occur predominantly and characteristically within high angle vein structures. Formation of oxides and mixed ore can be attributed to supergene enrichment processes close to surface. Weathering and oxidation therefore has a huge impact on the material types (oxide, transition and sulphide) found within the deposit.

8.6 Exploration techniques

A number of exploration techniques have been applied to the Kansanshi deposit from the time of discovery to date. The prominent method has been through drilling mainly to investigate continuity of the already known mineralisation trends. A lot of work was done by Cyprus Amax in the late 90's and early 2000 on geochemical and geophysical surveys to better understand the deposit. This was achieved through soil sampling, aeromagnetics and radiometrics. This was set as the base of all exploration work that was to follow.

Owing to the limited outcrop cover in the Kansanshi area, field mapping has not been effective in understanding the regional geology. This has facilitated FQM to focus on other techniques such as geophysics, geochemical surveys to identify dome structures and Cu anomalies respectively and diamond drilling to test these anomalies. Geophysical surveys such as magnetics and radiometrics have also been applied to identify structural traps and correlate stratigraphy. A lot of this information has been useful to better understand the characteristics of the Kansanshi Antiform and the related domes.

Because of the nature of the Kansanshi deposit (Main pit) which is vein hosted, the focus of the majority of exploration work has been to understand the occurrence, distribution and geometry of the veins. The presence of sulphides such as pyrrhotite makes the deposit suitable for magnetic and conductivity methods of investigation such as EM, CSAMT and IP. Although these methods were not effective in picking out the veins, they were useful in identifying the highly conductive units such as CBPH (associated with sulphide mineralisation) and structures. Radiometric surveys have not been widely used around the Kansanshi deposit probably because of its shortcomings in conditions of thick soil or laterite cover which are characteristic of the study area. Airborne gravity has not been applied at Kansanshi but could be useful in mapping out the lithological units and better define the gabbro sills/bodies. As highlighted in Chapter 4, the intrusives could have an influence on mineralisation; therefore it would be in FQMs interest to investigate gravity

as a targeting tool. Seismic, a technique similar to ultrasound (sound waves transmitted down the rock units, reflected or refracted back to surface and then detected by geophones for interpretation) can also be considered as an accurate method of determining the thickness of lithological units and the presence of major structures such as faults and fractures which are known to be associated with the mineralisation within the Kansanshi deposit. This can be used to assist in targeting for drilling. This information can also be useful for geotechnical purposes when designing support systems for mining the deposit. Predictability of mineralisation in a vein hosted deposit is critical for vein modelling purposes especially when dealing with wider spaced data at exploration or resource development level. These methods will not only assist in locating anomalies but will also help in refining the geological model(s) not just for exploration but also for production or grade control purposes.

CHAPTER 9: Conclusion/Summary

The aims of this thesis have been detailed and discussed in the preceding chapters with focus being on geology, mineralisation and alteration characteristics in the Main pit.

Review of literature and work done within the Main pit and the Kansanshi deposit as a whole in the last couple of years has helped to better understand the critical attributes of the ore body. Characterisation work done by Torrealday (2000), Barron (2003) and Cyprus Amax (2000) suggest that mineralisation is associated with deformation events experienced during the formation of the Lufilian fold belt. Logging and pit mapping has confirmed that structures in the form of reverse, normal faults and drag folds (structural architecture) are key controls of mineralisation within the Main pit. The presence of domal structures associated with second and third phases of deformation were critical in the emplacement of mineralisation especially in the vicinity of the dome apex. Low angle faults occurring below the current pit elevation are believed to have served as major fluid pathways during mineralisation, these account for the abundant vein injection, breccia development along the 4800 and 5400 zones. These ideas also serve to clarify issues of the genesis of the Kansanshi ore body relative to the other deposits of the ZCB. Thickening of favourable (ductile) units such PS and clastics through folds and low angle faults facilitated conduits for mineralising fluids. Failures within the units through supra-lithostatic pressure resulted in the omni-directional distribution of veins, whereas presence of mineralisation parallel to foliation and bedding resulted in veinlets and disseminations.

The source of mineralisation within the Kansanshi deposit and the Copperbelt as a whole is still unknown. Various ideas have been put across which include introduction of metals during diagenesis of the Katangan basin and the red beds. However recent work by Koziy et al. (2009) suggests that the deep seated basement of granites, gneisses and schists could be the potential source of mineralisation. Later stage deformation events within the Domes region could have resulted in re-mobilisation of this mineralisation higher up the stratigraphy.

Earlier drilling campaigns had ruled out mineralisation beyond the phyllites of the LM in the Main pit. Deeper drilling in the vicinity of the dome (LPS and LD units) has confirmed the presence of mineralisation in the form of veinlets and disseminations (included in MRE done by Titley, 2012). This can be attributed to hydrofracturing of the

units resulting in mineralising fluids moving up the sequence. The presence of mineralisation below the LM has changed the strategy for resource development with more effort being placed in defining deep seated mineralisation beyond the apex of the dome as a possible mineable resource.

Alteration within the Main pit occurs as discrete 'envelopes' around mineralised veins. The type and intensity of alteration is dominantly controlled by the lithological units, with albitisation occurring in phyllites and schists whereas dolomitisation is prevalent in calcareous units. Alteration, in particular albite alteration is a result of carbon, biotite and oligoclase destruction, thereby faciltating an influx in metals such as Cu, Au, Mo, V, U, Th, Ti. Carbonate alteration (Dolomitisation) results in formation of ferroan dolomite which is also associated with mineralisation. Both albite and carbonate alteration show association with mineralisation, however the albite-rich stage began a little earlier and the ferroan dolomite stage persisted a little longer. Sericite alteration usually occurs in association with albite alteration and is normally found at the margins of the albite bleached zones. Scapolite alteration normally occurs in calcareous units and has been observed to be associated with sulphide disseminations.

The Kansanshi deposit is unique in that it has a high Au tenor. Gold mineralisation occurs in association with sulphide and quartz dominated veins or veinlets and also stratiform mineralisation in CBPH. Work done by Goodship (2010) suggests that gold occurs as free grains in association with melonite ($NiTe_2$) and microfractured pyrite intergrown with chalcopyrite. Analysis of Au grades in the Main pit shows a clear indication of gold concentration along the major north-south trending structures like the 4800 and 5400 zones which are also characterised by high Cu grades. This suggests that Cu and Au could have existed in the same mineralising fluid. However the effects of supergene enrichment makes the grades inconsistent especially in oxide and transitional ores. Work done by Cyprus Amax (2000) suggests poor correlation of Au and Cu in the calcareous units lower down the stratigraphic sequence. A lot more work needs to be done to fully understand the relationship between of Au and Cu at a regional and localised scale.

9.1 Further study/recommendations

Owing to the higher Au tenor and the relatively favourable Au price there is need to expand on the work done by Goodship (2010) and Coetzee (2011) through confirmation of controls on Au mineralisation and it's relationship with Cu and other accessory mineral such U and Mo. There's need for in-depth fluid inclusion and isotope studies (C, O and S) on the different domal structures (associated with mineralisation) along the Kansanshi antiform so as to characterise the mineralising fluids in terms of Cu and Au and also to get a better understanding on metal source and ore genesis. This can be achieved through a research based MSc or PhD project.

Additional regional drilling within the Kansanshi area, especially the deep drilling on holes KRX082, KRX077, KRX066 and KRX055, gives a better understanding of the stratigraphy within the Kansanshi area; however correlation with the 'traditional' Copperbelt deposits is still problematic. There is need to further investigate the influence of the basement on the overlying lithological units in terms of depositional history and mineralisation.

With more drilling and pit mapping activities in the pit, there's currently a better understanding of vein geometries and characteristics especially in the Main pit, however more can be done to relate alteration and mineralisation to structures within the pit. This can therefore be used as a vein or mineralisation predictive tool especially in a grade control scenarios.

More conventional exploration techniques such as gravity and seismic surveys need to be investigated so as to aid in locating and understanding the influence of intrusives and mapping out of structures respectively.

References

Annels, A.E. (1989). Ore genesis in the Zambian Copperbelt, with particular reference to the northern sector of the Chambishi basin. *Geological Association of Canada*, Special Paper **36**, 427-452.

Arthurs, J.W. and Legg, C.A. (1974). The Geology of the Solwezi Area: Explanation of degree sheets 1226, NW Quarter and 1126, part of SW Quarter. *Geological Survey of Zambia*, **36**, 45pp.

AUSIMM (Australian Institute of Mining and Metallurgy) (2011) *Field Geologist Manual*, 5, 479pp.

Barra, F., Broughton, D.W., Ruiz, J. and Hitzman, M.W. (2004). Multi-stage mineralisation in the Zambian Copperbelt based on Re-Os isotope constraints. *Geological Society of America Abstracts with Program*, 36, 516.

Barron, J.W. (2003). *The stratigraphy, metamorphism and tectonic history of the Solwezi Area, Northwest Province, Zambia: Integrating geological field observations and airborne geophysics in the interpretation of regional geology*. PhD thesis (unpublished), Colorado School of Mines, Golden, Colorado, USA, 233pp.

Beeson, J., de Luca, K., Halley, S., Nielson, I., Wood, D., Chasaya, G., Clynick, G., Lewis, S., Pascall, J. and Shaw, A. (2008). Report and recommendations for Kansanshi. Unpublished Confidential report to First Quantum Minerals, Kansanshi Mine, Jigsaw Geoscience Pty Ltd, 105pp.

Beeson, J., Augenstein, C., Nielson, I., Wood, D., Hitzman, M.W., Williams, J., Kaemba, R., Shaw, E., Selwood, R., Mpokosa, L., Mkandawire, H., Lee, R., Kidder, J., Ghilissen, A. and Deltenre, A. (2013). Kansanshi Geological Campaign: Results and Implications. Unpublished Confidential report to First Quantum Minerals Limited, Jigsaw Geoscience Pty Ltd and Model Earth Pty Ltd, 53pp.

Binda, P.L. and Porada, H. (1995). Observations on the Katangan breccias in Zambia. In: M. Wendorff and L. Tack (Editors), *Late Proterozoic Belts in Central and Southwestern Africa*. Proceedings IGCP302, Annales Musee Royal Afrique, Central Tervuren Belgique, 49-62.

Blair, R.G. (1997). A Petrologic and Chemical Investigation of Selected, Pre-1997 Drill Core and Early 1997 Surface Samples from the Kansanshi Copper Deposit, NW Zambia, Unpublished Cyprus Amax Minerals Company internal report.

Broughton, D.W., Hitzman, M.W. and Stephens, A.J. (2002). Exploration history and Geology of the Kansanshi Cu (-Au) deposit, Zambia. *Society of Economic Geologists*, Inc, Special Publications **9**, 141-153.

Brown, A. C. (1984). Alternative sources of metals for stratiform copper deposits. *Society Precambrian Research*, **25**, 61-74.

Cahen, L., Snelling, N.J., Delhal, J., Vail, J.R., Bonhomme, M. and Ledent, D. (1984). *Geochronology and Evolution of Africa*. Clarendon, Oxford. 512pp.

Cailteux, J., Binda, P.L., Katekesha, W.M., Kampunzu, A.B., Intiomale, M.M., Kapenda, D., Kaunda, C., Ngongo, K., Tshiauka, T. and Wendorff, M. (1994). Lithostratigraphy correlation of the Neoproterozoic Roan Supergroup from Shaba (Zaire) and Zambia, in the Central African Copper-Cobalt metallogenic province. In: A.B. Kampunzu and R.T. Lubala (Editors), *Neoproterozoic belts of Zambia, Zaire and Namibia (Special Issue)*. Journal of African Earth Sciences, **19** (4), 265-278.

Cailteux, J., Binda, P.L., Katekesha, W.M., Kampunzu, A.B., Kaunda, C., and Wendorff, M. (1995). Results of Lithostratigraphic correlation of the late Proterozoic Roan Supergroup between Zambia and Zaire, Central African Copperbelt, Royal Museum of Central Africa (Belgium). *Annales Science Geology*, **101**, 21-27.

Cailteux, J.L.H. (2003). Comment from the Organiser. In: *Neoproterozoic Guide book to the Field Trip, IGCP No. 450, Proterozoic Sediment-hosted Base Metal Deposits of Western Gondwana*. Conference and Field workshop Lubumbashi 2003, Lubumbashi, 204-205.

Cailteux, J.L.H., Kampunzu, A.B., Lerouge, C., Kaputo, A.K., and Milesi, J.P. (2005a). Genesis of sediment-hosted stratiform copper-cobalt deposits, Central African Copperbelt. Journal of African Earth Sciences, **42**, 134-158.

Coetzee, L.L. and Glossop, L.N. (2011). Gold deportment study on Concentrate samples from a Cu-Au Exploration project: Mineralogical report No: MIN 0611/106. Unpublished Test report to First Quantum Minerals, Kansanshi Mine, SGS South Africa, 43pp.

Cosi, M., DeBonis, A., Gosso, G., Hunziker, J., Martinotti, G., Morrato, S., Robert, J.P., and Ruhlman, F. (1992). Late Proterozoic Thrust Tectonics, High-pressure Metamorphism and Uranium mineralisation in the Domes Area, Lufilian Arc, Northwest Zambia. *Precambrian Research*, **9**, 15-240.

Cyprus Amax (2000). Kansanshi Prefeasibility Study: Geology. Technical Report prepared for Cyprus Amax, 66pp.

Darnley, A.G., Horne, J.E.T., Smith, G.J., Chandler, T.R.D., Dance, D.F., Preece, E.R. (1961). Age of some uranium and thorium minerals from East and Central Africa. Mineralogist Magazine, **32**, 716-724.

First Quantum Minerals. (2012) Kansanshi fact sheet, www.first-quantum.com/Our-Business/operating-mines/Kansanshi/default.aspx.

Fourie P.H., Mulendwa, C., Shaw, E. and Kaemba R. (2012). Current understanding of the Kansanshi Antiform geology, Unpublished FQM Technical Meeting presentation, Solwezi, 61pp.

Fleisher, V.D., Garlick, W.G. and Haldane, R. (1976). Geology of the Zambian Copperbelt. In: K.H. Wolf (Editor), *Handbook of Strata-bound and Stratiform Ore deposits*. Elsevier, Amsterdam, pp. 223-352.

Garlick, W.G. (1961). The syngenetic theory. In: Mendelsohn (Editor), *The Geology of the Northern Rhodesian Copperbelt*. McDonald, London, pp. 146-165.

Goodship, A. (2010). *Occurrence of gold at Kansanshi Cu-Au deposit*. MSc. thesis (unpublished), University of Exeter, Camborne School of Mines, UK, 73pp.

Google Earth. (2012). Kansanshi satellite imagery.

Grey, A. (1930). The correlation of the ore-bearing sediments of the Katangan and Rhodesian Copperbelt. *Economic Geology*, **25**, 783-801.

Hason, R.E., Wilson, T.J., Wardlaw, M.S., Brueckner, H.K. and Onstott, T.C. (1990). A review of new Geochronological Data for the Proterozoic of Central and Southern Zambia. *Zambian Journal of Applied Earth Sciences*, **4**, 6-18.

Hason, R.E., Wardlaw, M.S., Wilson, T.J. and Mwale, G. (1993). U-Pb zircon ages from the Hook Granite massif and Mwembeshi dislocation: Constraints on Pan-African deformation, plutonism, and transcurrent shearing in central Zambia. *Precambrian Research*, **63**, 189-209.

Hanssen, M.G. (2010). Mineral Resource Estimate for First Quantum Minerals Ltd, Kansanshi Copper Mine, Zambia. NI43-101 Technical Report prepared for First Quantum Minerals, Digital Mining Services, Zimbabwe, 154pp.

Hitzman, M.W. (1999). The Zambian Copperbelt-A new look at a classic World–class District, Denver Region Exploration Geologists Society News Letter.

Hitzman, M.W. (2000). Source basins for sediment hosted stratiform copper deposits—Implications for the structure of the Zambian Copperbelt. *Journal of African Earth Sciences*, **30,** 855-863.

Hitzman, M.W., Kirkham, R., Broughton, D.W., Thorson, J. and Selley, D. (2005). The Sediment-hosted stratiform copper ore system. *Economic Geology 100th Anniversary volume*, 609-642.

Hitzman, M.W., Selley, D. and Bull, S. (2010). Formation of Sediment-hosted stratiform copper deposits through Earth history. *Economic Geology*, **105**, 627-640.

Hitzman, M.W., Broughton, D.W., Selley, D., Woodhead, J., Wood, D. and Bull, S. (2012). The Central African Copperbelt: Diverse Stratigraphic, Structural and Temporal Settings in the World's Largest Sedimentary Copper District. *Society of Economic Geologists*, Inc, Special Publications **16**, 487-514.

Hitzman, M.W. (2013). Kansanshi Campaign Observations, Unpublished report to First Quantum Minerals, Colorado School of Mines, 109pp.

Jackson, M.P. A., Warrin, O.N., Woad, G.M. and Hudec, M.R. (2003). Neoproterozoic allochthonous salt tectonics during the Lufilian Orogeny in the Katangan Copperbelt, Central Africa. *Geological Society Am. Bulletin*, **115** (3), 314-330.

Jowett, E.C. (1986). Genesis of Kupferschiefer Cu-Ag deposits by convective flow of Rotliegende brines during Triassic rifting. *Economic survey of Canada*, Special paper **36**, 3-38.

Kampunzu, A.B. and Cailteux, J. (1999). Tectonic evolution of the Lufilian Arc (Central African Copperbelt) during Neoproterozoic Pan-African Orogenesis. *Gondwana Research*, **2**, 401-421.

Kansanshi Resource and Exploration team. (2013). Kansanshi: a unique sediment hosted Copperbelt deposit, Unpublished Kansanshi Introductory presentation, Solwezi, 35pp.

Key, R.M., Liyungu, A.K., Njamu, F.M., Somwe, V., Banda, J., Mosley, P.N. and Armstrong, R.A. (2001). The western arm of the Lufilian Arc in NW Zambia and its potential for Copper mineralisation. *Journal of African Earth Sciences*, **33**, 503-528.

Koziy, L., Bull, S., Large, R. and Selley, D. (2009). Salt as a fluid driver and basement as a metal source for Stratiform Sediment hosted Copper deposits. *Geology*, **37**(12), 1107-1110.

Masiatis, V.L. (1998). Petrographic study of Kansanshi core samples, Unpublished report for Cyprus Amax Co.

Mason, D.R. (2013). Petrographic Description for 68 drill core samples from the Kansanshi Copper Mine, Zambia: Report No: 3891, Unpublished Petrographic report to First Quantum Minerals, Mason Geoscience Pty Ltd, 206pp.

Master, S., Rainaud, C., Armstrong, R.A., Phillips, D. and Robb, L.J. (2005). Provenance ages of the Neoproterozoic Katanga Supergroup (Central African Copperbelt), with implication of basin evolution. *Journal of African Earth Sciences*, **42**, 41-60.

Master, S. and Wendorff, M. (2011). Neoproterozoic glaciogenic diamictites of the Katangan Supergroup, Central Africa. In: E. Arnaud, G.P. Halverson and G. Shields-Zhou (Editors), *The Geological record of Neoproterozoic Glaciations*. Geological Society, London, pp. 173-184.

Meheghel, L. (1981). The occurrence of uranium in the Katanga system of Northwest Zambia. *Economic Geology*, **76**, 56-68.

Natural Resource Management: Geophysical mapping products. Available from: http://spatial.agric.wa.gov.au/geophysics/radiometrics.asp

Person, M. and Garvin, G. (1994). A sensitivity study of the driving forces on fluid flow during continental-rift basin evolution. *Geological Society of America*, **106**, 461-475.

Pirajno, F. (2010). *Hydrothermal Processes and Mineral Systems*. 1st edition. Springer Science+ Business Media, Perth. 1272pp.

Pirmolin, J. (1970). Inclusions fluids dans la dolomie du gisement stratiforme de Kamoto (Katanga occidental). *Annales Soc. Geol. Belgique*, **93**, 193-202.

Porada, H. and Berhost, V. (2000). Towards a new understanding of the Neoproterozoic-early Palaeozoic Lufilian and northern Zambezi belts in Zambia and the Democratic Republic of the Congo. *Journal of African Earth Sciences*, **30**, 727-771.

Rainaud, C., Master S., Armstrong R.A. and Robb, L.J. (2005). Geochronology and nature of the Palaeoproterozoic basement in the Central African Copperbelt. *Journal of African Earth Sciences*, **42**.

Renfro, A.R. (1974). Genesis of evaporite associated stratiform metalliferous deposits- a sabkha process. *Economic Geology*, **69**, 33-45.

Selfe, G.R. (2009). Report on CSAMT profiles undertaken south of Kansanshi Main pit. Unpublished report to First Quantum Minerals, GRS Consulting, South Africa, 5pp.

Selfe, G.R. (2010). Report on downhole geophysical logging of six holes in SE Dome area, Kansanshi. Unpublished report to First Quantum Minerals, GRS Consulting, South Africa, 4pp.

Selfe, G.R. (2011). Report on Gradient Array and Pole-Dipole IP in SE Dome area, Kansanshi. Unpublished report to First Quantum Minerals, GRS Consulting, South Africa, 9pp.

Selley, D., Broughton, D., Scott, R., Hitzman, M.W., Bull, S., McGoldrick, L.P., Croaker, M., Pollington, N. and Barra, F. (2005). A New Look at the Geology of the Zambian Copperbelt. *Economic Geology*, 100th Anniversary volume, 965-1000.

Sillitoe, R., Perello, J. and Garcia, A. (2010) Sulphide-bearing veinlets throughout the stratiform mineralisation of the Central African Copperbelt: Temporal and Genetic Implications. *Economic Geology*, **105**, 1361-1368.

Singer, D.A. (1995). World-class base and precious metal deposits: A quantitative analysis. *Economic Geology*, **90**, 88−104.

Speiser, A., Hein, F.U. and Porada, H. (1995). The Kansanshi Copper Mine (Solwezi Area, northwestern Zambia): Geology, wall-rock alteration and fluid inclusions. In: Pasava, Kfibek and Zak (Editors), *Mineral deposits*. Bulkema, Rotterdam, pp. 389-392.

Tembo, F., Kampunzu, A.B. and Musonda, B.M. (2000) Geochemical characteristics of Neoproterozoic A-type granites in the Lufilian belt, Zambia. *Journal of African Earth Sciences*, **30 (4A)**, 85.

Titley, M. (2012). Mineral Resource Estimate for First Quantum Minerals Ltd, Kansanshi and SE Dome, Zambia. NI43-101 Technical Report prepared for First Quantum Minerals, CSA Global Consultants, UK, 125pp.

Torrealday, H.I., Hitzman, M.W., Stein, H.J., Markley, R.J., Armstrong, R. and Broughton, D. (2000) Re-Os and U-Pb dating of the vein-hosted mineralisation at the Kansanshi copper deposit, Northern Zambia. *Economic Geology*, **95**, 1165-1170.

Torrealday, H.I. (2000). *Mineralisation and Alteration of the Kansanshi Cu Deposit, Zambia*. MSc. thesis (unpublished), Colorado School of Mines, Golden, Colorado, USA, 148pp.

Unsworth, M. (2013). Geophysics 424F: Time domain EM. Unpublished report, University of Alberta, Canada, 20pp.

Unrug, R. (1998). Mineralisation Controls and Source of Metals in the Lufilian Fold Belt, Shaba (Zaire), Zambia and Angola. *Economic Geology*, **83**, 1247-1258.

Wendorff, M. (2003a). Stratigraphy of the Fungurume Group- evolving foreland basin succession in the Lufilian fold-thrust belt, Neoproterozoic-Lower Palaeozoic, DRC. *South African Journal of Geology*, **106**, 47-64.

APPENDIX ONE: Glossary

%	Percent
°C	Celsius degrees
ASCu	Acid Soluble Copper – copper grade recovered after digest by a 3 acid mix
Au	Gold grade measured in parts per million (g/t)
Bn	Bornite, copper-iron sulphide
CACB	Central African Copperbelt
CCB	Congolese Copperbelt
Co	Cobalt
Cpy	Chalcopyrite, copper-iron sulphide
CSAMT	Controlled-Source Audio Magnetotellurics, a geophysical survey method
Cu	Copper, grade measured in %
EM	Electromagnetic geophysical method
FQML	First Quantum Minerals Limited
KMP	Kansanshi Mining Plc
LAT	Laterite (weathering profile)
m	metre
Ma	Million years
Mo	Molybdenite
MRE	Mineral Resource estimate
Mt	million tonnes
NI43-101	National Instrument 43-101
OK	Ordinary Kriging
Po	Pyrrhotite, iron sulphide
Py	Pyrite, iron sulphide
TCu	Total copper grade as a % of the sample mass
Th	Thorium
TSF	Tailings Storage Facility
U	Uranium
ZCB	Zambian Copperbelt

APPENDIX TWO: Quick logs of mineralised intervals for Kansanshi Boreholes and Kansanshi Mine logging codes

Borehole id: KRDD 662 **Location: KMP Main** **EOH: 282**

From	To	Min style	Lithology	Stratigraphy	Comments
0	32.1		FIL		No mineralisation
32.1	40.1		LAT		
40.1	159.6		DIO	UMC	
159.6	221		KS	UMC	
221	229.1		PHY	UMC	
229.1	248.5		KS	UMC	
248.5	254.5		CBPH	UMC	
254.5	257.2		RES	UMC	
257.2	266.5		MAR	UMC	
266.5	277.5		PHY	MMC	
277.5	282.5		BS	MMC	

Borehole id: KRDD 535 **Location: KMP Main** **EOH: 542.4**

From	To	Min style	Lithology	Stratigraphy	Comments
43.9	46	DSVN	PHY	MMC	Strong albite alteration
67.9	72.9	DSSFSV	PHY	MMC	
98.3	106.8	DSSFSV	PHY	MMC	
131.8	136	DSSV	MAR	LCS	
177	180	DSSFSV	MAR	LM	
196.4	199.4	DSSFSV	CBPH	LM	
330.4	344.4	DSVN	PS	LPS	
380.2	382.6	DSVN	PS	LPS	
407.1	409	DSVN	PS	LPS	
462.4	470.4	DSVN	PS	LPS	
478.8	516.4	DSVN	PS	LPS	
516.4	525		BS	LPS	
525	542.4		DOL	LD	

Borehole id: KRDD 609 **Location: KMP Main** **EOH: 353.9**

From	To	Min style	Lithology	Stratigraphy	Comments
7.8	9.9	DSSF	PHY	LM	Albite alteration
18.7	29.7	DSSFSV	PHY	LM	Albite alteration
33.9	38	DSSF	PHY	LM	Albite alteration
104.9	106.8	DSVN	PS	LPS	
276	278.9	DSSF	DOL	LD	
302.9	308.9	DSSF	DOL	LD	
308.9	353.9		DOL	LD	

Borehole id: KRDD 475 **Location: KMP Main** **EOH: 458.6**

From	To	Min style	Lithology	Stratigraphy	Comments
274	281.6	DS	MAR	UM	
320.6	326.6	DS	PHY	MMC	
360.6	368.6	DS	PHY	LCS	
377.4	379.6	DS	BS	LCS	
379.6	419.4		MAR	LM	
419.4	458.6		PS	LPS	

Borehole id: KRDD 533 **Location: KMP Main** **EOH: 344.5**

From	To	Min style	Lithology	Stratigraphy	Comments
81	82.95	SV	KS	UMC	
137.95	141.8	DSSV	MAR	UM	
144.9	146.85	DSSV	MAR	UM	
168.75	170	DSSV	PHY	MMC	
174.95	177.75	DSSFSV	CLBS	MMC	
180.2	184.65	DSSF	CBPH	MMC	
196.33	198.02	DSVN	MAR	LCS	
202.7	204.45	DS	CLBS	LCS	
218.8	221.4	VNSV	PHY	LCS	
221.4	297.95		MAR	LM	
297.5	344.5		KS	LPS	

Borehole id: KRDD 420 **Location: KMP Main** **EOH: 416.6**

From	To	Min style	Lithology	Stratigraphy	Comments
223.5	227.2	DSSFSV	PHY	MMC	
233	234.5	DSSV	PHY	MMC	
248.2	250.2	DSSV	PHY	MMC	
268	269.6	DS	MAR	LCS	
289.2	292	DS	PHY	LM	
378.6	381.6	VNSV	MAR	LM	
402.6	404.1	DSSV	PS	LPS	
404.1	416.6		PS	LPS	

Borehole id: KRDD 455 **Location: KMP Main** **EOH: 440.6**

From	To	Min style	Lithology	Stratigraphy	Comments
214.6	218.6	DSSF	PHY	UM	Albite alteration
224.6	230	DSVNSV	PHY	MMC	Albite alteration
263.4	268.45	DSSV	PHY	MMC	Albite alteration
268.45	289.15		KS	MMC	
289.15	314.68		CLBS	LCS	
314.68	325.3		KS	LCS	
325.3	422.6		MAR	LM	
422.6	440.6		PS	LPS	

Borehole id: KRDD 660 **Location: KMP SE Dome** **EOH: 543.3**

From	To	Min style	Lithology	Stratigraphy	Comments
140.15	142.65	VN	VNQ	UMC	Albite alteration
354.35	355.55	VN	VNQ	MMC	Albite alteration
369.8	370.65	VN	VN	MMC	Albite alteration
466.1	467.55	VN	VNC	LM	Carbonate alteration
494.8	499.15	VN	VN	LM	Albite alteration
499.15	520.75		MAR	LM	
520.75	543.3		PS	LPS	

Borehole id: KRDD 625 **Location: KMP SE Dome** **EOH: 446.2**

From	To	Min style	Lithology	Stratigraphy	Comments
139.35	141.5	DS	MAR	TMM	Albite alteration
233.45	233.8	DSVN	KS	UMC	Albite alteration
278.2	287.55	DSVN	PHY	UMC	Albite alteration
292.0	293.25	DSVNSV	PHY	UMC	Albite alteration
304.65	306.5	DSSV	KS	UMC	Albite alteration
332.75	335.2	VN	VNC	UMC	Carbonate alteration
393.05	393.6	VN	VNC	MMC	Carbonate alteration
426.95	427.9	DSSV	MAR	LM	Albite alteration
427.9	446.2		MAR	LM	

Borehole id: KRDD 704 **Location: KMP Main** **EOH: 374.5**

From	To	Min style	Lithology	Stratigraphy	Comments
170.5	173.2	VN	VN	MMC	
267.24	270.22	VN	VNC	LM	Carbonate alteration
270.22	314.5		MAR	LM	
314.5	317.17		PS	LPS	
317.17	324.0	DS	BXH	LPS	Hydrothermal Breccia
324.0	350.5		PS	LPS	
350.5	367.3		KS	LPS	Albite alteration
367.3	374.5		PS	LPS	Scapolite alteration

Borehole id: KRX 029 **Location: KMP Main** **EOH: 835**

From	To	Min style	Lithology	Stratigraphy	Comments
26.2	114.4		QFMS		
558.9	562.1	VN	VN	UMC	
669.8	670.3	VN	VN	MMC	
670.3	743.3		MAR	LCS	
743.3	754.6		DOL	LCS	
754.6	760.4		KS	LCS	
760.4	773.7		DOL	LM	
773.7	778.9		BS	LPS	
778.9	817.1		PS	LPS	
817.1	827.9		DOL	LD	
827.9	831.8		PHY	LD	
831.8	835		DOL	LD	

Borehole id: KRDD 559 **Location: KMP NW** **EOH: 253.5**

From	To	Min style	Lithology	Stratigraphy	Comments
122.0	127.5	VNC	VN	MMC	Carbonate alteration
129.5	133.9	VNSV		MMC	
135.0	139.5			MMC	
139.5	160.5		KS	MMC	
160.5	200.0		CLBS	LCS	De-dolomitisation
200	220.4		MAR	LM	
220.4	253.5		PS	LPS	

KANSANSHI MINE LOGGING CODES

MINERAL STYLE	
SF	Stratiform
DS	Disseminated
SV	Stringer Vein
VN	Vein
DSSF	Disseminated and stratiform
DSSV	Disseminated and stringers
SFSV	Stratiform and stringers
DSVN	Dissem and veins
SFVN	Stratiform and veins
VNSV	Veins and stringers
DSSFSV	Dissem, stratiform and stringers
SFSVVN	Stratiform, stringers and veins
DSSFVN	Dissem, stratiform and veins
DSVNSV	Dissem, veins and stringers
VNDSSV	Vein, dissem and stringers
VNSFSVDS	Vein, stratiform, stringers, dissem

LITHOLOGY	
DSS	Dolomitic Sandstone
PHY	Phyllite
PS	Pebble Schist
SS	Quartzite or Sandstone
DIO	Diorite
CBPH	Carbonaceous Phyllite
BS	Biotite Schist
CLBS	Calcareous Biotite Schist
DOL	Dolomite
CBKS	Carbonaceous Knotted Schist
CSS	Calcareous Sandstone
SAP	Saprolite
KS	Knotted Schist
MAR	Marble
NC	No core
SOIL	Soil
RES	Residual
BX	Breccia
BXC	Collapse Breccia
BXF	Fault Breccia
BXH	Hydrothermal Breccia
VN	Vein
VNC	Carbonate vein
VND	Dolomite vein
VNQ	Quartz vein
VNS	Sulphide vein

APPENDIX THREE: Plan showing location of boreholes that were quick-logged

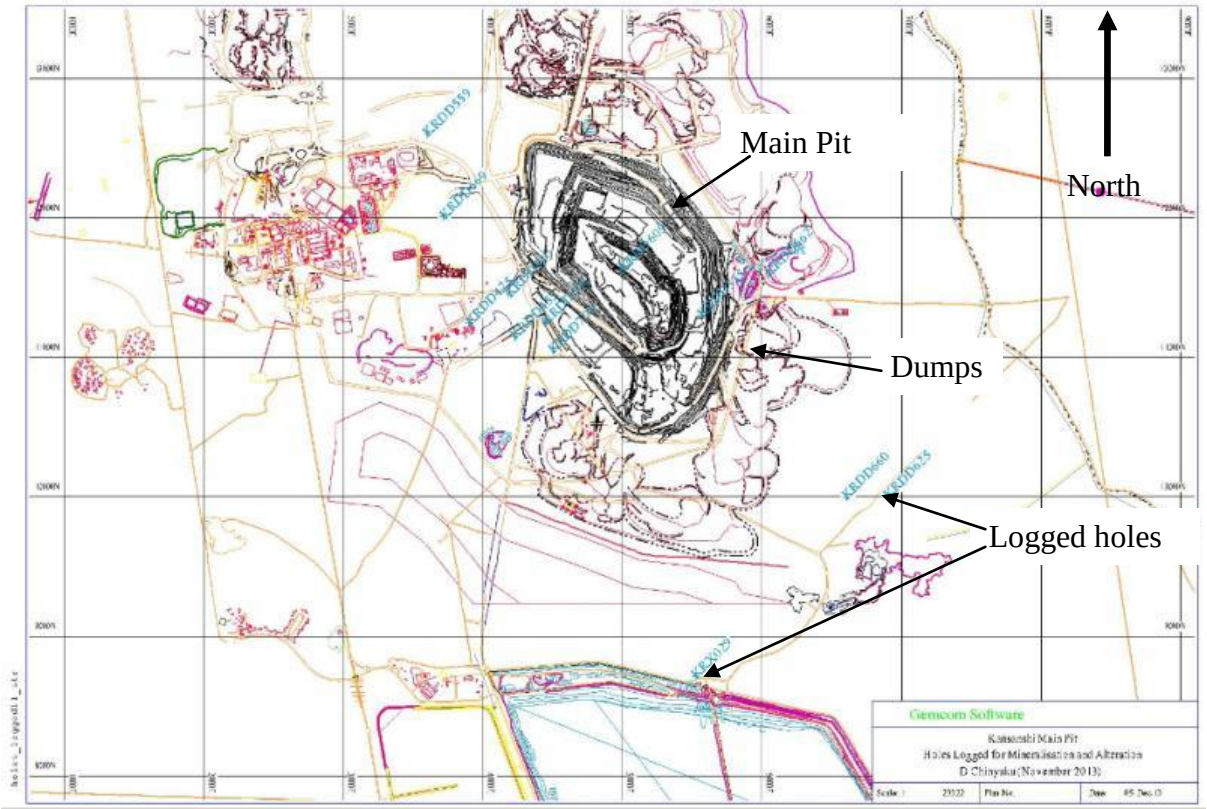

APPENDIX FOUR: Geology plan of Main pit showing mineralisation, alteration and lithologies